(2)

UNIVERSIDAD POLITECNICA DE MADRID

U. P. M.

Department of Electronic Engineers

HIGH SPEED ELECTRONICS LABORATORY

Telecommunication Engineering School

Ciudad Universitaria s/n
28040 MADRID
SPAIN

(2)

FINAL SCIENTIFIC REPORT
on
ELECTRICAL BEHAVIOR ON N-TYPE DOPANTS
IN AlGaAs ALLOYS:
SHALLOW LEVELS AND DX CENTERS

Period Covered
15 September 1988 - 14 September 1990

Sponsoring Office
AIR FORCE OFFICE OF SCIENTIFIC RESEARCH
GRANT AFOSR-88-0316

REPORT DOCUMENTATION PAGE

Form Approved
OMB No. 0704-0188

1. AGENCY USE ONLY (Leave blank)	2. REPORT DATE	3. REPORT TYPE AND DATES COVERED
	NOV 90	FINAL 15 SEP 88 - 14 SEP 90

4. TITLE AND SUBTITLE

ELECTRICAL BEHAVIOR OF N-TYPE DOPANTS IN AlGaAs ALLOYS: SHALLOW LEVELS AND DX CENTERS

5. FUNDING NUMBERS

6. AUTHOR(S)

PROFESSOR ELIAS MUNOZ

7. PERFORMING ORGANIZATION NAME(S) AND ADDRESS(ES)

UNIVERSIDAD POLITECNICA DE MADRID
DEPT OF ELECTRONICS ENGINEERING
CIUDAD UNIVERSITARIA
28040 MADRID , SPAIN

8. PERFORMING ORGANIZATION REPORT NUMBER

AFOSR-88-0316

9. SPONSORING/MONITORING AGENCY NAME(S) AND ADDRESS(ES)

SPONSORING AGENCY: AFWAL
WRIGHT-PATTERSON AFB, OH 45433-6523
MONITORING AGENCY: EUROPEAN OFFICE OF AEROSPACE RESEARCH AND DEVELOPMENT, BOX 14, FPO, NY 09510-0200

10. SPONSORING/MONITORING AGENCY REPORT NUMBER

EOARC
TR-91-01

11. SUPPLEMENTARY NOTES

12a. DISTRIBUTION/AVAILABILITY STATEMENT

APPROVED FOR PUBLIC RELEASE;
DISTRIBUTION UNLIMITED

12b. DISTRIBUTION CODE

13. ABSTRACT (Maximum 200 words)

The electrical properties of n-type AlxGal-xAs for x > 0.2, are governed by deep donor states, formerly called DX centers, and created by the isolated donor atoms. At very low AL compositions, such deep donors become resonant with the gamma minimum. For GaAs and x < 0.1 compositions, the electron thermal emission has been studied under hydrostatic pressure. For x > 0.2, the structure of spectra obtained by deep level transient spectroscopy (DLTS), has been analyzed for Si and Se dopants. It is suggested that deep donors show a discrete structure of energy levels, revealed in their thermal emission kinetics.

An analysis of the capacitance behavior of AlGaAs n- type regions (x > 0.2) has been performed for Si and Sn donors. Electron capture kinetics has been modeled. Photoluminescence in Si- doped AlGaAs has been studied in a large variety of samples. The behavior of AlGaAs/GaAs heterojunction bipolar transistors at low temperature has been explored for Si- and Sn-doped emitters. It has been found that the internal photoionization of the Si deep donors is produced, allowing a better transistor performance at 77K than at 300K. Finally, impact ionization of Se- related DX centers has been detected and analyzed.

14. SUBJECT TERMS	15. NUMBER OF PAGES
CaAlAs Doping, Deep Levels	70
	16. PRICE CODE

17. SECURITY CLASSIFICATION OF REPORT	18. SECURITY CLASSIFICATION OF THIS PAGE	19. SECURITY CLASSIFICATION OF ABSTRACT	20. LIMITATION OF ABSTRACT
UNCLASSIFIED	UNCLASSIFIED	UNCLASSIFIED	

This report has been reviewed and is releasable to the National Technical Information Service (NTIS). At NTIS it will be releasable to the general public, including foreign nations.

This technical report has been reviewed and is approved for publication.

EIRUG DAVIES, Ph.D.
Chief, Semiconductor/S.S. Phys

FRED T. GILLIAM, Lt. Col, USAF
Chief Scientist

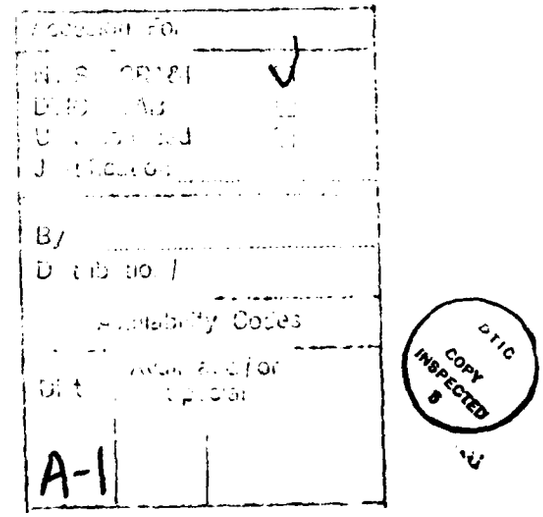

FINAL SCIENTIFIC REPORT

ON

ELECTRICAL BEHAVIOR OF N-TYPE DOPANTS IN AlGaAs ALLOYS SHALLOW LEVELS AND DX CENTERS

PERIOD COVERED
15 SEPTEMBER 1988 - 14 SEPTEMBER 1990

SPONSORING OFFICE
AIR FORCE OFFICE OF SCIENTIFIC RESEARCH
GRANT AFOSR-88-0316
EOSRD-LONDON

DEPARTAMENTO DE INGENIERIA ELECTRONICA
E.T.S. INGENIEROS DE TELECOMUNICACION
UNIVERSIDAD POLITECNICA DE MADRID

PRINCIPAL INVESTIGATOR PROF. ELIAS MUÑOZ

FINAL SCIENTIFIC REPORT

Electrical behavior of n-type dopants in $Al_xGa_{1-x}As$ alloys : shallow levels and DX centers

GRANT AFOSR 88-0316
PERIOD : SEPTEMBER 1988-SEPTEMBER 1990

PRINCIPAL INVESTIGATOR : PROF. ELIAS MUNOZ
RESEARCH PERSONNEL :
ENRIQUE CALLEJA
IGNACIO IZPURA
FERNANDO GARCIA
ANGEL L. ROMERO

UNIVERSIDAD POLITECNICA DE MADRID
DEPARTAMENTO DE INGENIERIA ELECTRONICA
ETS INGENIEROS DE TELECOMUNICACION. MADRID

OCTOBER 1990

ABSTRACT

The electrical properties of n- type $Al_xGa_{1-x}As$, for $x > 0.2$, are governed by deep donor states, formerly called DX centers, and created by the isolated donor atoms. At very low Al compositions, such deep donors become resonant with the Γ minimum. For GaAs and $x < 0.1$ compositions, the electron thermal emission has been studied under hydrostatic pressure. For $x > 0.2$, the structure of spectra obtained by deep level transient spectroscopy (DLTS) has been analyzed for Si and Se dopants. It is suggested that deep donors have a discrete structure of energy levels, revealed in their thermal emission kinetics.

An analysis of the capacitance behavior of AlGaAs n- type regions ($x > 0.2$) has been performed for Si and Sn donors. Electron capture kinetics has been modeled. Photoluminescence in Si- doped AlGaAs has been studied in a large variety of samples. The behavior of AlGaAs/ GaAs heterojunction bipolar transistors at low temperature has been explored for Si- and Sn-doped emitters. It has been found that the internal photoionization of the Si deep donors is produced, allowing a better transistor performance at 77K than at 300K. Finally, impact ionization of Se- related DX centers has been detected and analyzed.

TABLE OF CONTENTS

I. INTRODUCTION

Silicon device engineering has benefit from the fact that, in Si, X conduction band minima are the lowest ones, and they are far from the L and Γ minima. Then, the useful dopants behave as effective mass-like, rather shallow levels. However, III-V compound semiconductors, that offer a wide range of applications because the conduction band can be engineered, have their CB minima, in many cases, separated just by a few tens of meV. The states created by the donor atoms show, then, a much more complex behavior because such multivalley effects.

GaAsP was probably the first III-V ternary semiconductor where it was shown that the standard donors introduce extra deep levels not linked to the Γ minimum [1,2]. Later on, research on AlGaAs material and devices revealed the presence of donor- related deep levels, with features similar to those found in GaAsP. These levels were coined DX centers, X indicating that something was accompanying the donor D, but its specific nature was unknown [3,4]. Deep donor levels, linked to upper conduction band minima, and related to the dopant atoms, were also found in other III-V alloys, as InGaP [5,6]. It was also shown that these levels, apparently tied to the L, or X, minima, could be made to emerge into the forbidden band by the use of hydrostatic pressure. Their presence as resonant states with the Γ minimum was also demonstrated in GaAs [7,8]. Finally, a large experimental evidence backs today the idea that the so called DX center is just due to the isolated donor atom itself, although its sitting into the lattice may be distorted in relation to an ideal substitutional dopant. Although it is still a matter of controversy, most of the experimental data seems to favor a large donor- atom displacement after capturing one (or two) electron, then becoming neutral (or negatively charged). Chadi and Morgan have proposed models along such direction [9,10]. A different school proposes a small lattice relaxation model, or even considers that the DX center is just the donor effective mass state linked to the L minima [11,12].

Basically from studies in AlGaAs, a significant number of properties of such deep donors have been obtained today, involving photoionization, Hall effect, low temperature persistent photoconductivity, and thermally activated electron emission and capture. However, a proper.

selfconsistent description of the electrical behavior of such deep donors is not available. Their nature and microscopic origin have not been resolved yet, and, although some structures have been shown to decrease the effects of such DX centers, a definitive answer concerning ways to avoid, or to minimize, such deep donors is still lacking.

Today it is well known that the behavior of AlGaAs/ GaAs HEMT transistors at low temperature is drastically influenced by such deep donors, and these problems have motivated the research efforts around the behavior of donors in AlGaAs. New HEMT structures based on InGaAs and InGaP have emerged. Current views indicate that we face a band structure problem, then, a general one for III-V semiconductors and even other compound semiconductors, but the deleterious effects (amount) seem to be dependent on the specific dopant, host lattice and alloy composition.

Present research addresses the objective of determining the electrical behavior of such deep donors in AlGaAs, to obtain information about the structure and nature of such donors by electrical and optical techniques, and to explore the implications for AlGaAs based devices.

Most of the research effort in this program has been focused in understanding and modeling the capacitance behavior of n -AlGaAs regions, for $x > 0.2$, where the deep donors have a dominant role. Such information has been revealed as a fundamental one to understand the electron emission and capture results from measurements that use space charge capacitance techniques (deep level transient spectroscopy - DLTS, thermally stimulated capacitance, photocapacitance, etc.). These experimental tools are based in capacitance waveform analysis and processing, to extract the physics involved in the electron capture - emission kinetics. To separate, or deconvolve, the features of such waveforms due to the space charge region evolution, from those due to the intrinsic electronic structure of the deep donors, is the ultimate goal of such studies.

The development of methods to obtain the energy position of the deep donors (referred to the lowest CB minimum), by static and quasi- static capacitance measurements, has been a major issue. These new techniques have been applied to characterize Si and Sn deep donors. The electron capture kinetics, showing its intrinsic non exponential nature, has been also

modeled. Another result is that we have found significant evidence that the infrared luminescence coming from Si- doped AlGaAs is not related to the DX center.

The effects of the local environment on the properties of DX centers in Si- doped GaAs, and dilute $Al_xGa_{1-x}As$, have been studied by DLTS under hydrostatic pressure. For group IV donors, our past findings for Sn related DX's, and present data for Si DX's, show the presence of four peaks in the DLTS spectra that we relate to donor atoms being interstitial with 0, 1, 2, or 3 Al nearest neighbors atoms. Multiple thermal emission rates in ordinary alloy compositions (0.2 to 0.6 Al mole fractions) have been observed for Sn, Se, and Si- related DX centers.

An important motivation for our research has been to link the basic properties of DX centers with AlGaAs- based device behavior. In this context, the behavior at low temperatures of AlGaAs/ GaAs heterojunction bipolar transistors has been considered, showing an interesting improvement. For the first time, impact ionization of DX centers has been observed. Its implications in device performances need an extra effort.

As a summary of the most relevant parameters of the DX centers, table I shows the values of the thermal activation energy for emission (E_e), and capture (E_b) processes, the "intrinsic" capture barrier (E_σ), and the photoionization threshold (E_{io}).

TABLE I

Activation Energies of DX Centers in GaAlAs Alloys

Donor	Ee (eV)	Eb (eV)	Eσ (eV)	Eio (eV)	x
S	0.28				0.43
S	0.20	0.10			0.40
Se	0.29	0.16	0.09		0.35
Se	0.28				0.43
Se	0.28	0.18		0.85	0.40
Se	0.29				0.50
Te	0.28	0.18		0.85	0.40
Te	0.24	0.14		0.60	0.65
Te	0.27	0.16			0.65
Te	0.28				0.43
Te	0.32				0.50
Si	0.43	0.33		1.25	0.40
Si	0.43				0.30
Si	0.43	0.21		1.40	0.35
Si	0.43		0.20		
Si	0.44	0.33			0.30
Si	0.44	0.24			0.35
Ge	0.33				0.30
Sn	0.19	0.10		1.10	0.40
Sn	0.19	0.09	0.02		0.35
Sn	0.21				0.30
Sn	0.19				0.30
Sn	0.21	0.08	0.01		0.35
Sn	0.20				0.35

REFERENCES

1. M.G. Craford, G.E. Stillman, J.A. Rossi, and N. Holonyak, Phys. Rev., **168**, 867, (1968).
2. J.A. Gaj, A. Majerfeld, and G.L. Pearson, phys. status solidi (b), **48**, 513, (1971).
3. D.V. Lang and R.A. Logan, Phys. Rev. Lett., **39**, 635, (1977).
4. D.V. Lang, R.A. Logan, and M. Jaros, Phys. Rev., **B19**, 1015, (1979).
5. R. A. Craven and D. Finn, J. Appl. Phys., **50**, 6334, (1979).
6. S. Nojima, H. Tanaka, and H. Asahi, J. Appl. Phys., **59**, 3489, (1986).
7. M. Mizuta, M. Tachikawa, H. Kukimoto, and S. Minomura, Jap. J. Appl. Phys., **24**, L143, (1985).
8. D.K. Maude, J.C. Portal, L. Dmowski, T. Foster, L. Eaves, M. Nathan, M. Heiblum, J.J. Harris, and R.B. Beall, Phys. Rev. Lett. **59**, 815, (1987).
9. T. N. Morgan, in "Defects in Semiconductors 15", ed. by G. Ferenczi, Materials Science Forum, Vol. 38 - 41 (Trans. Tech. Publications, Switzerland, 1989) p. 1079.
10. D. J. Chadi and K. J. Chang, Phys. Rev. Lett., **61**, 873, (1988).
11. J. Henning and J. Ansems, Semicond. Sci. Technol., **`**. 1, (1987).
12. S. Alaya, H. Maaref, and J.C. Bourgoin, Aμpl. Phys. Lett., **55**, 1406, (1989).

II. LOCAL ENVIRONMENT EFFECTS ON THE PROPERTIES OF DX CENTERS IN Si-DOPED GaAs AND DILUTE $Al_xGa_{1-x}As$ ALLOYS

II.I. INTRODUCTION

DX centers have been mostly studied in Si- doped AlGaAs alloys with compositions beyond 20%, where these levels lie below the bottom of the conduction band. The rapid change in the DX center electron occupancy with alloy composition, together with the constant value of the thermal emission activation energy, led to some authors to conclude that the DX center is a localized state not related to the Γ minimum of the conduction band [1,2]. The first direct evidence of this picture was found by Mizuta in Si- doped GaAs [4], where a clear DLTS signal with a thermal activation energy of 0.33 eV appeared under hydrostatic pressures higher than 30 Kbar. In GaAs and AlGaAs alloys with AlAs mole fractions of $x < 0.2$, DX levels are found to be resonant states [5] (lying above the bottom of the conduction band).

The presence in Si- doped dilute AlGaAs alloys (4% and 8%) of three discrete DLTS peaks has been reported [6]. This indicates that there are, at least, three discrete thermal emission rates, and this fact has been interpreted as evidence *of three different local environments for the Si atoms* [6]. This suggests that the lattice relaxation associated with electron capture at DX centers involves the motion of Si atoms from their substitutional sites to interstitial sites, and that the three emission rates correspond to relaxed configurations having 0, 1, or 2 Al atoms as nearest neighbors [7,8]. It is also consistent with measurements of the fine structure in the DLTS spectrum in alloys with higher AlAs mole fraction (for both Sn and Si donors), which show no more than four DLTS peaks [9,10], as presented in the next section of this report. These results also agree with a recent experiment [11] using an ordered alloy/ superlattice structure which also showed only four discrete DLTS peaks.

We have now revised such studies in dilute AlGaAs alloys, and included data for $x = 0.14$ alloys. A fourth peak, that we think is linked to a local configuration of one Si donor surrounded by 3 Al atoms, has been detected. Then, a very good agreement with results in ordered alloys and in

high Al- composition homogeneous alloys, has been achieved.

We have studied the change in DLTS spectra under applied hydrostatic pressure of Si- doped GaAs and AlGaAs having x = 0.04, 0.08, and 0.14. It was found that for the range of pressures available, up to 13 Kbar, the emission activation energies are independent of the magnitude of the applied pressure.

II.2. SAMPLES AND RESULTS

In this work, Si- doped GaAs and GaAlAs (4%, 8%, and 14%) samples grown by molecular beam epitaxy (MBE), with a doping level in the 10^{18} to 10^{19} cm^{-3} range, have been used. A top layer of undoped GaAs was needed to obtain Mo-Schottky barriers with low leakage current. A cylinder-piston type cell, with kerosene as liquid medium, was used for hydrostatic pressure experiments. Pressure values were always measured at the DLTS temperature with a 0.5 $\pm$ Kbar accuracy.

As preliminary information, a summary of published DLTS spectra for Si- doped GaAs and AlGaAs samples, for a wide range of compositions, is shown in figure 1 [6].

Figures 2, 3, 4 and 5 show the evolution of various DLTS spectra with pressure. In figure 2, a single, featureless DLTS peak is observed for Si- doped GaAs. As the pressure increases, the peak amplitude (trap occupancy) gets larger, following an exponential rate. The thermal emission activation energy is found to be constant (0.35 $\pm$ 0.02 eV) for all pressure values. The peak position does not move with pressure, as expected from an exponential emission process if the sampling times are kept constant.

DLTS spectra in figure 3 reveal a similar evolution with pressure in a Si- doped GaAlAs sample with 4% Al content. Here, two distinct peaks are observed, and again, neither their emission energies nor their temperature positions move when the pressure is increased. From these two parameters we can conclude that the coldest peak corresponds to the one

observed in GaAs (note that the time constants are not the same), and the second peak corresponds to the well established DX center in AlGaAs alloys with $x > 0.2$, as indicated in figure 1 [6,7]. Both peak amplitudes follow an exponential increase as a function of pressure. These peaks have been attributed to local environments with 0 and 1 Al atoms as nearest neighbors.

Figure 4 shows the evolution with pressure of DLTS signals corresponding to a Si- doped GaAlAs sample with 8% Al content. There is a dominant peak (0.43 eV) that correlates to the one observed in the 4% Al content GaAlAs sample, since the emission energy, position (note again the difference in time constants), and amplitude change with pressure are similar. At the highest pressure available, a second peak (coldest) is resolved, being characterized by a thermal emission energy of 0.35 eV. We want to remark that this energy has been derived from much better resolved DLTS spectra, using shorter filling pulses. All DLTS spectra on figures 2, 3, 4, and 5 were obtained under saturation filling pulse conditions in order to derive true trap electron occupancies. A third peak, appearing at the highest temperature, has an amplitude that barely changes with pressure. This peak merges with the dominant one, making very difficult an emission energy assignment. However, if we compare data in figure 3 with the summary shown in figure 1, it is reasonable to assume that this peak is associated with the DX center having 2 Al nearest neighbors, with an emission energy around 0.43 eV. We will then refer as P_0, P_1, and P_2, the three different DLTS peaks, where the subscript indicates the number of Al nearest neighbors.

Following the same arguments, the DLTS experiments under pressure for the sample with $x = 0.14$ (figure 5) shows a new peak, P_3, that we claim is due DX centers with 3 Al atoms as near neighbors. Its thermal emission activation energy is $E_e = 0.45$ eV.

In figures 6, and 7 we represent the pressure dependence of the DLTS peak amplitudes in samples with different Al contents. All amplitudes increase with pressure and, eventually, they saturate sequentially with pressure. As it will be discussed later, this is understood as an indication that *the larger the number of Al neighbors, the lower the energy of the DX level.*

The measured values of the thermal emission energies are summarized in figure 8, where the DLTS emission energies corresponding to the resolved peaks are plotted versus hydrostatic pressure. Labels "GaAs-like" and "GaAlAs-like", that point to the different emission energies, will make more sense after the discussion.

II.3. DISCUSSION

A thermal emission energy of 0.35 eV is clearly representative of Si- DX centers in GaAs, that is, corresponding to donor local environments where there are no Al atoms. Once the Al concentration is slightly increased (4%), a second DLTS signal with thermal emission energy of 0.43 eV appears, but we still observe the former one. There is a simple explanation for this result if we consider that, in AlGaAs with 4% Al content, there are donors with no Al atoms around (GaAs-like), as well as donors with Al atoms around (GaAlAs-like). This difference in donor local environments might change the DX center thermal emission energy and/ or its total energy, taking into account the strong localized character of the DX centers.

As the Al content is further increased to 8%, the GaAs- like peak becomes smaller. Following the previous picture, this is consistent with a lower probability to find donor local environments with no Al atoms around, and to be able to charge them. In fact, a reasonable intense signal is only obtained at high pressures, that is, when the trap electron occupancy is increased by pushing down the trap towards the Fermi level.

A third DLTS peak (at the highest temperature) emerges in the 8% Al content sample. There is a clear indication from data in reference (6), that increasing the Al mole fraction in Si- doped GaAlAs beyond 8% moves the dominant DLTS peak to higher temperatures, but the thermal emission energy remains constant, in good agreement with previous data [12]. Then, it is reasonable to assign the two peaks on the right side of figure 4 to DX centers with different donor local environments, that is, with one or two close Al atoms (dominant and weak peaks respectively). In the sample with 14% of Al, the peak appearing at the highest temperatures has E_e= 0.45 eV, and is linked with a DX center surrounded by 3 Al atoms. For this alloy

composition the probability of such environment is much higher than in the previous samples, where it could not be detected. It agrees with the results in the next section for much higher Al composition samples.

The dependence of each DLTS peak amplitude with pressure can be studied for the various Al compositions, and then compared with the evolution of the various conduction band minima. The difficulty arises because the occupation of the DX center is controlled by the Fermi level. Then, the pressure evolution of the P_i peak does not give information about the pressure coefficient of E_{DXi} with respect to any band edge minima, but only with respect to E_F.

In the 8% sample, the electron occupancy of the different DX levels increases exponentially with pressure, but the amplitude of P_2 saturates at about 4 Kbar. This can be understood as if at these pressures the level E_{DX2} lies below the Fermi level, while E_{DX1} still lies above it. For the dilute alloys the probability of a Si atom having 1 or 2 Al atoms as near neighbors should be much smaller than having 0 Al atoms. However, because the larger amplitude of peak P_1 as compared to P_0, we may conclude that E_{DX1} lies below E_{DX0}. Then we suggest that $E_{DX0}>E_{DX1}>E_{DX2}$. Energies E_{DXi} are measured respect to the CB bottom.

A full picture of the emission (or capture) process of one electron from the DX ground state to the CB has to be based on thermodynamic concepts. The total transition energy (free energy) has to be considered as an increase of an entropy term and an entalpy term. Since at a given temperature, the emission rates for P_1 and P_2 are quite different, and taking into account that their thermal activation energies seem to be equal, above argument leads to consider that the values of the transition entropies for both centers must be different. In a simple scheme where the top of the capture barrier E_{cap}, measured from the bottom of the conduction band minimum, is the same for the various configurations, the energy change needed for an electron to be emitted from the DX center over the barrier is expressed as the total change in free energy (Gibbs free energy) as follows:

$$\Delta G_{DX} = \Delta H_{DX} - T\Delta S_{DX} = E_{cap} - E_{DX} \qquad [1]$$

DLTS experiments prove that the energy ΔH_{DX} remains constant

(0.43 eV) with both pressure and alloy composition [6,7] for Si- doped GaAlAs. Then P_1 and P_2 should have a different entropy factor associated with each configuration, explaining the temperature shift of the two DLTS peaks. As it is indicated in the next section, this result is consistent with the idea that the temperature independent prefactors in the emission rates reflect the DX local environments. This analysis should be pursued in a future research program.

Another point of discussion concerns the choice of a DX center microscopic model that might answer why the emission process is so sensitive to the number of Al atoms around the donor and how many different contributions to the emission process should we expect. We start considering that the electron trapped at the DX center has a very localized wave function, then, being most sensitive to atomic configurations of first and second neighbors. When Si replaces a group III host atom in GaAlAs, there are 12 group III atoms as first neighbors. Since not all configurations with a given number of Al atoms are equivalent, the number of different environments with Al atoms as second neighbors is much higher. However, a maximum of four DLTS peaks has been reported in different experiments (see next section). A simple explanation is given by a model in which the Si atom moves to an interstitial site upon electron capture by the deep level [7,8]. In this case, there will be four different atomic configurations around the donor with different number of Al atoms as first neighbors, that is, 0, 1, 2, and 3 Al atoms.

The analysis of figures 6 and 7 allow to obtain the pressure coefficients of the P_i peaks. Preliminary analysis about the dependence of $(E_{DXi} - E_F)$ (experimental) and $(E_L - E_F)$ (theoretical) indicates that the pressure coefficients of the DX centers and that of the L minima are not the same. Thus, any special relationship between the DX levels and the L minima states is doubtful.

Finally, we want to comment briefly on the emission energy value obtained for DX centers in Si- doped GaAs. Following the proposed model, we should expect no change in the emission energy for donor local environments with 0 or 1 Al atom, but there is indeed a strong change (0.35 eV to 0.43 eV). Once a proper DX center microscopic model is available, and the effect of different donor local environments on the lattice relaxation is

understood, this point could be addressed.

II.4. SUMMARY

In summary, we have shown that hydrostatic pressure does not change the thermal emission energy of the DX centers (GaAs-like or GaAlAs-like). This result together with data in ref. (9) point out that this energy is constant once a minimum amount of Al atoms is present in the alloy. An entropy term shift, due to different donor local environments, seems to be the origin of multiple, discrete contributions to the emission process from DX centers. This alloy effect would also be responsible for the non- exponential behavior of the capacitance transients. From the change in the electron occupancy with pressure, for each peak in the DLTS spectra, it is suggested that a deepening of the trap energy position takes place as the number of Al atoms close to the donor increases. This change in DX_i energy position is in very good agreement with the mentioned transition entropy shift. For a given sample, the pressure coefficients of the individual DX levels are similar, but they are in general different from that of the L minima.

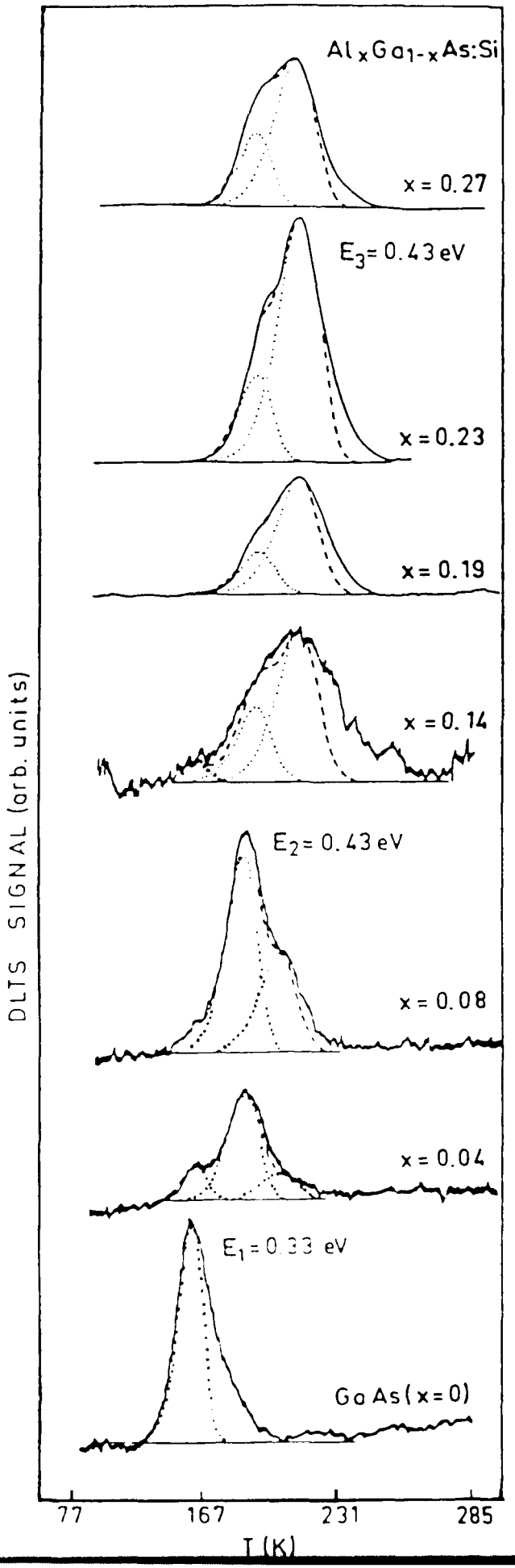

Fig. 1. DLTS spectra for Si-doped GaAs and AlGaAs samples of various compositions. Solid lines are the experimental spectra. (REF 6)

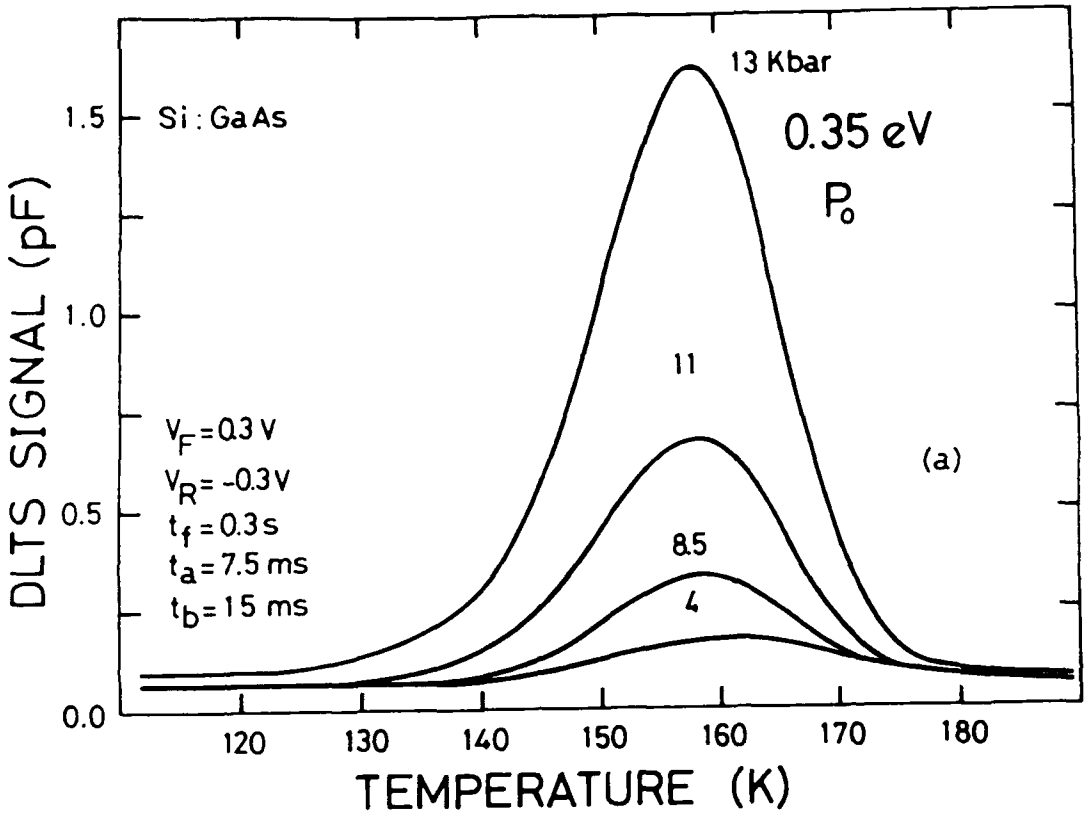

Figure 2. Evolution of DLTS spectra of DX centers in Si-doped GaAs with applied hydrostatic pressure

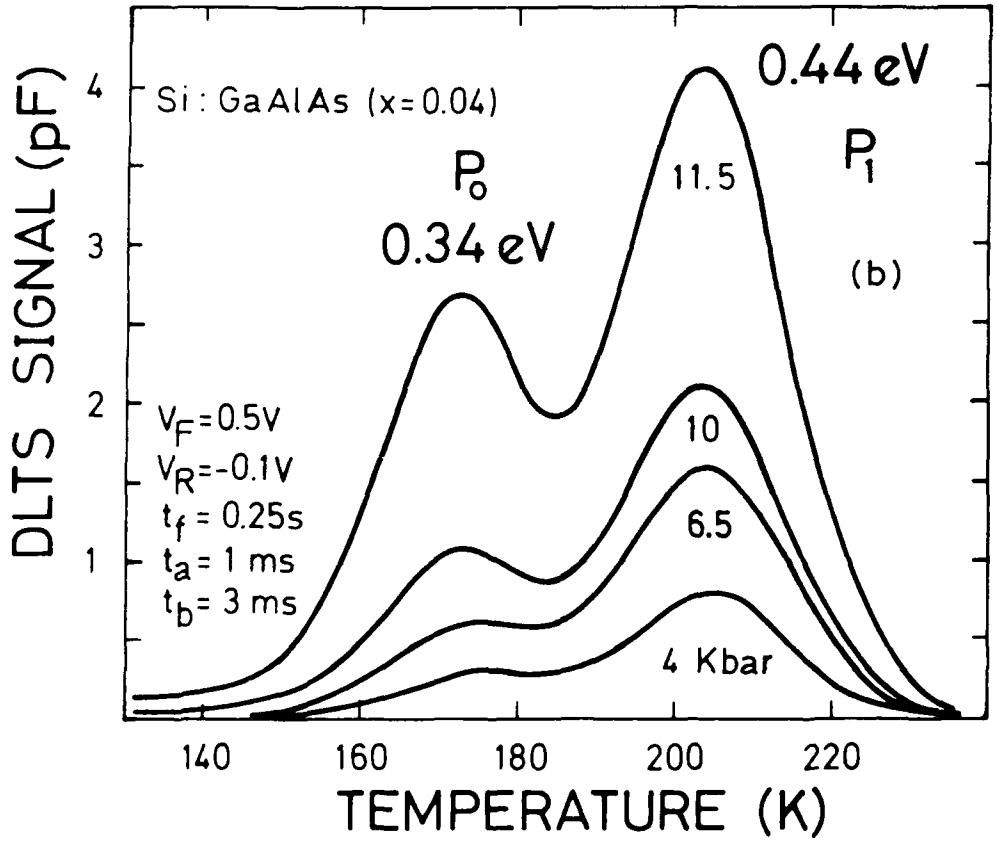

Figure 3. Evolution of DLTS spectra of DX centers in Si-doped AlGaAs (x=0.04) with applied hydrostatic pressure.

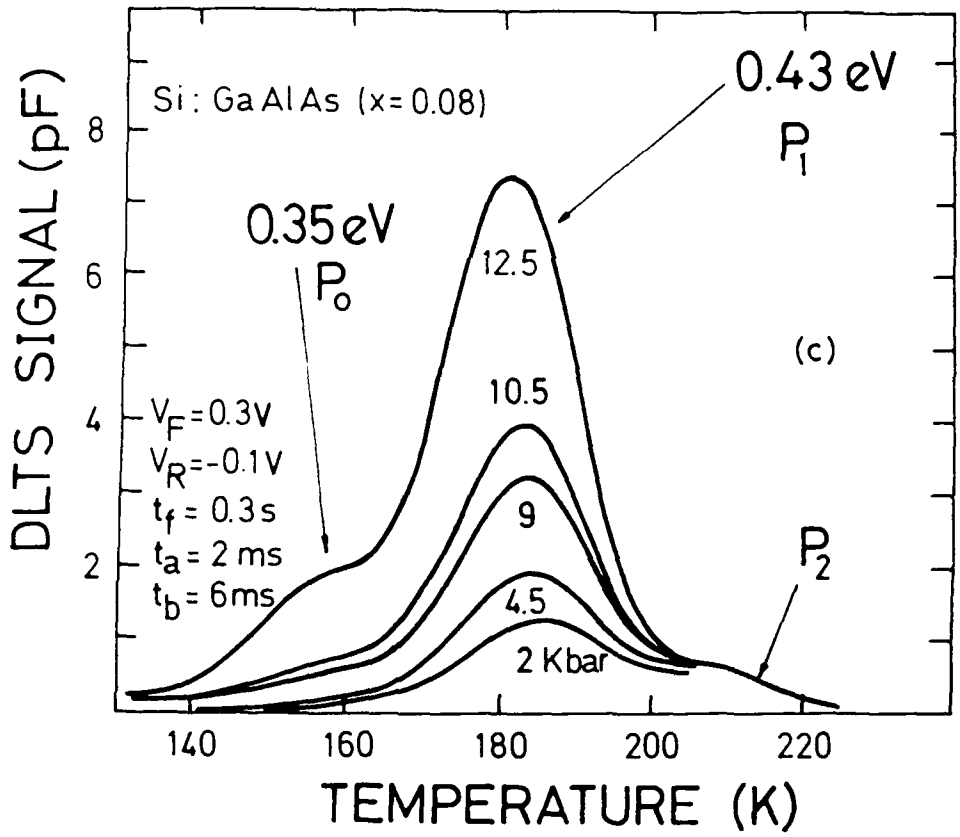

Figure 4.- Evolution of DLTS spectra of DX centers in Si-doped AlGaAs (0.08) with applied hydrostatic pressure.

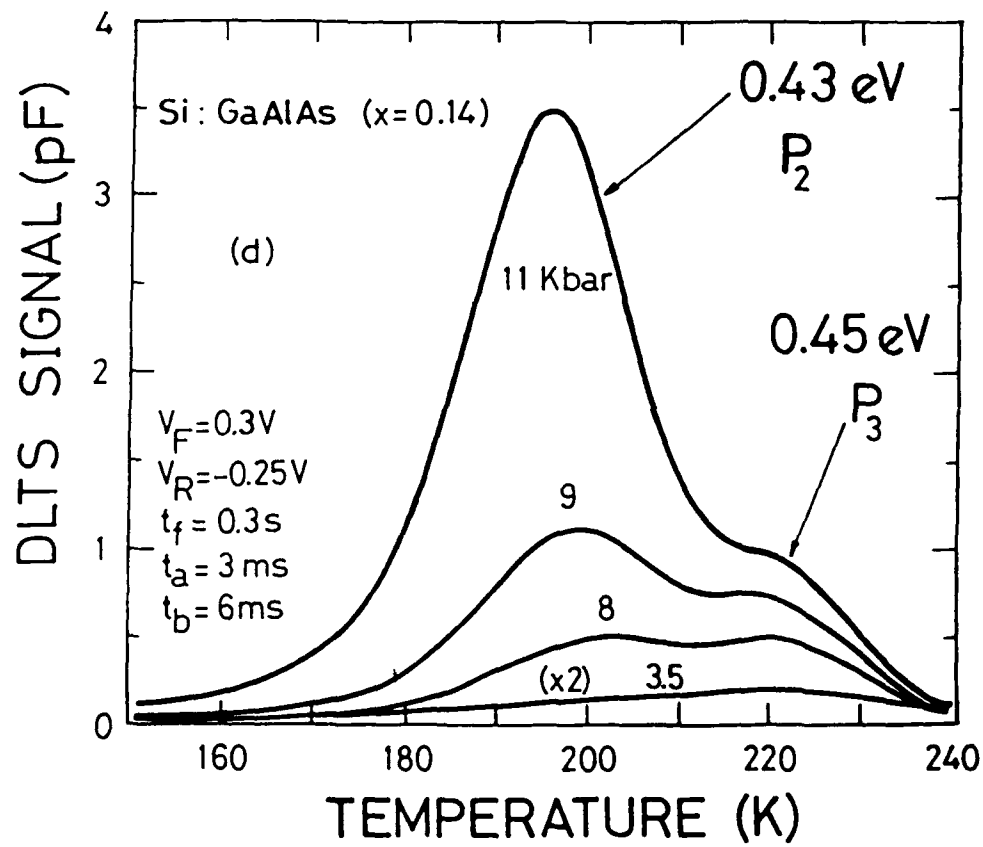

Figure 5.- Evolution of DLTS spectra of DX centers in Si-doped AlGaAs (0.14) with applied hydrostatic pressure.

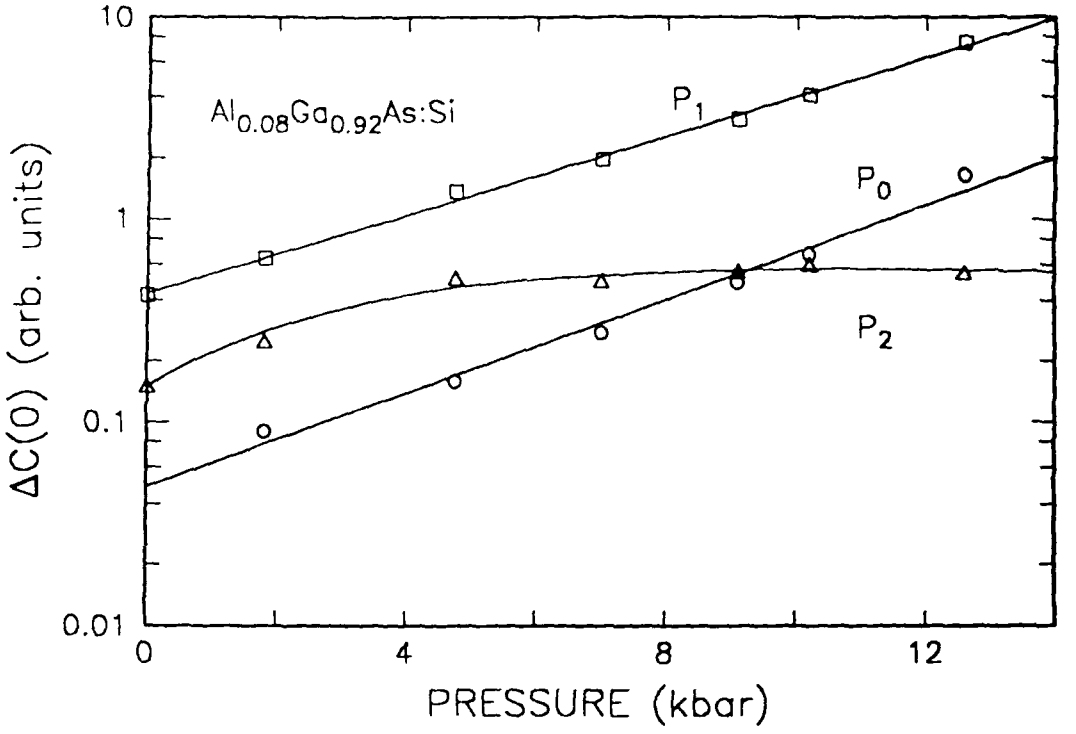

Figure 6.- Amplitude of the capacitance transient of each DX level as a function of the applied pressure in Si:AlGaAs (0.08).

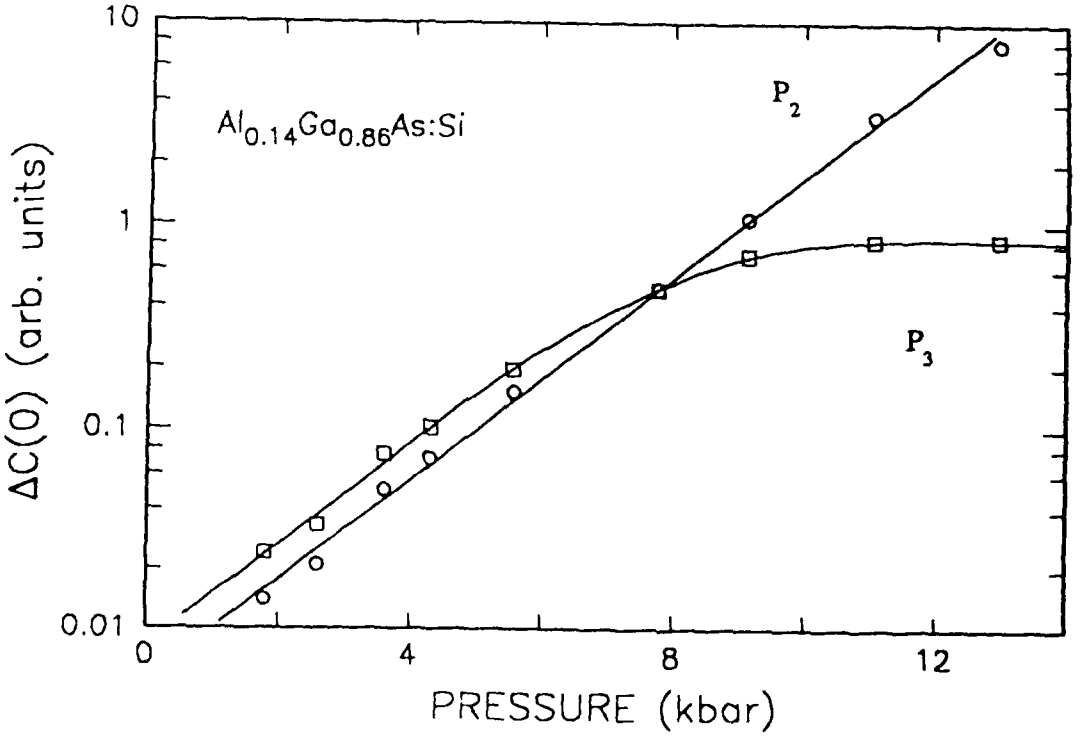

Figure 7.- Amplitude of the capacitance transient of each DX level as a function of the applied pressure in Si:AlGaAs (0.14).

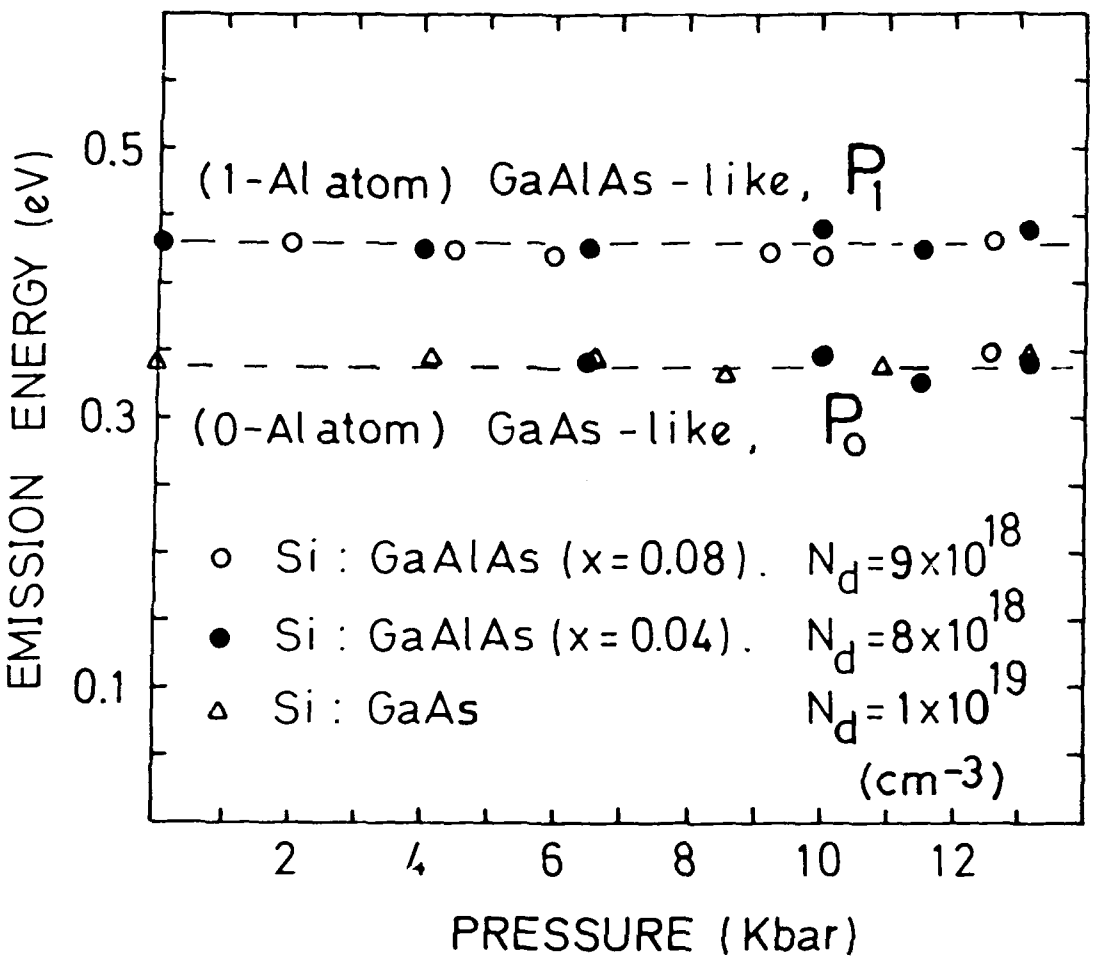

Figure 8.- Dependence of the thermal emission energy of P_0 and P_1 on hydrostatic pressure.

REFERENCES

1) D.V. Lang, R.A. Logan, and M. Jaros, Phys. Rev., **B19**, 1015, (1979); and D.V. Lang in "Deep Centers in Semiconductors" ed. by S.T. Pantelides, (New York, Gordon & Breach) pp. 489-539, (1986).
2) K. Kaneko, M. Ayabe, and N. Watanabe, Inst. Phys. Conf. Ser. No **33a**, 216, (1977).
3) P.K. Bhattacharya, A. Majerfeld, and A.K. Saxena, Inst. Phys. Conf. Ser. No **45**, 199, (1979).
4) M. Mizuta, M. Tachikawa, H. Kukimoto, and S. Minomura, Jap. J. Appl. Phys., **24**, L143, (1985).
5) P.M. Mooney, T.N. Theis, and S.L. Wright, Inst. Phys. Conf. Ser. No **91**, 359, (1987).
6) P.M. Mooney, T.N. Theis, and S.L. Wright in "Defects in Semiconductors", Materials Science Forum, vol. 38-41, p. 1109 (1989).
7) T. N. Morgan, in "Defects in Semiconductors 15", ed. by G. Ferenczi, Materials Science Forum, Vol. 38 - 41 (Trans. Tech. Publications, Switzerland, 1989) p. 1079.
8) D. J. Chadi and K. J. Chang, Phys. Rev. Lett., **61**, 873, (1988).
9) E. Calleja, A. Gomez, E. Muñoz, and P. Camara, Appl. Phys. Lett., **52**, 1877, (1988).
10) E. Calleja, A. Gomez, A. Criado, and E. Muñoz, Proc. **15th** Int. Conf. on Defects in Semiconductors, Budapest, Hungary, (1988).
11) T. Baba, M. Mizuta, T. Fujisawa, J. Yoshino, and H. Kukimoto, Jap. J. Appl. Phys., **28**, L891, (1989).
12) E. Calleja, A. Gomez, and E. Muñoz, Appl. Phys. Lett., **52**, 383, (1988).

III. MULTILEVEL STRUCTURE OF Si- AND Se- RELATED DX CENTERS IN HIGH Al CONTENT $Al_xGa_{1-x}As$ ALLOYS

III.1. INTRODUCTION

Since the first report on DX centers by Lang [1], the peculiar phenomenology of these centers has been increased by a number of properties that are not yet well understood. For instance, the dependence on alloy composition of both the thermal broadening of the deep level transient spectroscopy (DLTS) signals and the non- exponentiality of the isothermal capacitance transients, has been interpreted in terms of an alloy-broadening effect [2-4]. It has been generally assumed that this effect produces a spread of the thermal emission and capture energies, partly because this hypothesis allows a simple and effective analytical treatment for experimental data fitting [5,6]. However, there is no direct evidence of such a broadening of the thermal emission and capture energies.

On the other hand, the presence of shoulders and multiple peaks in DLTS signals, generated by electron thermal emission from DX centers, has been frequently found, and explained in various ways, including the existence of several types of DX centers. An early report on this subject is due to Lang [7], who attributed this effect to a shift in the thermal emission energy, due to the relative probabilities of particular Ga and Al arrangements around the defect (DX center). This idea was further developed by Omling [2] to explain the thermal widening of the DLTS signals, and the concept of alloy- broadening was established. More recently, Calleja et al. [8] have shown that a DLTS spectra fine structure can be observed, under adequate experimental conditions, being qualitatively explained in terms of and alloy- broadening effect affecting just the DX center capture cross section, σ^{∞}_{n}.

In this work we present a detailed study of the thermal emission processes. First, from Si- DX centers in GaAlAs layers, using both DLTS and isothermal emission transients. Trap filling times, sampling conditions, and the selfconsistency of isothermal emission transient components analysis

to generate DLTS spectra, that are later compared with the recorded ones, have been investigated. Second, a similar study has been made in Se -doped samples by using DLTS under hydrostatic pressure.

III.2. EXPERIMENTAL

--Si doped samples

P^+-GaAs / n- GaAlAs (30 %) heterojunctions for resolved DLTS measurements, and GaAs/ GaAlAs (35 %) modulation- doped field effect transistors (MODFET) for isothermal emission transients as well, as for DLTS spectra fittings, have been used in this work. Both sets of devices were Si- doped, with donor concentrations in the 10^{17} cm^{-3} range. Capacitance DLTS spectra were obtained, at constant reverse voltage, with a Boonton 72-BD bridge linked to a hardware DLTS system. An HP-4280 bridge, with an external pulse generator, was used for short filling pulses and small sampling times. MODFET's were also characterized by single shot isothermal voltage transients at constant capacitance.

--Se doped samples

MOVPE grown AlGaAs layers with 30%, 34%, 49%, and 77% Al content were used in this work. These samples were 1 μm thick and Se- doped in the 10^{18} cm^{-3} range. An undoped GaAs cap layer, 100A thick, was deposited to obtain better Ti/ Au Schottky diodes. The DLTS system has been described above, as well as the hydrostatic pressure set up.

III.3. RESULTS AND DISCUSSION

For a Si- doped GaAs/ GaAlAs (30%) heterojunction, the evolution of the DLTS spectra with experimental conditions is shown in figure 1. A dramatic change of the DLTS structure is observed when the charging time is reduced. Better resolved peaks are obtained for shorter sampling windows. As it was shown in a previous work, the activation energies corresponding to

the resolved peaks are the same, within the experimental error [8], being however their σ_n^{∞} values quite different (they are in a six orders of magnitude range).

In figure 2 we represent the Arrhenius plots corresponding to the thermal emission processes from a GaAs/ GaAlAs (35 %) Si- doped MODFET. In this case we have characterized the device by measuring both DLTS signals and isothermal voltage transients at constant capacitance. The parallel plots correspond to the fast, medium and slow parts of the transient, obtained by a three exponential function fit, taking special care to minimize errors [4]. Again, a single value for the activation energy is obtained, whereas a big spread for the thermal capture cross section, σ_n^{∞}, is found.

The same MODFET structure has been characterized by DLTS for a set of sampling times, and double peak structures are also obtained (Fig.3). The two peaks present are better resolved for small sampling window widths. Then, we have tried to compare these experimental DLTS signals with those, computer generated, from the above isothermal transient components analysis. As the number, and the relative weights, of the various contributions to the DLTS signal are not known, we have used the experimental values of the single activation energy and the various σ_n^{∞} values obtained from Fig.2. Thus, the selfconsistency of our model is checked, since we are dealing with the same sample. The results are shown in Fig.3. As it can be seen, the shape of the experimental and simulated signals is very similar, and they follow the same pattern with sampling times. The differences in their temperature width and position can be understood if we consider that a small change in the σ^{∞}_n values shifts the temperature at which the DLTS signal appears. On the other hand, we have used only three values of σ^{∞}_n with a separation and relative weight that might be unexact. Until some physical guidelines are drawn for the electron emission components selection, any overestimation of the range of σ^{∞}_n values used would imply that a more broaden and shifted DLTS spectrum is obtained.

Concerning the Se- doped AlGaAs samples, the structure of the DLTS spectra, at atmospheric pressure, for the various Al compositions is depicted in figure 4. For the same sampling conditions indicated in the figure insert, a double peak structure is only seen for x = 0.49. The

activation energies of the thermal electron emission in all measured samples are in the $E_e = 250 \pm 20$ meV range.

The evolution of the DLTS spectra with pressure for three Al compositions is shown in Fig. 5. A clear two-peak structure (P_1, P_2) is always detected at high pressures, corresponding to equivalent Al compositions in the 40 - 50%. range. A third, saturated peak (P_0), is barely seen at the low temperature side of the DLTS spectrum for the x = 0.34 sample. An important feature is that the temperature position of P_1 and P_2 moves towards higher temperatures with pressure, in contrast with the behavior observed in Si- doped samples.

The evolution with hydrostatic pressure of P_1 and P_2 heights, indicates that P_2 saturates first, and then P_1. P_2 is the dominant one at low pressures, while P_1 is clearly enhanced at high pressures. Electron thermal emission has been studied at various pressures, although single peak activation energies cannot be resolved in most of the cases. E_e is again in the 250 meV range, indicating that the emission activation energy of P_1 and P_2 is the same or very close.

Thermally activated electron capture experiments have been performed at atmospheric pressure. At high Al compositions the difficulty arises because of the interaction of the P_1 and P_2 peaks, and again an effective capture barrier energy (E_b) is determined. For 30%, 34%, 49%, and 77%, E_b energies are 170, 160, 190, and 240 meV respectively. The dependence of E_b on Al composition seems to follow an V- shaped profile, as it does in the case of Si- doped AlGaAs [11]. This behavior is shown in figure 6, where data from Si- DX centers is also plotted. In this figure, the experimental point corresponding to 43% is obtained from the 30% Al content sample under hydrostatic pressure (13 Kbar). Capture experiments under hydrostatic pressure may allow to differentiate between P_1 and P_2 capture abilities, and this point is a subject of further work.

The assignment of the various DLTS peaks for the Se- DX centers is difficult because the lack of data in dilute Se- doped alloys. On the basis of the probabilities for the different local environments with Al atoms as near neighbors, and from the results for Te- doped ordered alloys, we assign P_2 to the Se- DX configuration with two Al atoms, while P_1 will

correspond to a one Al atom local environment. This model agrees with previous data in Si and Te -doped AlGaAs, where a lower energy level corresponds to a higher number of Al atoms. Then, the lowest lying energy level should appear at the lowest pressure and also the intensity of the peak should saturate first. In a sequential way, they become closer (even cross it) to the Fermi level, and their intensity increase, until they saturate. Such behavior is observed for P_1 and P_2 peaks. In x = 0.30 and x = 0.34 a third peak seems to be present at temperatures around 110K, with a very small intensity, which is almost masked by P_1. This peak may correspond to Se- DX environments with no Al atoms as near neighbors (P_0). Such assignment is again in good agreement with those made in Te modulation- doped ordered alloys [9,10]. An important feature is that peaks P_1 and P_2 shift with the applied pressure, in a similar way as it is reported in Te-doped ordered alloys for donor environments with 2 and 3 Al atoms [9].

III.4. SUMMARY

We have characterized the electron thermal emission process from DX centers in Si- doped GaAlAs alloys, by DLTS and isothermal capacitance transients, under various filling and sampling conditions. Within the experimental error, a single value for the activation energy is obtained in samples that exhibit multiple emission constants (non- exponential behavior). However, the value of the thermal capture cross section spreads over several orders of magnitude. It is concluded that the alloy- broadening affects mainly the parameter σ_n^{∞}, rather than the thermal emission energy. That the alloy-broadening effect is responsible for the fine structure found in DLTS spectra is supported by the fact that no such a structure is found in samples with 85% Al content, where the alloy effect is quite small [4]. Simulated DLTS spectra, using the components from experimental isothermal transient analysis, agrees with the measured DLTS structure in the same sample, thus supporting the hypothesis of a spread of the σ^{∞}_n value.

Concerning Se- related DX's, for the various Al compositions and pressures, the emission activation energy seems to be rather constant $E_e = 250 \pm 20$ meV. Two peaks, tentatively assigned to configurations with 1 and 2 Al atoms, have been detected. The total energies corresponding to

these local environments seem to differ in their entropy term, that has been revealed to be pressure dependent for Se but not for Si.

Finally, as a qualitative argument, we want to point out that this idea of an alloy effect, that changes discretely the value of the entropy term (or the equivalent thermal parameter σ_n^{∞}), is consistent with the fact that very good exponential waveforms (constant capacitance) are obtained when the DX centers are optically activated. Indeed, if the electron activation energies (both thermal and optical ones) are not modified by the Al composition, but just the thermal capture cross section σ^{∞}_n, we should expect the optically activated capacitance transients being single exponential functions, independently of the Al mole fraction.

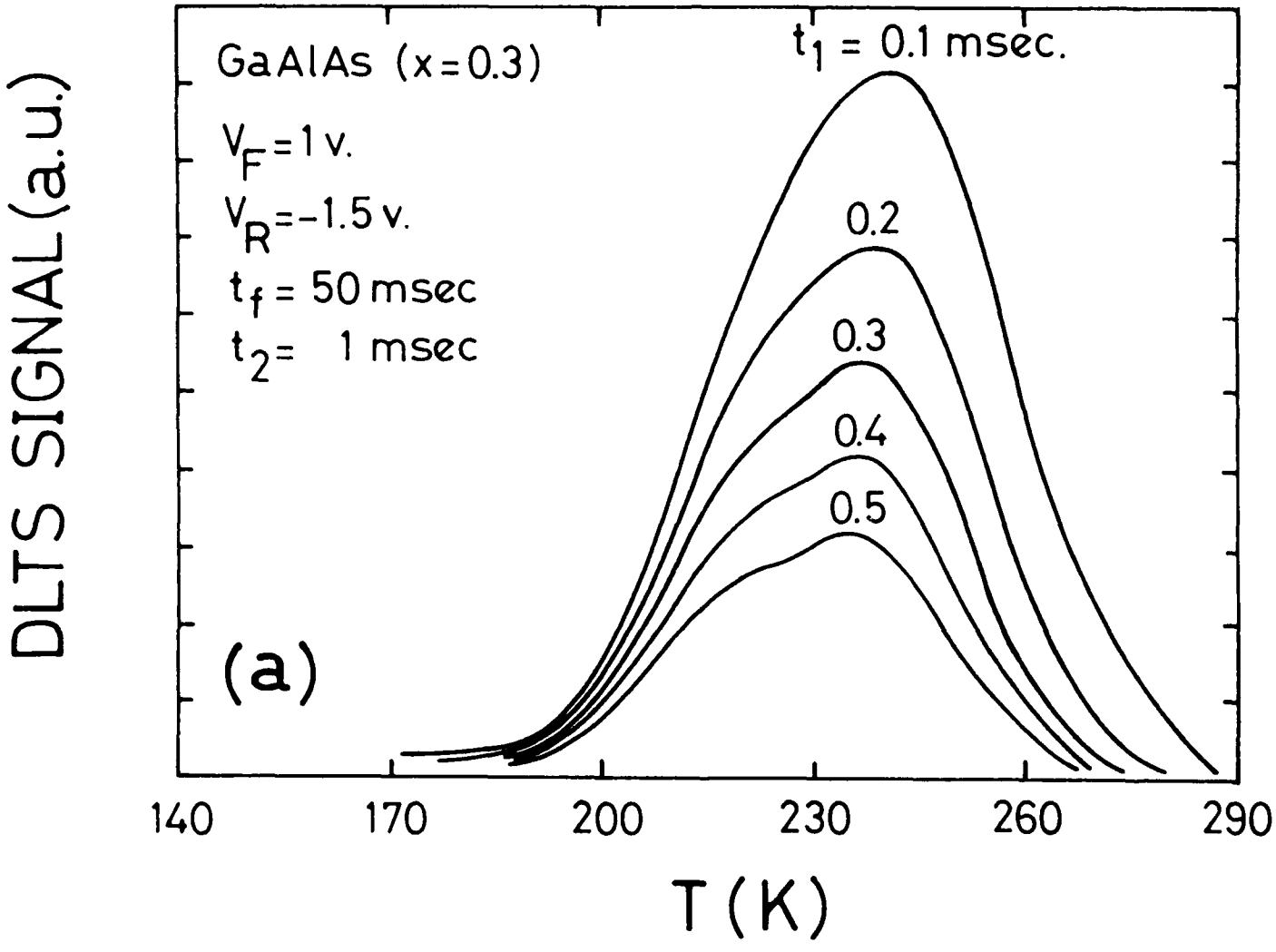

Fig. 1. DLTS spectra from DX centers in Si-doped GaAlAs with 30% Al. The evolution with the charging and sampling conditions is shown (Fig. 1.a, 1.b, 1.c, 1.d).

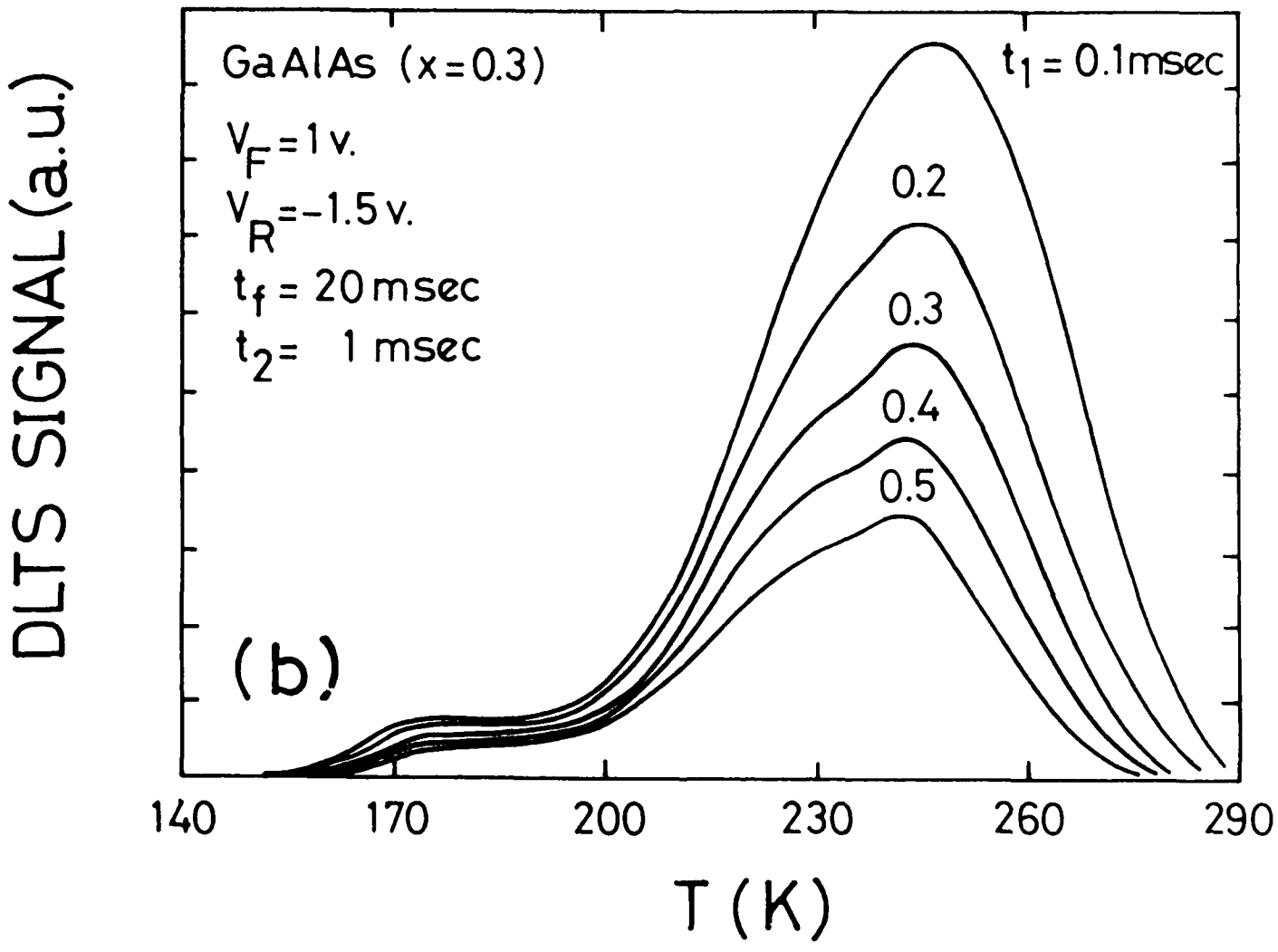
GaAlAs (x=0.3)
V_F=1 v.
V_R=-1.5 v.
t_f = 20 msec
t_2= 1 msec
t_1 = 0.1msec
0.2
0.3
0.4
0.5
(b)
DLTS SIGNAL (a.u.)
140
170
200
230
260
290
T (K)

Fig. 1.b

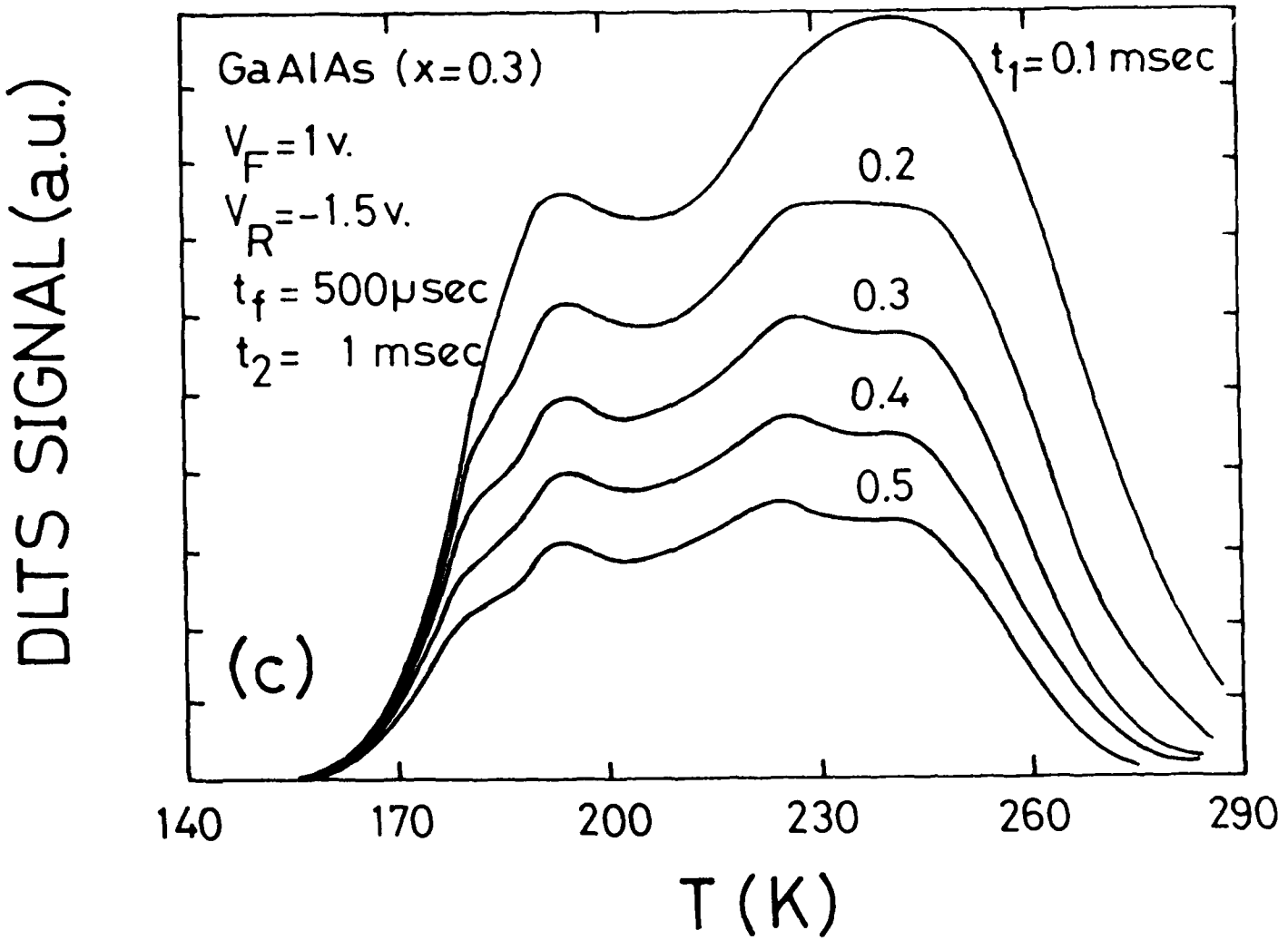
GaAlAs (x=0.3)
V_F=1v.
V_R=-1.5v.
t_f = 500μsec
t_2= 1 msec
t_1=0.1 msec
0.2
0.3
0.4
0.5
(c)
DLTS SIGNAL (a.u.)
140
170
200
230
260
290
T (K)

Fig. 1.c

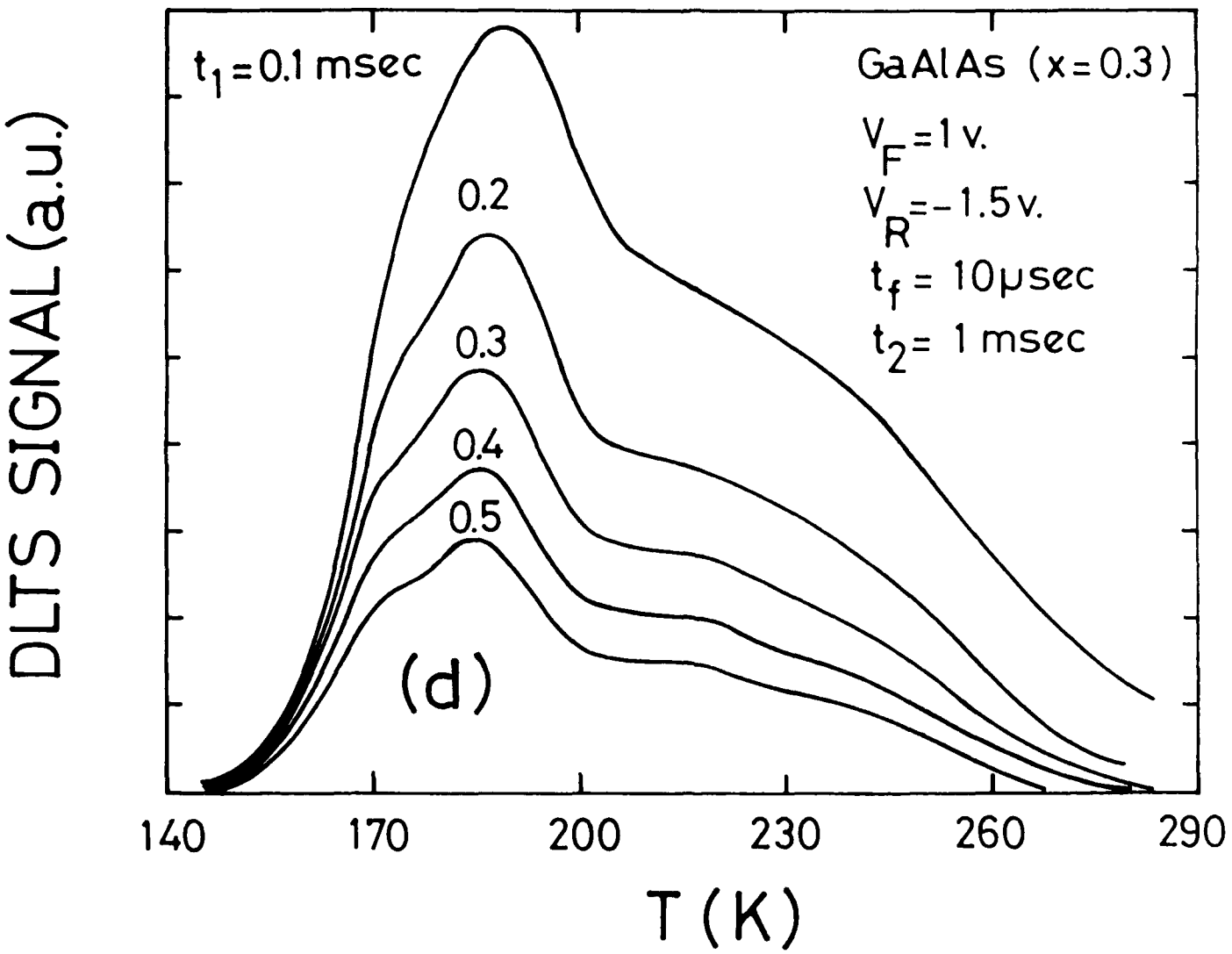
DLTS SIGNAL (a.u.)
t1 = 0.1 msec
GaAlAs (x = 0.3)
VF = 1 v.
VR = -1.5 v.
tf = 10 μsec
t2 = 1 msec
0.2
0.3
0.4
0.5
(d)
140
170
200
230
260
290
T (K)

Fig. 1.d

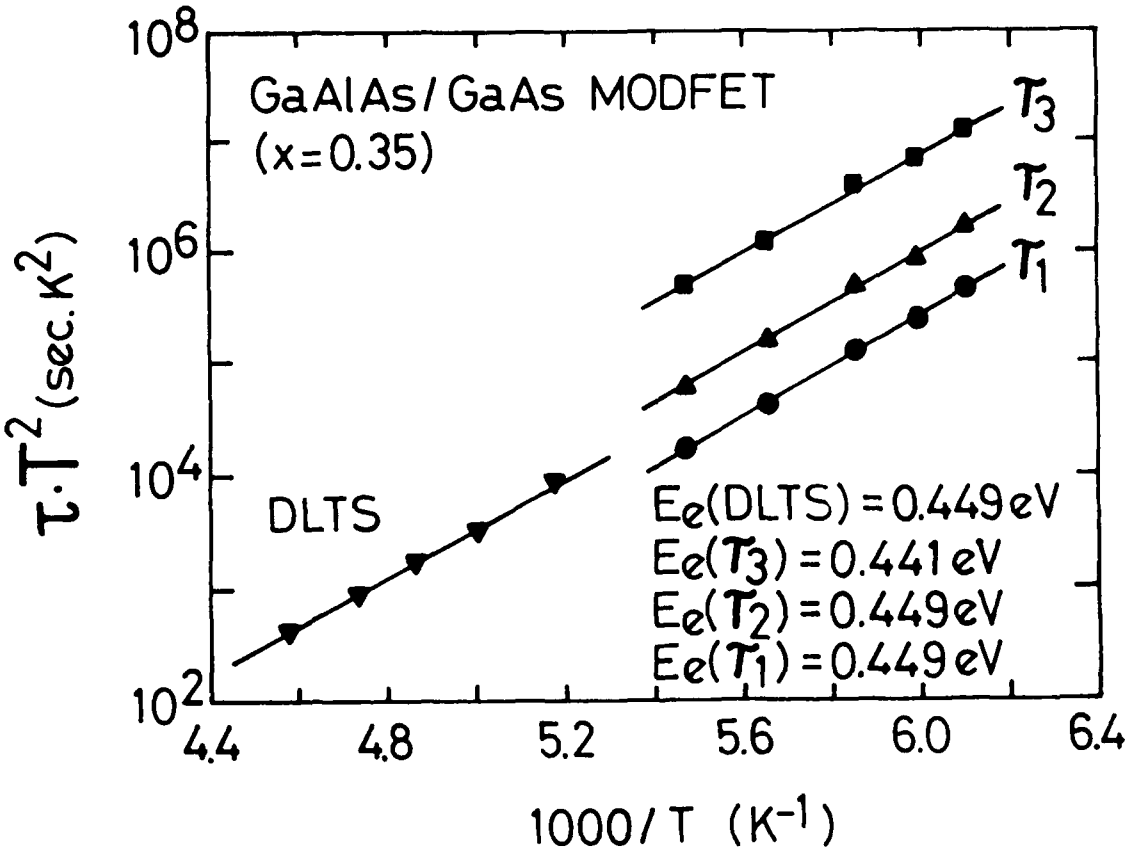

Fig. 2. Arrhenius plots obtained from DLTS and isothermal emission transients in Si-doped GaAlAs (35%).

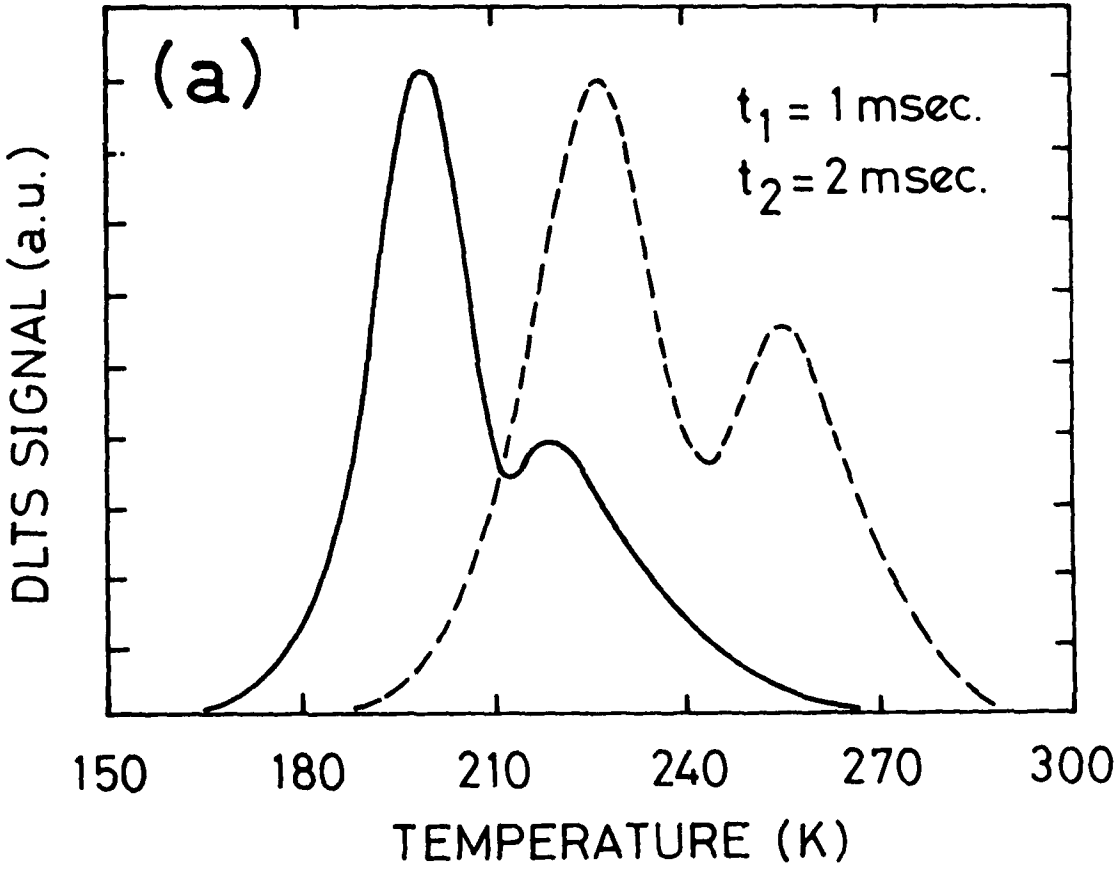

Fig. 3. Experimental (solid line) and simulated (dashed line) DLTS spectra in a GaAs/GaAlAs (35%) MODFET. Simulated signals are obtained using the experimental data from Figure 2. (Figs. 3.a, 3.b, 3.c).

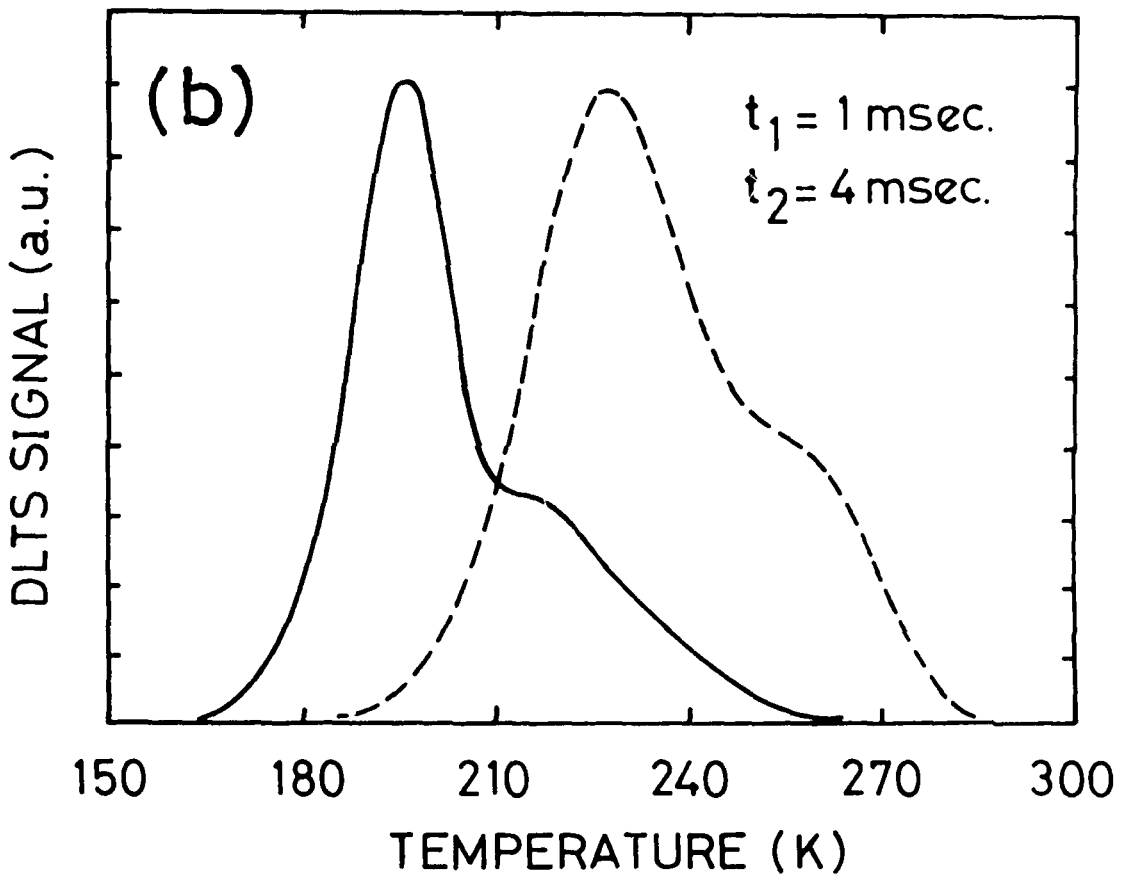
(b)
t_1 = 1 msec.
t_2 = 4 msec.
DLTS SIGNAL (a.u.)
150
180
210
240
270
300
TEMPERATURE (K)

Fig. 3. b

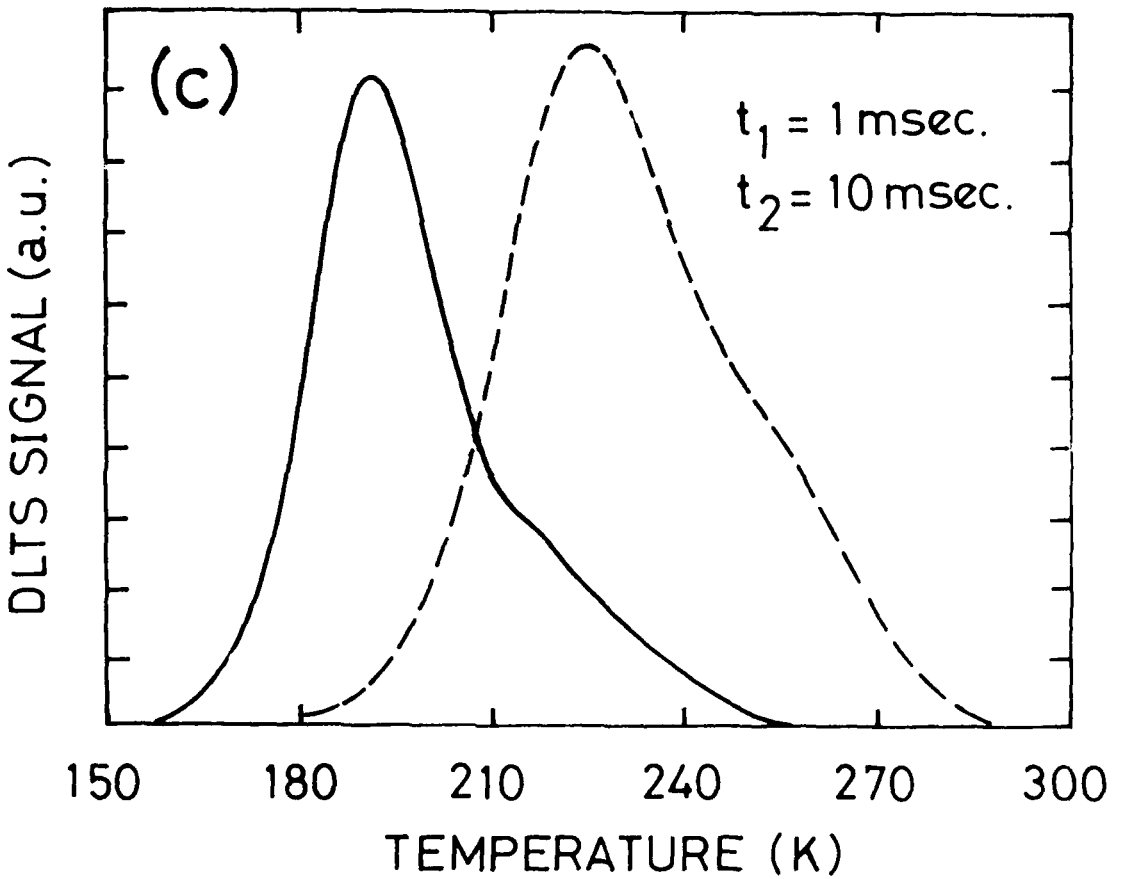
(c)
t_1 = 1 msec.
t_2 = 10 msec.
DLTS SIGNAL (a.u.)
150
180
210
240
270
300
TEMPERATURE (K)

Fig. 3. c

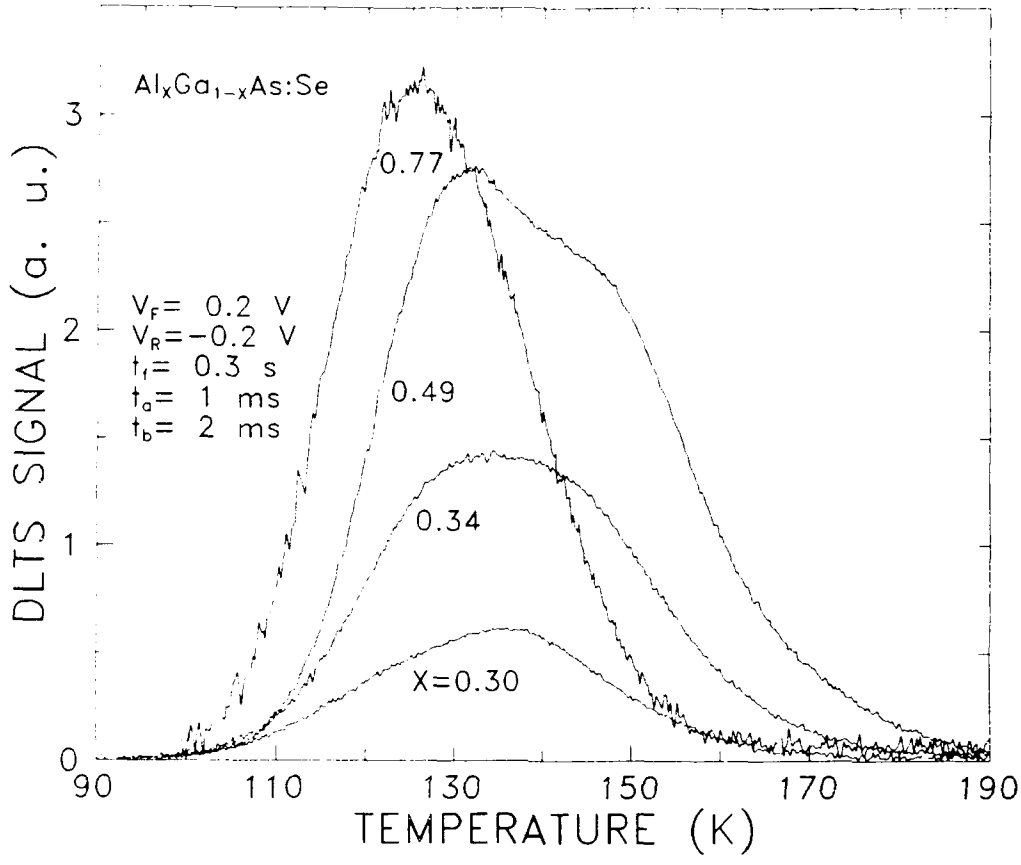

Figure 4. DLTS spectra from Se-doped AlGaAs of different Al content.

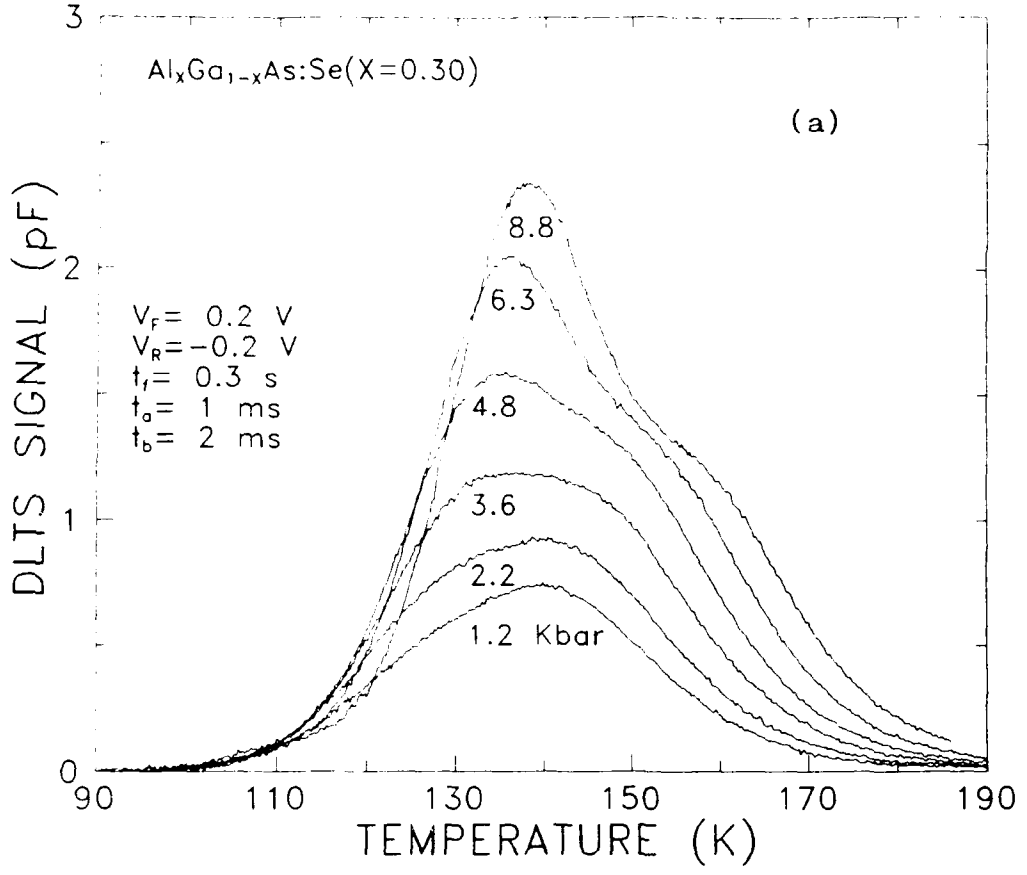

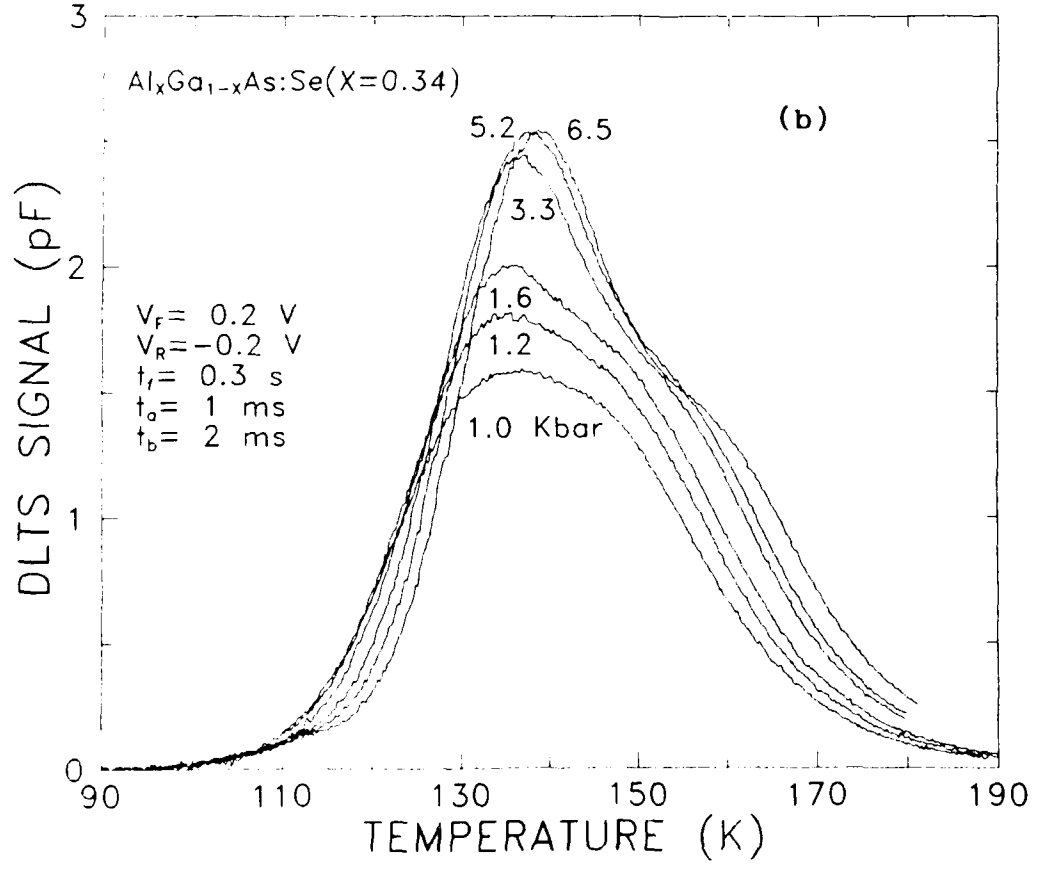

Figure 5. DLTS spectra as a function of hydrostatic pressure:
a) Se -doped AlGaAs (30%),.
b) Se- doped AlGaAs (34%).

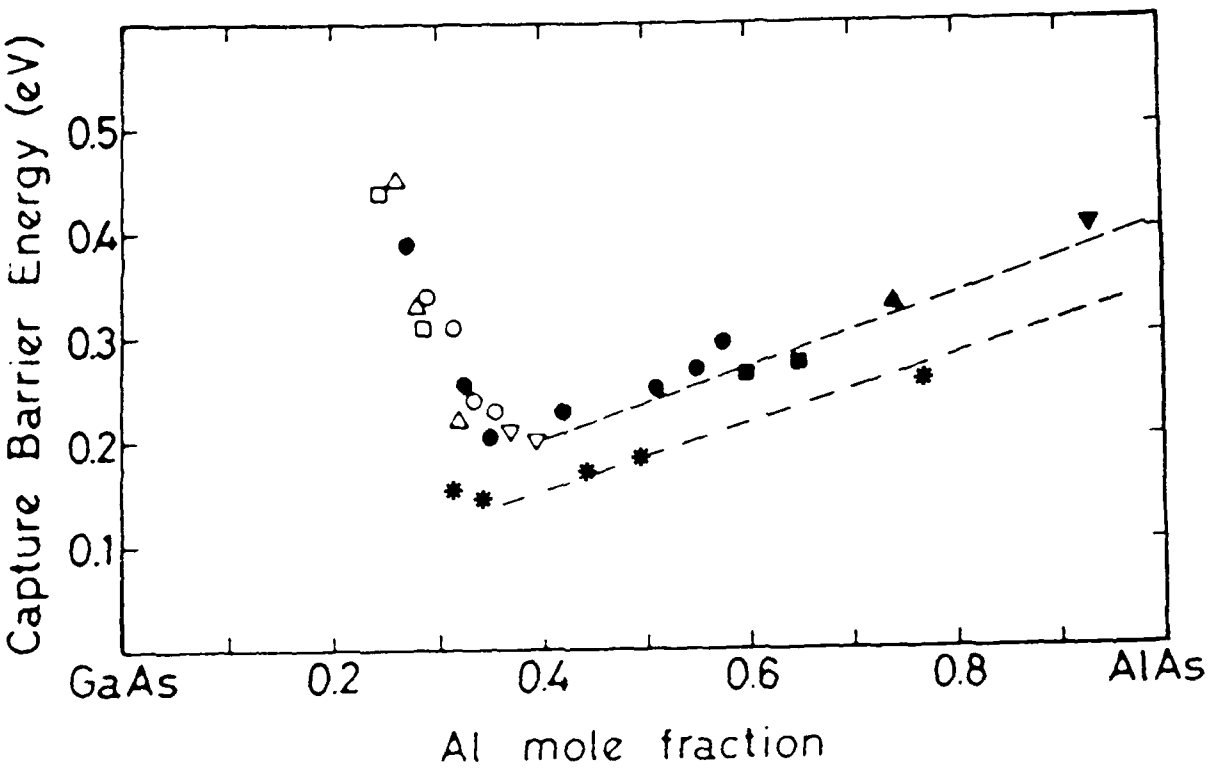

Figure 6.- Thermal capture barrier versus Al composition in Si:AlGaAs (upper curve) and Se:AlGaAs (lower curve). Dashed line represents the L-X energy separation versus Al composition. Si data is from reference (11).

REFERENCES

1. Lang, D.V. and Logan, R.A., Phys. Rev. Lett., 1977, **39**, 635.
2. Omling, P.,Samuelson, L., and Grimmeiss, H. G., J. Appl. Phys., 1983, **54**, 5117.
3. Yoshino, J., Tachikawa, M., Matsuda, Mizuta, M., and Kukimoto, H., Jap. J. Appl. Phys., 1984, **23**, L29.
4. Calleja, E., Mooney, P. M., Wright, S. L., and Heiblum, M., Appl. Phys. Lett., 1986, **49**, 657.
5. Caswell, N. S., Mooney, P. M., Wright, S. L., and Solomon, P.M., Appl. Phys. Lett., 1986, **48**, 1093.
6. Calleja, E., Gomez, A., and Munoz, E., Solid-State Electronics, 1986, **29**, 83.
7. Lang, D. V., Logan, R. A., and Jaros, M., Phys. Rev. B, 1979, **19**, 1015.
8. Calleja, E., Gomez, A., Munoz, E., and Camara, P.: Appl. Phys. Lett., 1988, **52**, 1877.
9. Baba, T., Mizuta, M., Fujisawa, T., Yoshino, J.,and Kukimoto, H., 1989, MRS Fall Meeting.
10. Mizuta, M., Baba, T., Fujisawa, T., Yoshino, J., and Kukimoto, H., Int. Phys. Conf. Ser. No. **106**, Chapter 5, pp. 321-326, 1990.
11. Calleja, E., Gomez, A., and Muñoz, E., Appl. Phys. Lett., **52**, 383, 1988.

IV. CAPACITANCE PROPERTIES OF N-TYPE $Al_xGa_{1-x}As$ ALLOYS

IV.1. INTRODUCTION

The electrical properties of n-type $Al_x Ga_{1-x} As$, for $x > 0.2$, are governed by deep donor states (formerly called DX centers) created by the isolated donor atoms. We have studied the capacitance properties of such layers for Si and Sn dopants. The meaning of the capacitance- voltage carrier profiling, and the capacitance dependence with temperature, have been considered. Techniques to determine the donor state energy position with respect to the Γ minimum are presented.

N- type $Al_x Ga_{1-x} As$ layers play an important role in a large family of, heterojunction- based, electronic and optoelectronic devices. The free electron concentration of such layers, for $x > 0.2$, is governed by deep donor states created by the isolated n- type dopant atoms. The detailed microscopic structure, and the optical and electrical properties of these donor states, are still under study [1-3]. Deep level transient spectroscopy (DLTS) allowed to identify the Si, Se, Te, Sn, etc. deep donors by means of the thermal activation energies of both electron emission and capture processes [3-5]. The question about to which conduction band minima the electrons are emitted from the deep states, has been initially answered by performing DLTS studies under hydrostatic pressure, indicating that the deep donor states behave as apparently bound to the L minima [3,6,7], although, as it is pointed out in **Section II**, recent measurements indicate that this link may be just a coincidence with no physical basis.

Because the electron capture is thermally activated, DLTS experiments do not give information about the absolute energy level position of such deep states. The important point of knowing the binding energy to the conduction band (CB) minima needs extra complementary measurements. Such information has been usually derived from Hall effect data, although uncertainties in a number of parameters, and the effects of other traps, limit in practice the accuracy of this method. An alternate source of information to be explored is the capacitance behavior of n-type $Al_x Ga_{1-x} As$ layers. In this context, a quasi static C-V technique has been

used by Oh et al. to determine the absolute energy position of Se deep states in $Al_x Ga_{1-x} As$ [8].

In this work we address the study of the thermal equilibrium capacitance of n-type AlGaAs layers doped with Si and Sn, mainly because Si and Sn show the highest and the lowest capture barrier energies (E_b). As an example, for x = 0.25, E_b is about 360 meV and 170 meV, for Si and Sn, respectively [4,5]. Our objectives are to establish the validity of the usual $1/C^2$ vs. voltage profiling technique, to study the behavior with temperature of such capacitance, and to present techniques to determine the binding energy of the deep donor states.

IV.2. EXPERIMENTAL AND RESULTS

A number of Schottky barriers on MBE grown AlGaAs:Si layers, and several sets of MOCVD and LPE grown AlGaAs p^+-n junctions, have been used in this study. Capacitance measurements have been made using a Boonton 72BD and an HP 4191A bridges. The basis for our study is that, for $0.2 < x < 0.4$ compositions, n- type non- degenerate layers are basically governed by a single deep donor, several tens of meV below the Γ minimum (depending on the Al mole fraction), and whose concentration is close to the donor doping density (N_d).

Let us first consider the small signal capacitance of a Schottky barrier on an n-type layer, governed by a shallow donor of concentration N_d. It is modeled as the reaction of mobile electrons at the end of a space charge region (SCR) of $\rho(z) = N_d^+ \cong N_d$ net charge density, and width W_1 (defined by the 50% N_d^+ point). In the quasi neutral region, the ionization factor is very high ($I \cong 1$), the free electron concentration is $n_o = I \times N_d$, and it decreases to practically zero as we approach the SCR edge. The condition of $n = 0.5\ n_o$ occurs at a distance W_2 from the metal-semiconductor barrier, and we will label this distance as the carrier depleted region width (CDR). For a shallow level, edges W_1 and W_2 practically coincide, $W_1 = W_2$, determining the width of the space charge region. This is the usual full depletion approximation, $W_1 = W_2 >> L_D$ (Debye extrinsic length). A detailed computer analysis indicates that, as I decreases below 0.5, W_2

starts to be clearly greater than W_1, being $W_2 - W_1 \cong L_D$ for $I < 0.1$.

Figure 1 reflects the evolution of the depletion region with ionization energy. Figure 1.a shows the normalized (to N_d) net charge density and free electron concentration for a 0.3 μm width, n- type, GaAs region (donor depth 6 meV), with a donor concentration $N_d = 10^{17}cm^{-3}$. N_d is the normalizing parameter, temperature is 200 K, and there is an ideal ohmic contact at x = 0 and a metallisation at x = 0.3 μm. The Schottky barrier height is 1 eV. In spite of the incomplete ionization of the donors in the quasi- neutral region ($I \cong 61$ %), still we have $W_1 \cong W_2$. This is the typical behavior of shallow donors.

If we replace the GaAs material by $Al_{0.3}Ga_{0.7}As$, where the donor depth is about 120 meV, maintaining the same barrier height and temperature, we obtain the result shown in figure 1.b. Now the normalizing parameters are N_d for the net charge density and n_o for the free electron concentration, since the low I factor ($I = 3.5$ %) present in this case makes difficult to see where the $n = 0.5\ n_o$ point (W_2 edge) is. As we can see in figure 1.b, only at the ideal ohmic contact the electron concentration corresponds to the equilibrium neutral region one, *being nearly all the n-type region a non neutral one* as the continuosly varying free electron concentration suggests.

Let us now consider the study of the depletion capacitance in an n- type region governed by a deep level (figure 2). In our case the deep donor is just due to the dopant atom itself. Under this assumption, the donors are partially ionized at room temperature, I decreases markedly as temperature lowers, L_D increases, and the edges of SCR and CDR regions (W_1 and W_2) are far apart. A computer simulation example is shown in figure 2.c, indicating that the free electron concentration near W_1 is much lower than $n_o = I \times N_d$, it increases over a distance of about three L_D and reaches the $n \cong n_o$ condition at the ideal ohmic contact in real finite samples. Then, at these temperatures where $I < 0.1$, the presence of the deep donor implies that $W_2 - W_1 \cong W_1 \cong L_D$, and that the so called quasi- neutral region has now a net positive charge, showing a clear non- constant free electron profile over a $3L_D$ distance.

To make the problem analytically tractable at temperatures when I is moderate, we will use the rectangular approximations indicated in figure

starts to be clearly greater than W_1, being $W_2 - W_1 \cong L_D$ for $I < 0.1$.

Figure 1 reflects the evolution of the depletion region with ionization energy. Figure 1.a shows the normalized (to N_d) net charge density and free electron concentration for a 0.3 μm width, n- type, GaAs region (donor depth 6 meV), with a donor concentration $N_d = 10^{17}cm^{-3}$. N_d is the normalizing parameter, temperature is 200 K, and there is an ideal ohmic contact at x = 0 and a metallisation at x = 0.3 μm. The Schottky barrier height is 1 eV. In spite of the incomplete ionization of the donors in the quasi- neutral region ($I \cong 61$ %), still we have $W_1 \cong W_2$. This is the typical behavior of shallow donors.

If we replace the GaAs material by $Al_{0.3}Ga_{0.7}As$, where the donor depth is about 120 meV, maintaining the same barrier height and temperature, we obtain the result shown in figure 1.b. Now the normalizing parameters are N_d for the net charge density and n_o for the free electron concentration, since the low I factor ($I = 3.5$ %) present in this case makes difficult to see where the $n = 0.5\ n_o$ point (W_2 edge) is. As we can see in figure 1.b, only at the ideal ohmic contact the electron concentration corresponds to the equilibrium neutral region one, *being nearly all the n-type region a non neutral one* as the continuosly varying free electron concentration suggests.

Let us now consider the study of the depletion capacitance in an n- type region governed by a deep level (figure 2). In our case the deep donor is just due to the dopant atom itself. Under this assumption, the donors are partially ionized at room temperature, I decreases markedly as temperature lowers, L_D increases, and the edges of SCR and CDR regions (W_1 and W_2) are far apart. A computer simulation example is shown in figure 2.c, indicating that the free electron concentration near W_1 is much lower than $n_o = I \times N_d$, it increases over a distance of about three L_D and reaches the $n \cong n_o$ condition at the ideal ohmic contact in real finite samples. Then, at these temperatures where $I < 0.1$, the presence of the deep donor implies that $W_2 - W_1 \cong W_1 \cong L_D$, and that the so called quasi- neutral region has now a net positive charge, showing a clear non- constant free electron profile over a $3L_D$ distance.

To make the problem analytically tractable at temperatures when I is moderate, we will use the rectangular approximations indicated in figure

2.b. Then, the charge density between W_1 and W_2 is taken as due to the depletion of I x N_d electrons. The capacitance bridge ac signal, f_s, will try to modulate both the W_1 and W_2 edges, and if the electron emission and capture rates (f_t) from the donor level are high enough to follow f_s, the small signal capacitance, per unit area, $C(V_r)$, will be determined by the reacting charge contributions from W_1 and W_2. Clearly W_1 dominates, and we obtain:

$$\frac{1}{C^2(V_r)} = \frac{2}{q \times N_d \times \varepsilon}\left[V_r + \phi - \frac{E_t}{q}\left(1 - I\right)\right] \qquad (1)$$

This equation indicates that the $1/C^2$- V plot will tend to give information about N_d, although the free electron concentration in the quasi- neutral region may be much smaller (I<<1). This fact explains why the room temperature $1/C^2$-V profiling is not adequate to obtain *n* in AlGaAs layers. For Al compositions greater than 20%, such a profile gives $N_d^+ = N_d$ instead of n, as it has been reflected in significant discrepancies between Hall effect and C-V measurements in AlGaAs [9].

As temperature lowers, the ionization factor of the deep donors decreases, and both $\rho(z)$ and *n* profiles are those indicated in figure 2.c. For a given bias, the total barrier height, U, will be nearly constant because the displacements of the Fermi level are small (meV) as compared to U, and the W_1 edge remains nearly fixed for such temperature range. The emission- capture processes become slower as temperature diminishes, the W_2/W_1 ratio increases, and the role of the charges reacting to f_s at the W_1 edge become even smaller. Therefore, C(T) decreases as we cool down, becoming only determined by the CDR region reacting at the W_2 edge. Then, if the $f_s >> f_t$ condition is met, and if we make a C-V scanning fast enough not to allow the W_1 edge to adjust itself as the reverse voltage is varied, only then the measured C^{-2}-V profile will give $N^+ \cong I \times N_d << N_d$, that we approximate as the free electron concentration, n, at this temperature. From these results, we propose now two techniques to determine the deep level binding energy.

First, once T is low enough to make $f_s >> f_t$, only the free electrons at the W_2 edge will respond to the f_s signal, and under this conditions C-T measurements will give information about $W_2(T)$. We may remind that at these low temperatures ($E_d >> kT$), and at thermal equilibrium, for our simple model,

$$n(T) = F \times N_d \cong \frac{N_d}{g} \times exp\left[\frac{-E_t}{kT}\right] \qquad (2)$$

and

$$E_t = \frac{E_d}{2} + \frac{kT}{2} \times ln\left[\frac{N_d}{g \times N_c(T)}\right] \qquad (3)$$

In our samples, and for the characterization temperature range, $N_c(T)$ is just the Γ minimum density of states, and non degenerate statistics have been used because the low electron gas concentration present. If $E_t << U$ and $F << 1$ (figure 2.b), we obtain

$$W_2(T) = W_1 + L_D(T) \cong \sqrt{\frac{\varepsilon}{q^2 \times N_d}}\left[\sqrt{2\,U} + \sqrt{g\,k\,T}\,exp\left(\frac{E_t}{2\,k\,T}\right)\right] \qquad (4)$$

Then, cooling from high temperatures, for the range where the $f_s >> f_t$ condition is met, only the W_2 edge will react to the f_s signal, and then $C(T) = \varepsilon / W_2(T)$. Defining $C_1 = \varepsilon / W_1$, we obtain

$$\frac{W_2(T) - W_1}{W_1} = \frac{C_1 - C(T)}{C(T)} = \sqrt{\frac{g\,k\,T}{2\,U}} \times exp\left(\frac{E_t}{2\,k\,T}\right) \qquad (5)$$

and this expression summarizes the first, **static**, proposed technique to obtain E_t and E_d from C (T) measurements. In practical situations, the n- type layer must be thicker than $W_1 + L_D(T)$, and the bridge signal amplitude much smaller than $V_L = E_t/q$. As an example, for a 2×10^{17} cm^{-3} Si doped $Al_{0.32}Ga_{0.68}As$ layer, $L_D(150K) \cong 1.2 \times 10^{-5}$ cm, and $L_D(130K) \cong$

$1.7x10^{-5}$cm. We can also use a second, **quasi- static**, method to determine directly the free electron concentration in the quasi neutral region. Once we are in the low temperature region, ($f_s >> f_t$), under thermal equilibrium at T_b and zero bias, if we obtain the C-V data very fast (W_1 does not change), going towards reverse bias, the $1/C^2$-V_r plot allows to obtain $n(T_b)$, and, using equations 2 and 3, E_d can be deduced.

We now present some experimental results in Si (x = 0.26) and Sn doped (x=0.25) (p^+)GaAs/ (n)AlGaAs heterojunctions. For Si, both methods are easy to apply because its large emission and capture barriers make f_t low, but, due to this fact, C(T) measurements have to be taken after assuring that thermal equilibrium has been reached. Figure 3 shows, for both dopants, the dependence of above junction capacitances with temperature.

For Si, detailed C-T data obtained for a measuring frequency of 4 MHz are shown in figure 4.a. Using these data we plot in figure 4.b the $Ln(C_1 / C(T)-1)$ versus 1000/ T (see equation 5) and we find a linear region corresponding to the structure reacting only at the W_2 edge. This condition is better fulfilled at higher measuring frequencies (a more clear linear region is obtained). By applying equations 5 and 3 to the C(T) data just before the plateau, and taking g = 2, and activation energy E_d (x=0.26) = 80 meV is obtained. Also for the same sample, the quasi- static method gives E_d = 70 meV (T = 130K). For Sn, E_d(x = 0.25) = 70 meV has been estimated at T = 70K. These thermal activation energies are relative to the lowest CB minimum, are about 30 - 40 meV larger than the reported apparent Hall effect activation energies, and closer to DLTS estimations assuming that the deep donor is linked to the L minima [1,2,4,5]. This result needs further study, but in this Al composition range E_d is a very steep function of the Al composition, and then prone to an uncertainty range. A comparative analysis of both methods is also needed. For the objectives of this work, we do not want to discuss here the appropriate g value to take. We have used g = 2 as an example, although depending on the real nature of these deep donors, the right degeneracy factor has to be considered.

IV. DISCUSSION

The low temperature C-T plateaus present in figure 3 may have various physical origins. When their value depends on the cooling rate, it indicates a capture barrier limiting mechanism, reflecting that the electrons need to surmount an energy barrier, E_b, to be trapped by the deep donors (persistent photoconductivity effect). To dbe detected, thick samples ($>>L_D$), depending on the Al composition, are required, and this is nearly found in the 26% AlGaAs: Si sample. In other cases, while cooling, the W_2 edge may reach the n^+ substrate, thus, determining the capacitance plateau (lowest C value). Such is the case for the 25% AlGaAs: Sn sample. This size effect is also present in the 33% AlGaAs: Si Schottky barrier, where the CDR reaches the n^+ substrate even at moderate temperatures, causing the very steep capacitance decrease indicated in figure 2.

As a conclusion, an analysis of the thermal equilibrium capacitance of a semiconductor layer governed by a single deep level has been presented and applied to n- AlGaAs. The experimental conditions to extract information from the C(T) and C(V) measurements have been deduced. Two techniques to determine the deep level absolute energy position have been indicated, and used to estimate the binding energy of Si and Sn deep states in AlGaAs with $x \cong 0.25$ compositions. Such study can also be applied to the analysis of deep donors in GaAsPSb, InGaAlP and InGaPSb, alloys, that have shown similar electronic properties.

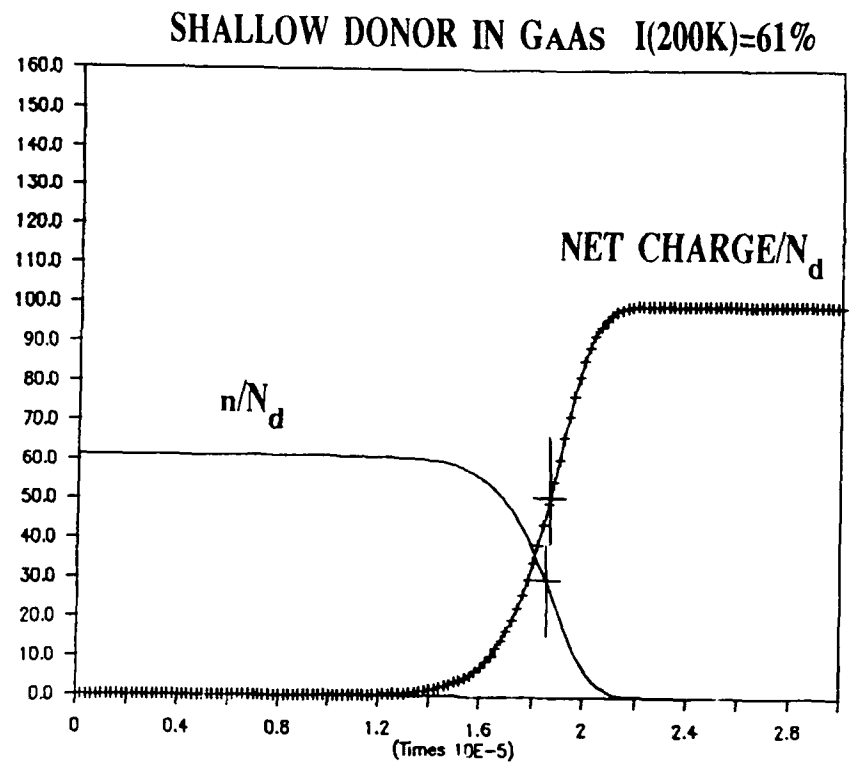

Fig. 1.a. Normalized net charge density and free electron concentration for a Schottky barrier on a 0.3 microns thick, n-type GaAs layer. T=200 K.

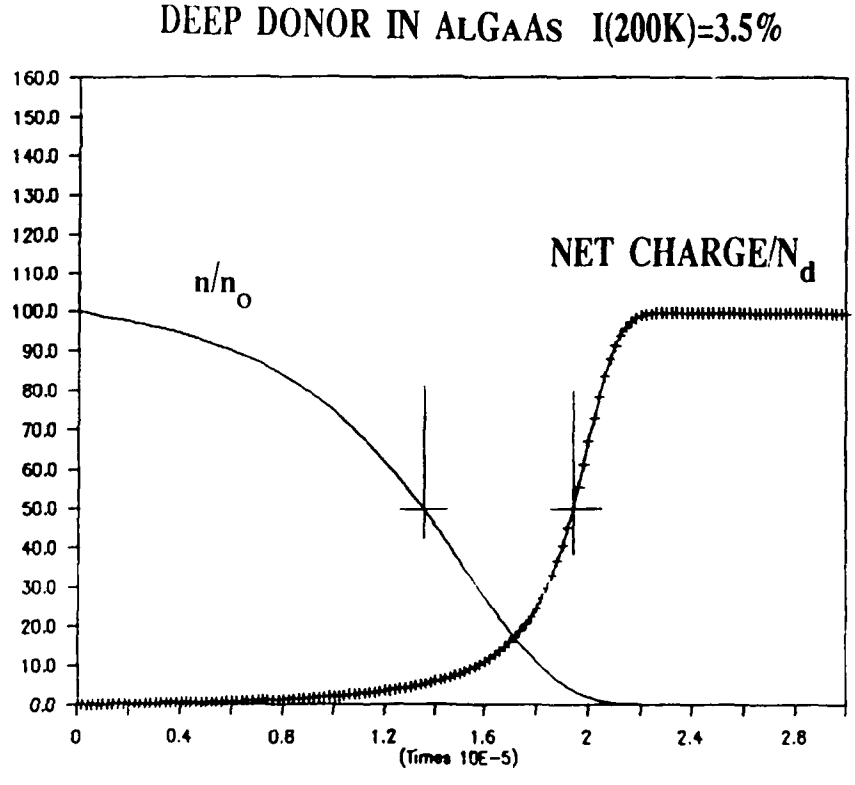

Fig. 1.b. Normalized net charge density (to N_d) and free electron concentration (to n_o) for a Schottky barrier on a 0.3 microns thick, n-type $Al_{0.3}Ga_{0.7}As$ layer. T=200 K.

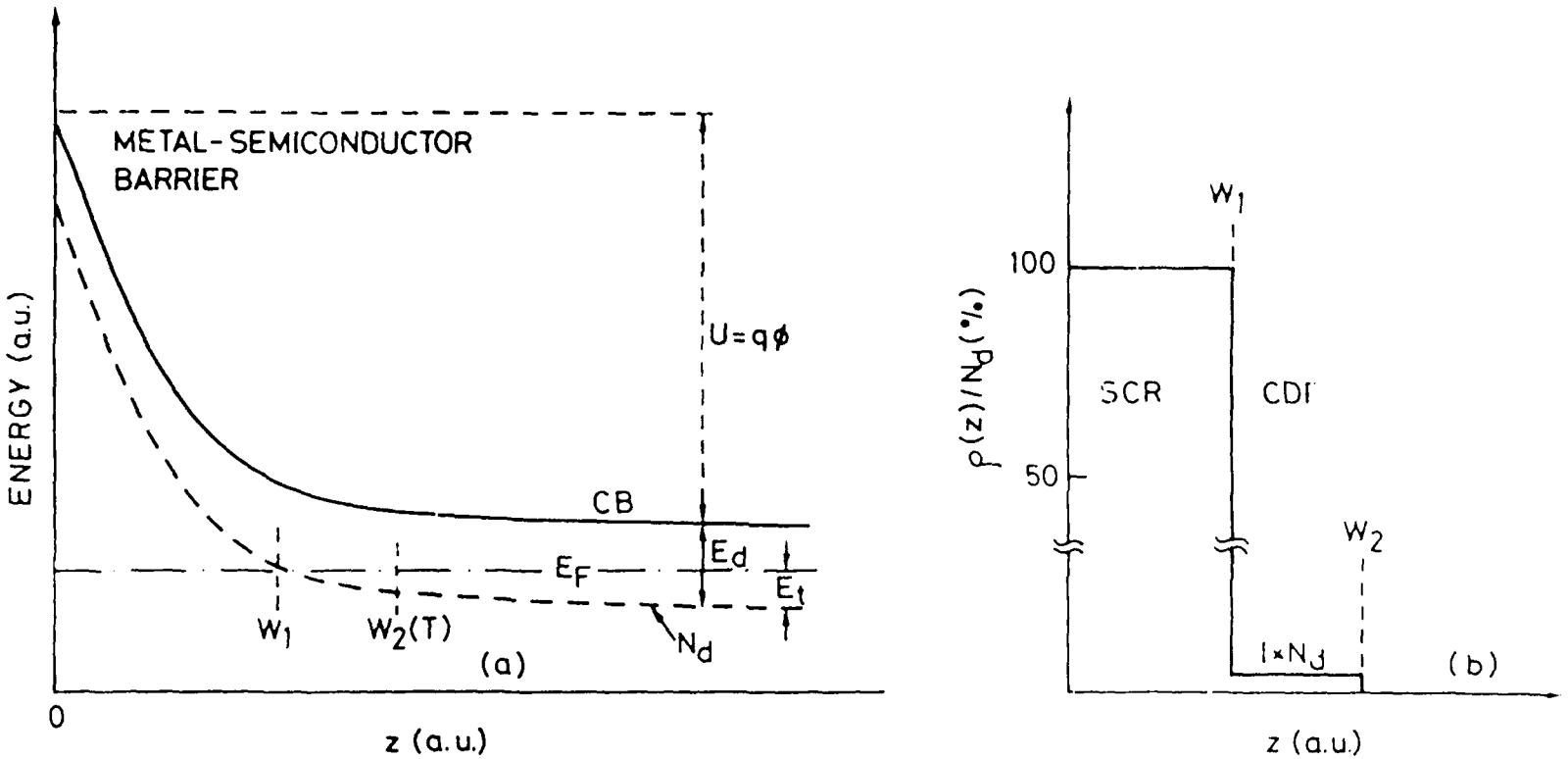

Fig. 2 . a. Band energy scheme in a metal-AlGaAs Schottky barrier governed by a deep donor.

b. Rectangular approximations of the SCR and CDR regions.

c. Computer simulation of free electron and net fixed charge concentrations. Densities are normalized to N_d and n_o.

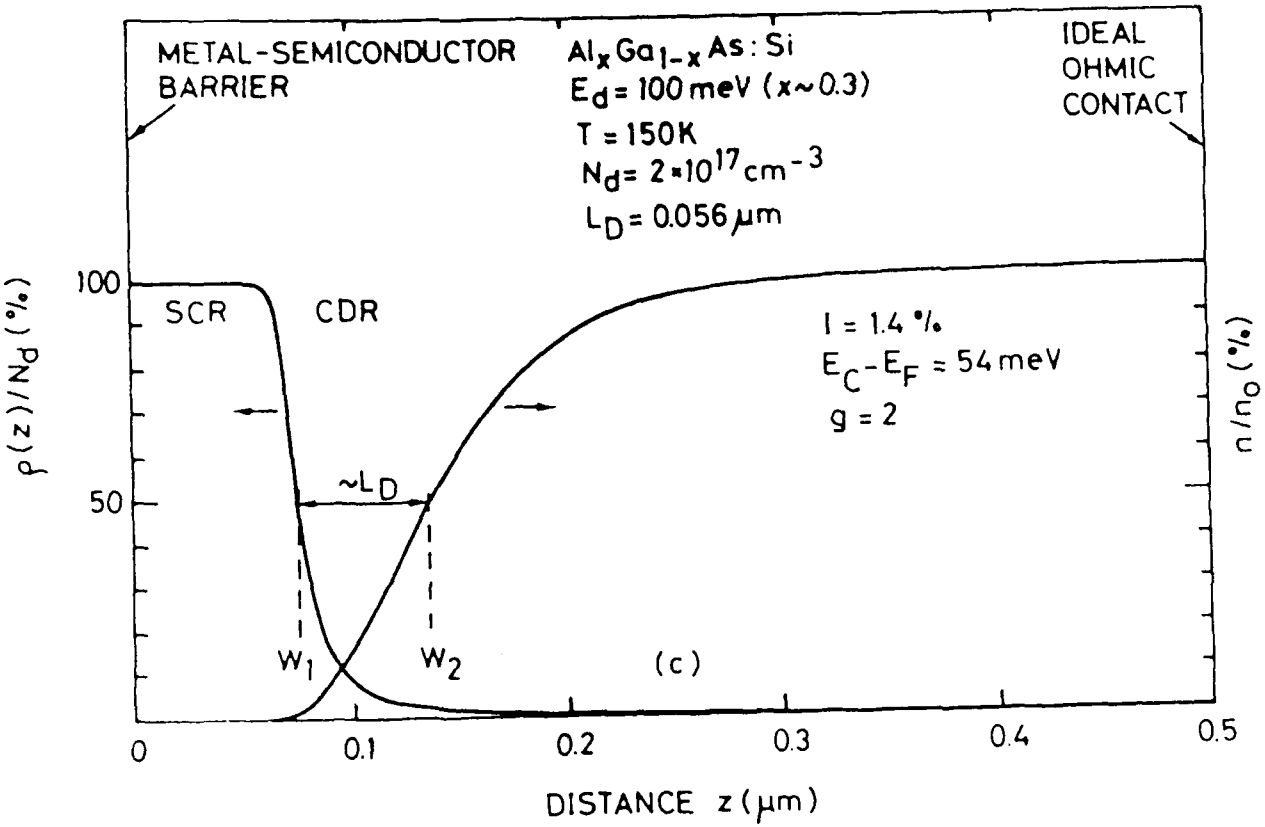
METAL-SEMICONDUCTOR BARRIER
$Al_xGa_{1-x}As$: Si
E_d = 100 meV (x~0.3)
T = 150K
$N_d = 2 \times 10^{17} cm^{-3}$
L_D = 0.056 μm
IDEAL OHMIC CONTACT
100
50
SCR
CDR
~L_D
W_1
W_2
(c)
I = 1.4 %
$E_C - E_F$ = 54 meV
g = 2
$\rho(z)/N_d$ (%)
n/n_o (%)
0
0.1
0.2
0.3
0.4
0.5
DISTANCE z (μm)

Fig. 2. c

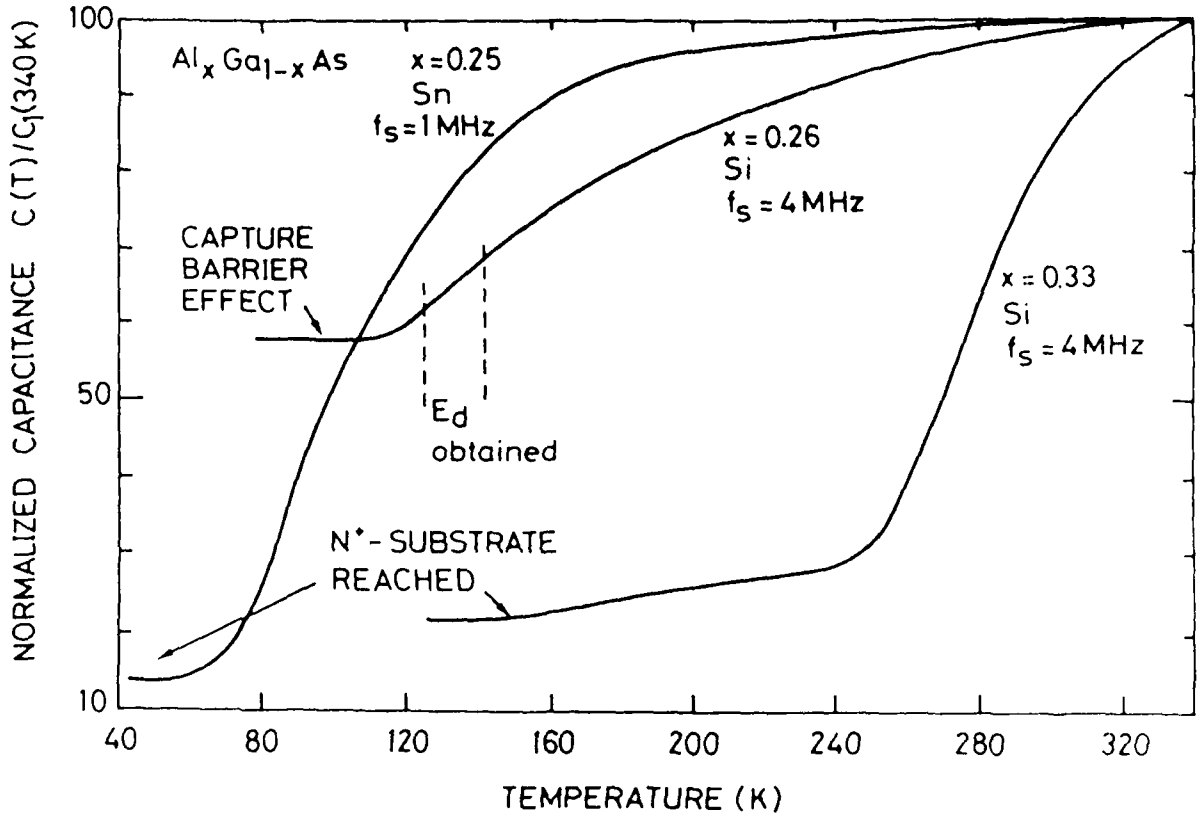

Fig. 3. Normalized depletion capacitance dependence on temperature for a set of Si and Sn doped AlGaAs samples. For the Si doped x=0.26 sample, E_d is determined in the temperature range indicated, and its capacitance shows a capture barier-induced plateau. In the thinner x=0.33 sample, at T=150K, W_2 reaches the n^+ substrate ohmic contact, and at higher temperatures both the W_1 and W_2 edges react to the bridge signal, and n cannot be determined. Concerning Sn, E_d has been estimated, but, because its very low capture barrier energy, the SCR meets the n^+ substrate before the capture-limited regime is achieved.

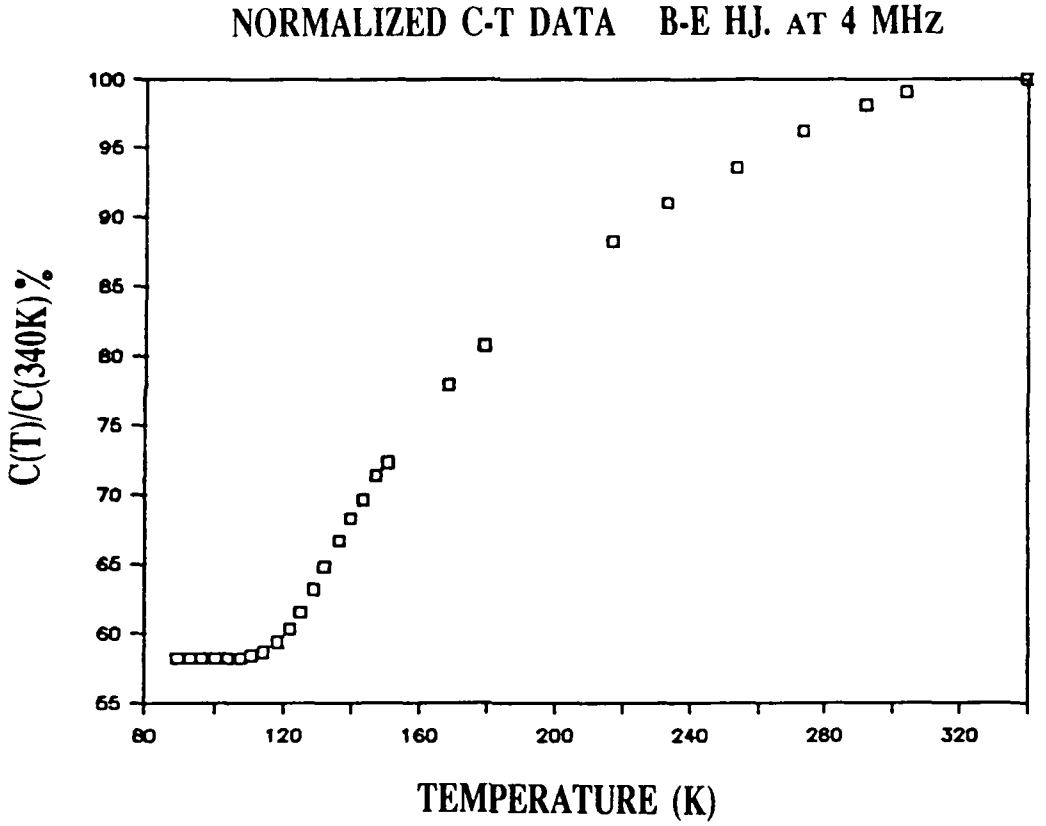

Fig. 4.a. C-T data measured at a small signal frequency of 4 MHz. Data are taken after long waiting times specially for T<160 K, to assure that thermal equilibrium is reached.

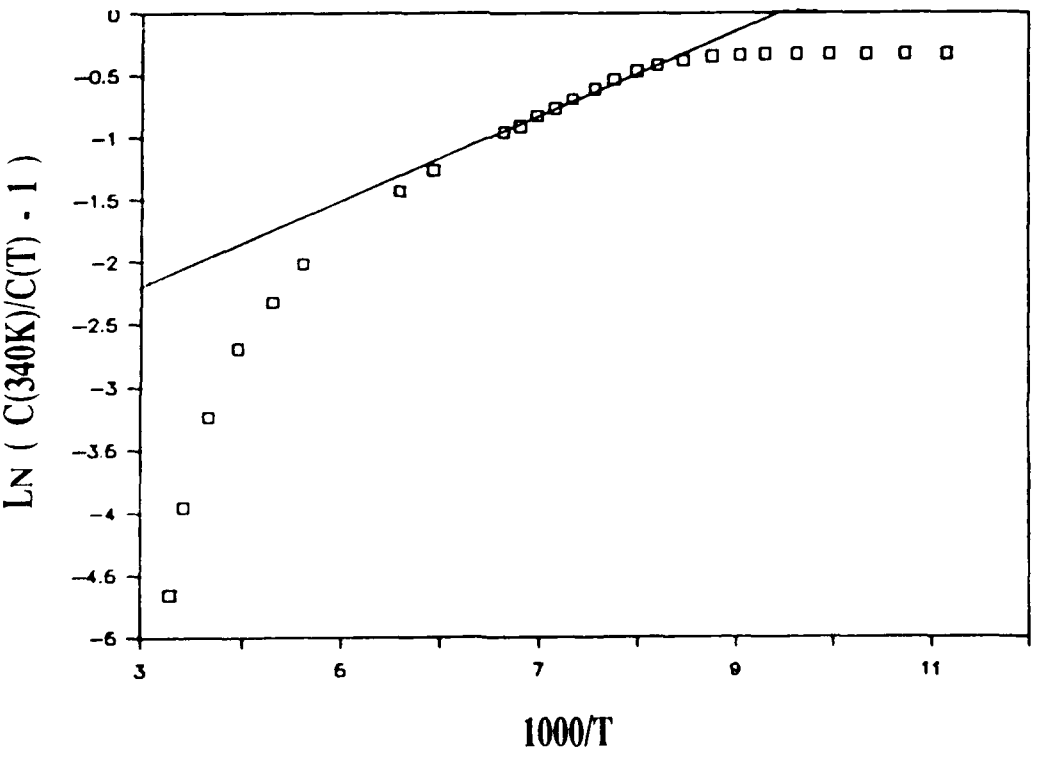

Fig. 4.b. Arrhenius plot of equation 5 using the C-T data shown in Figure 4.a to obtain E_d. C1=C(340K).

REFERENCES

1. D. V. Lang, in *Deep Centers in Semiconductors,* ed. by S.T. Pantelides, (Gordon & Breach, New York, 1986), pp. 489-539.
2. P.M. Mooney, J. Appl. Phys., **67**, R1, (1990).
3. M. Mizuta, M. Tachikawa, H. Kukimoto, and S. Minomura, Jpn. J. Appl. Phys., **24**, L143, (1985).
4. N. Lifshitz, A. Jayaraman, R.A. Logan, and H.C. Card, Phys. Rev. **B21**, 670, (1980).
5. N. Chand, T. Henderson, J. Klem, W.T. Masselink, R. Fisher, Y.C. Chang, and H. Morkoç, Phys. Rev. **B30**, 4481, (1984).
6. E. Calleja, P.M. Mooney, S.L. Wright, and M. Heiblum, Appl. Phys. Lett., **49**, 657, (1986).
7. E. Calleja, A. Gomez, and E. Muñoz, Appl. Phys. Lett., **52**, 383, (1988).
8. E.G. Oh, M.C. Hanna, Z.H. Lu, D.M. Szmyd, and A. Majerfeld, Electronic Materials Conf., Boulder, USA, 1980.
9. T.F. Kuech, E. Veuhoff, and B.S. Meyerson, J. Crystal Growth, **68**, 48, (1984).

V. ELECTRON CAPTURE KINETICS IN n-TYPE $Al_xGa_{1-x}As$ ALLOYS

V.1. INTRODUCTION

For $x > 0.2$, the electrical properties of n-type $Al_xGa_{1-x}As$, $GaAs_xP_{1-x}$ and related III-V alloys, are governed by deep donor states, formerly called DX centers. These deep donors are due to the behavior of the isolated dopant atoms, and they control the layer free electron concentration. Since the work of Lang and co- workers, it was shown that the electron capture process was temperature dependent, and it was modeled by a capture thermal activation energy (E_b) [1,2].

Electron capture and emission from the deep donors has been studied, basically, by transient capacitance techniques, being deep level transient spectroscopy (DLTS) a very useful experimental tool. Then, the electron emission and capture thermal activation energies (E_e and E_b, respectively) are determined from the evolution with temperature of space charge capacitance changes, due to the emission of electrons from the deep donors, and to their capture after filling pulses.

Concerning the electron capture process, its kinetics has being studied by monitoring the junction capacitance or voltage (constant capacitance technique), after applying controlled trap filling pulses. Then, one has to deconvolve the changes of such junction parameter to obtain the corresponding carrier concentration time-evolution. It was shown from the early experiments in GaAsP and AlGaAs, that the increments of the space charge capacitance with filling pulses had a clear non exponential behavior [3,4]. By extrapolation from the usual situation where a deep level coexists with a larger concentration shallow level (the capture transient evolves exponentially), present non exponential behavior was attempted to be described by a set of time constants. Because present views indicate that the deep donor concentration in AlGaAs and GaAsP, for $x > 0.2$, is close or equal to the doping level density, we face a quite different problem, and such extrapolation may have no meaning.

Detailed capture studies have been performed in AlGaAs:Si by

Mooney and co- workers, who, by monitoring the time dependence of a MODFET threshold voltage, were able to get rather direct information about the free electron trapping kinetics in AlGaAs [5]. Such technique is an improvement over monitoring the space charge capacitance, where the capacitance waveform needs a difficult deconvolution to obtain the true carrier concentration evolution . The capture times for the voltage to change by 50% of its total value was determined at each temperature, and then E_b was deduced. The results of Mooney et al. were interpreted as if for each Al composition a distribution of capture barrier heights is present, just to account for the range of fitting capture time constants used. For each alloy composition, an average capture barrier energy is then obtained, having a minimum near the direct to indirect gap cross over composition. The width of such distribution (Gaussian) was found to be maximum near such cross over, decreasing as x decreases towards 0, or increases towards 1. Such result was understood as due to an alloy broadening effect.

In a recent paper by Bourgoin et al. [6], they have suggested that such non exponential capture kinetics do not reflect an alloy effect, but that the thermal capture barrier is a well defined quantity. It has been claimed that the electron capture and emission kinetics in DX centers are just determined by the high DX concentration, and not by an alloy broadening effect.

The key point is then to determine which amount of non exponentiality, in the capture process, is due intrinsically to the deep donor high concentration, and if the specific electronic structure of such deep donor is an extra source of non exponentiality.

In this work the capture kinetics of electrons is presented, introducing some of the terms missed in previous publications. Such study is first applied to long structures, where the length of the n-type region (W) is much greater than the extrinsic Debye length, $L_D(T)$, at the measurement temperatures. Such results are then compared with those of Mooney et al. Finally, the lack of real neutral regions in most of the samples is considered, due to the fact that $L_D \cong W$. It is concluded that to describe the kinetics of electron capture by DX centers, the electron emission process has to be included in its formulation; that, intrinsically, the free electron concentration evolves with time in a non exponential way; and that

for long capture times, this evolution is significantly affected by small thickness effects in real samples.

V.2. ANALYSIS

Let us consider a Schottky barrier on a long n- type region of AlGaAs, with $x > 0.2$. The structure is then governed by a single deep donor, at E_d below the lowest conduction band minima, with a concentration close to the donor doping level (N_d). At the measurement temperatures $E_d >> kT$, the donors have a very low ionization factor (I), and a space charge region (SCR) of width W_1, with fully ionized donors, is present. The free electron concentration starts to rise (50%) at W_1, and it takes about $3L_D$ to reach the $n \cong n_O = I \times N_d$ condition in the long quasi neutral region (figure 1).

We consider that the capture process starts with a SCR region under reverse voltage, where the deep donors are fully ionized. Then, the voltage is suddenly returned to 0 V. A sea of electrons (N_d) will move into the SCR, screening the $N_d^+ = N_a$ ions. At t=0, the N_d donors begin to capture the electrons, but the emission processes from the donors also start to appear. Let us note that at t= 0, the SCR edge is rather abrupt because the extrinsic Debye length is very short, being determined by the initial $n = N_d$ free electrons. For very long capture times, at equilibrium, in the quasi neutral region, $(1-I) \times N_d$ donors would have captured their electrons, only $n \cong n_0 = I \times N_d$ free electrons remain, and the extrinsic Debye length is now much longer, as determined by n_0.

As compared to previous publications, the introduction of the emission processes while the capture takes place, as well as to insure a null net charge condition while capturing, are essential. Only in this way we can consider meaningful physical boundary conditions at $t \longrightarrow \infty$. Then, at any instant t, while capturing under zero bias, if n(t) is the free electron concentration (also equal to the empty donors in the quasi neutral approximation), the electrons being captured by unit time and volume are:

$$c_n \times n(t) \times n(t) = \sigma_n \times v_{th} \times n^2(t) \qquad (1)$$

Equation (1) applies only for a non- degenerate electron gas. Otherwise c_n would be concentration dependent. Also, for a given temperature, the capture cross section is constant. The electrons being emitted per unit time and volume will be

$$e_n \times \left(N_d - n(t) \right) \qquad (2)$$

Then, the net electron concentration at the quasi neutral region varies as

$$\frac{\partial n}{\partial t} = e_n \times \left(N_d - n(t) \right) - c_n \times n^2(t) \qquad (3)$$

If we would not have considered the emission processes, and with the boundary conditions $n(t=0)= N_d$, and $n(t \longrightarrow \infty)= 0$, the solution for equation (3) would be

$$n(t) = \frac{N_d}{1 + a \times t} \qquad (4)$$

being $a = c_n \times N_d$ as reported by Bourgoin and co- workers [6], and indicating an hyperbolic electron capture process. However, as indicated above, the emission process has to be taken into account to reach the equilibrium condition $n(t \longrightarrow \infty) = n_0 = I \times N_d$.

Equation (3) can be solved if a particular solution is known. This can be obtained when the emission and capture processes equate ($dn/dt = 0$), and

$$e_n \times \left(1 - I \right) \times N_d = c_n \times I^2 \times N_d^2 \qquad (5)$$

After some manipulation, and taking $n(t=0) = N_d$, we can obtain

$$n(t,I) = N_d \times \left[\frac{I \times \left(1 - I\right) \times \left(2 - I\right)}{\exp\left(\frac{2 - I}{I} \times e_n \times t\right) - \left(1 - I\right)^2} + I \right] \qquad (6)$$

If capture starts when the deep donors are not fully ionized, the initial condition would be $n(t=0) = P \times N_d$, being P a factor varying between I and the unity, and we obtain

$$n(t,I,P) = N_d \times \left[\frac{\dfrac{I \times \left(P - I\right) \times \left(2 - I\right)}{\left(I + P - I \times P\right)}}{\exp\left(\dfrac{2 - I}{I} e_n \times t\right) - \dfrac{\left(1 - I\right) \times \left(P - I\right)}{\left(I + P - I \times P\right)}} + I \right] \qquad (7)$$

The transient part of equation (7) is represented in figure 2 for I=1 %, and P=1, 1/e and $1/e^2$. The ionization factor I affects strongly the non-exponential behaviour. Capture transients appear nearly exponential for ionization factors higher than 40%. For low ionization factors, only the very end of the capture transient is exponential, being its time constant the argument of the exponential in equations (6) or (7). The main part of the transient occurs in a faster, non- exponential way. We can also notice in figure 2 that, for a given I (or temperature), the more filled the DX's are at t = 0, the more exponential is the capture waveform, in disagreement with the suggestions in ref. (6).

A more powerful way to represent n(t) for several ionization factors (I=1, 0.1, 0.01, and 0.001 %) is shown in figure 3. It is easy to see from equation (6) that, for low ionization factors, the capture transient reaches the 50 % of its amplitude at a time $t_a(T)$ that is very close to

$$t_a(T) = \frac{I^2(T)}{e_n(T)} \qquad (8)$$

For our dominant single deep donor and for low ionization factors, we can write

$$I^2(T) = \left(\frac{n(T)}{N_d}\right)^2 \cong \frac{N_C}{g \times N_d} \times \exp\left(\frac{-E_d}{kT}\right) \qquad (9)$$

where Maxwell- Boltzmann statistics for the electron gas, because its low concentration, and Fermi- Dirac for the deep donor ionization factor, have been used.

From detailed balance considerations, the emission rate is

$$e_n(T) = \sigma(T) \times v_{th} \times N_C \times \exp\left(\frac{-E_d}{kT}\right) \qquad (10)$$

From equations (8), (9), and (10), we conclude that $t_a \cong 1/(\sigma_n v_{th} g N_d)$, and it will not have any exponential dependence with T, except if the electron capture process is thermally activated. If $\sigma_n = \sigma_n^{\infty} \exp(-E_b/KT)$, then an Arrhenius plot of $t_a(T)$ will give the capture barrier height, and this may be a well defined parameter. This result justifies the technique used by Mooney and co- workers [5] to extract E_b from their data. Equation (4) can also be obtained from equation (6) for small time values, using a Taylor series for the exponential term and I<<1.

Let us now to compare the behavior predicted by equation (3) with the experimental results of Mooney et al. In their work, the MODFET threshold voltage vs. capture time tends to be non symmetric, with long tails at large capture times. For their x = 0.35 sample, capture extends for more than six time decades. If we consider our results shown in figure 3, for the case of an ionization factor of 0.001% (estimated as a real one for a 35% Si: AlGaAs, where E_d = 150 meV, and T = 87K), the free electron concentration evolution is symmetric, and only covers about four time decades.

Since equation (8) indicates that capture processes for deep

donors will be much faster than the emission ones, capture measurements usually require low temperatures where degeneration at the beginning of the capture transients is easily reached. In this case we must wait until degeneration has been removed in order to apply equation (1) and solve equation (3) under the appropriate boundary conditions. From a qualitative viewpoint, the effect of degeneration is to make c_n dependent of the dynamic state of the system, being greater as degeneration increases. Therefore, capture transients under degeneration will have decreasing c_n factors as capture takes place.

As an example, figure 4 shows the c_n evolution for a capture barrier height $E_b = 10 \times kT$ and a parabolic band, vs. the Fermi level position respect to the bottom of the conduction band. As we can see, c_n markedly increases as degeneration does, resulting in faster beginnings of the capture transients than equation (6) predicts. This c_n modulation should be responsible for more than four time decades of free electron evolution as it was the case in the samples of Mooney et al, since the transient will begin sooner as they said, and will finish following equation (3) with the appropriate boundary conditions.

Therefore, in order to obtain the capture barrier height from an Arrhenius plot of $t_a(T)$ measurements, a non-degenerate situation is required during capture. If this is no the case, we must wait until degeneration is removed, or otherwise we won't have an expression of $t_a(T)$ being inversely proportional to the thermally activated capture cross section.

V.3. EXPERIMENTAL

We want to describe now some capture experiments aimed to validate above model. These efforts showed later the presence of small size effects, that will be used to discuss capture experiments in MODFET's. From this viewpoint, the measuring technique we propose is less influenced by these effects, since we can use long samples (0.5 - 1 microns) instead of short ones as MODFET's (less than 0.1 microns).

The emitter-base junctions in the HBT's structures described in

Section VII, Si doped, were used in these measurements. The employed technique was based on the following procedure: a) a forward bias is applied to the junction, to photoionize practically all the electrons in the DX centers (see **Section VII**); b) next, a reverse voltage of V_r = 6 V is then applied, allowing a wide depleted region (≅0.2 μm) with fully ionized DX's and without free electrons to be captured; c) afterwards, junction voltage is switched to V = 0V. A sea of electrons will screen the deep donors and simultaneously the capture processes start. This new technique allows to study capture kinetics without using MODFET's, and because the internal photoionization, the emission-capture cycle can be made very fast, without the need to raise the sample temperature to empty the DX centers. During a controlled time, capture takes place in the quasi neutral region (≅ 0.12 μm) indicated in figure 1. At the end of the capture interval, the remaining free electron density is determined by performing a fast 1/ C^2-V_r scanning, for example from the original 0 V to -6 V. If the temperature has been selected so that $t_a(T)$ in equation (8) is at least one order of magnitude larger than the fast C-V scanning time, the 1/ C^2 slope will indicate the captured electron concentration. In our case T = 122.4 K, $\tau_n = 1/e_n \cong 10^6$s, $t_a \cong 361$ s and the C-V scanning lasted 10 s. Starting again from process a), and using a different capture time, the capture kinetics can be experimentally studied.

A series of results are shown in figure 5.a. The ionization factor at this temperature was calculated as 1.9 % from data obtained by the quasi-static method used in **Section IV** to obtain E_d. These data were: I(130K)=2.5 % and I(115K)=1.48 %, both giving E_d= 70 meV and easily obtained for Si by fast C-V scanning (quasi-static method). The above mentioned $\tau_n = 1/e_n \cong 10^6$s is obtained from DLTS data extrapolated to 122.4K. Equation (8) gives t_a(122.4K)=361 s, a much longer value than the 10 s scanning time. An important point to mention is that we face a degeneration condition during the early stages in the capture. That is, because for the Γ minimum (the dominant one at T=122.4K for our Al composition) the density of states is $N_C = 1.82 \times 10^{17} cm^{-3}$, and $N_d = 3.22 \times 10^{17}$ cm^{-3}, the initial c_n is larger than for the next capture times. This is the reason for the discrepancy shown in figure 5.a at short capture times. However there is good agreement in the slopes between theory and experiments, once the electron gas concentration decreases below ≅ $N_C/5$. A faster C-V scanning system will improve the results allowing to study the evolution of c_n with capture time in the

degeneration regime, as well as to increase the S/N ratio of measurements.

Different fittings were tried without success, using slightly different values of I in equation (6), as shown in figures 5.b. and 5.c. A detailed study of c_n under degeneracy conditions is planned in the next future.

Another series of capture experiments revealed the importance of insuring that a neutral, or quasi neutral, region is really available for capture in the samples under study. Thin samples, quite common in high speed structures, may have thicknesses not large enough (a few times L_D at the measuring temperature) to insure the presence of a neutral capturing region. A faster C-V system will allow to increase T, and then shorten L_D, making easier to fulfill this condition.

We want to talk about the presence of short size effects in the samples used in ref. (5), because at the capture temperatures $L_D > W$. We have to remind that, at a given capture temperature, L_D starts to increase as capture time increases and n(t) tends to n_0. For the lowest temperatures used in ref. (5), ionization factors are in the 10^{-4} to 10^{-5} range, $N_d \cong 10^{18}$ cm^{-3}, and then L_D is in the 2000 to 6000 Å range. As a result, in most of the practical situations L_D will be larger than the sample thickness. Evenmore, in MODFET's this size problem is even worse because the AlGaAs layer forms two SCR's that collides (two L_D values). In all cases the main result is that the structure does not have a quasi-neutral capturing region, the AlGaAs bands bend, being a region of net positive charge, with less free and less trapped electrons than if a quasi neutral region was present (flat bands). Under this condition equation (6) is not valid, and the capture processes are slowed down.

V.4. CONCLUSIONS

In conclusion, a detailed analysis of the electron capture process by deep donors in AlGaAs has been presented. It predicts for n(t) an strong non exponential behavior, validates the experimental determination of the capture barrier, and precludes the presence of important size effects, for

long capture times. However, because experimental capture data extends over many decades, and the analytical treatment of these size effects are rather complex, a direct proof that just size effects, or that the electronic structure of the deep donors (alloy broadening), are the origin of these extended capture data (extra non exponentiality), cannot be presented. Further experiments are needed to clarify the problem. Capture experiments have been performed, indicating the importance of the initial degeneration conditions in the capture kinetics. Besides, capturing regions really neutral are needed so present analysis can be applied. It has been shown that this is not the case in many circumstances for long capturing times.

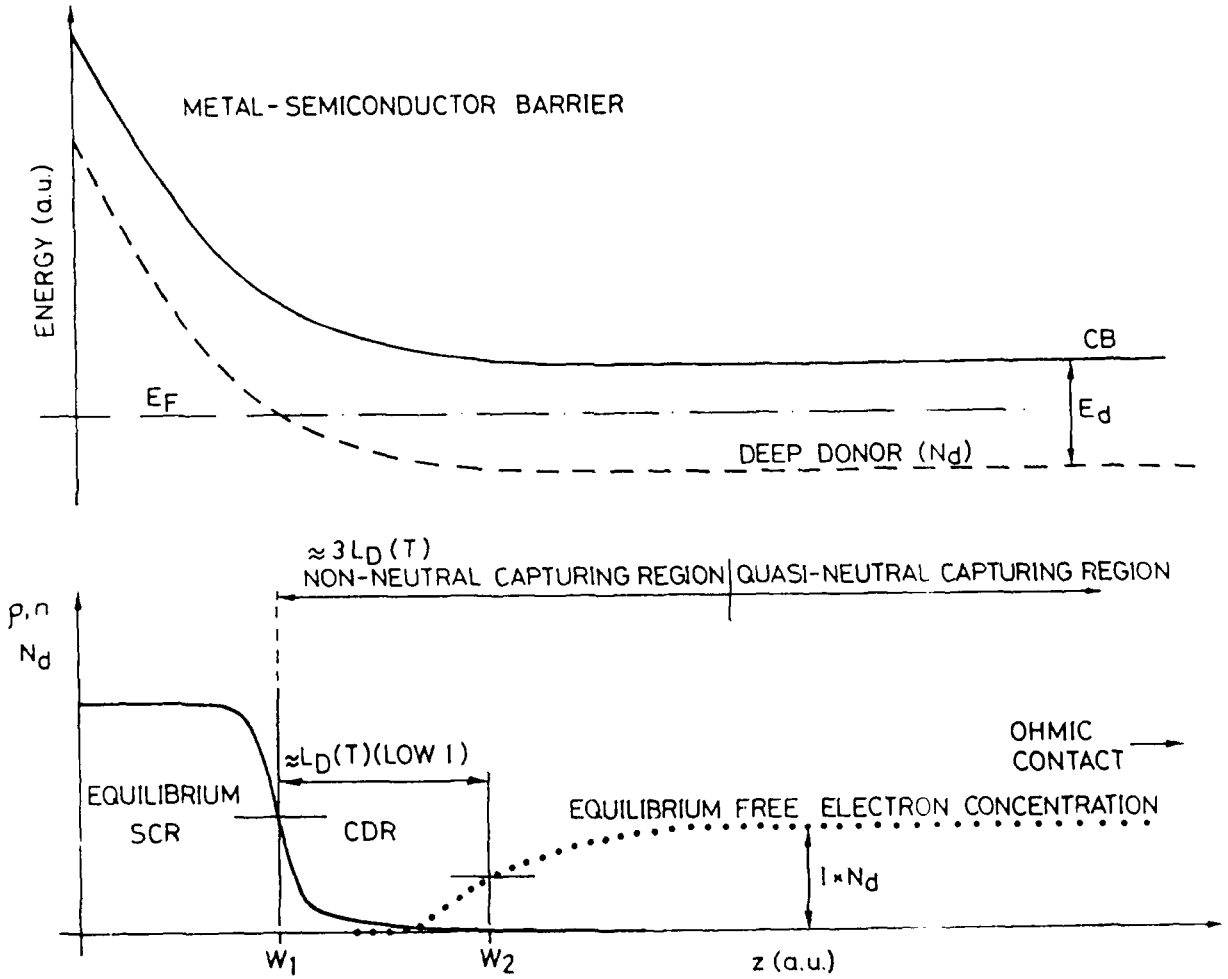

Fig. 1. Energy band, fixed charge and electron concentration scheme in a Schottky barrier at low temperatures. Various regions are displayed, indicating their role in the capturing process.

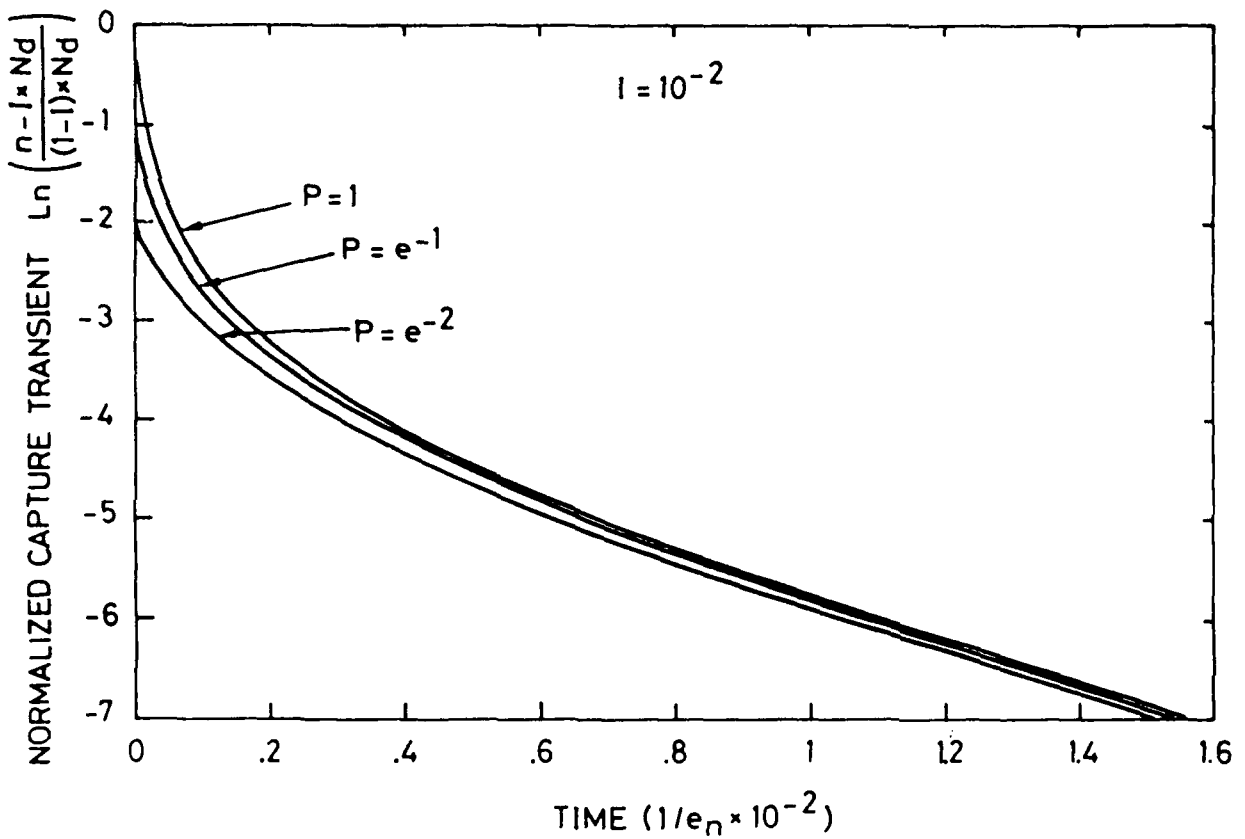

Fig. 2. Simulation of the free electron capture transient as a function of the filling factor P.

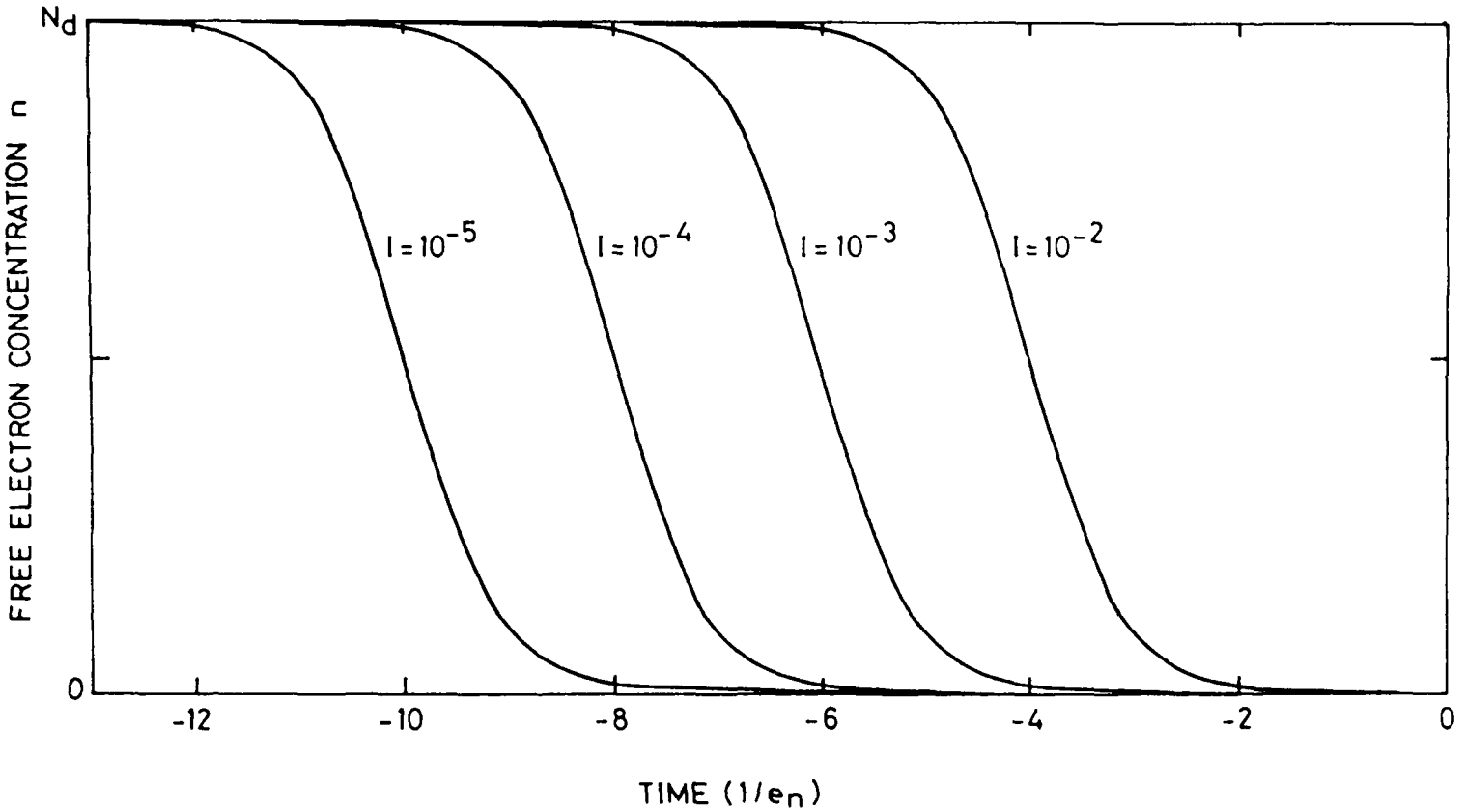

Fig. 3. Evolution with time of the free electron concentration during the capture process. Curres have been obtained for various ionization coefficients (I).

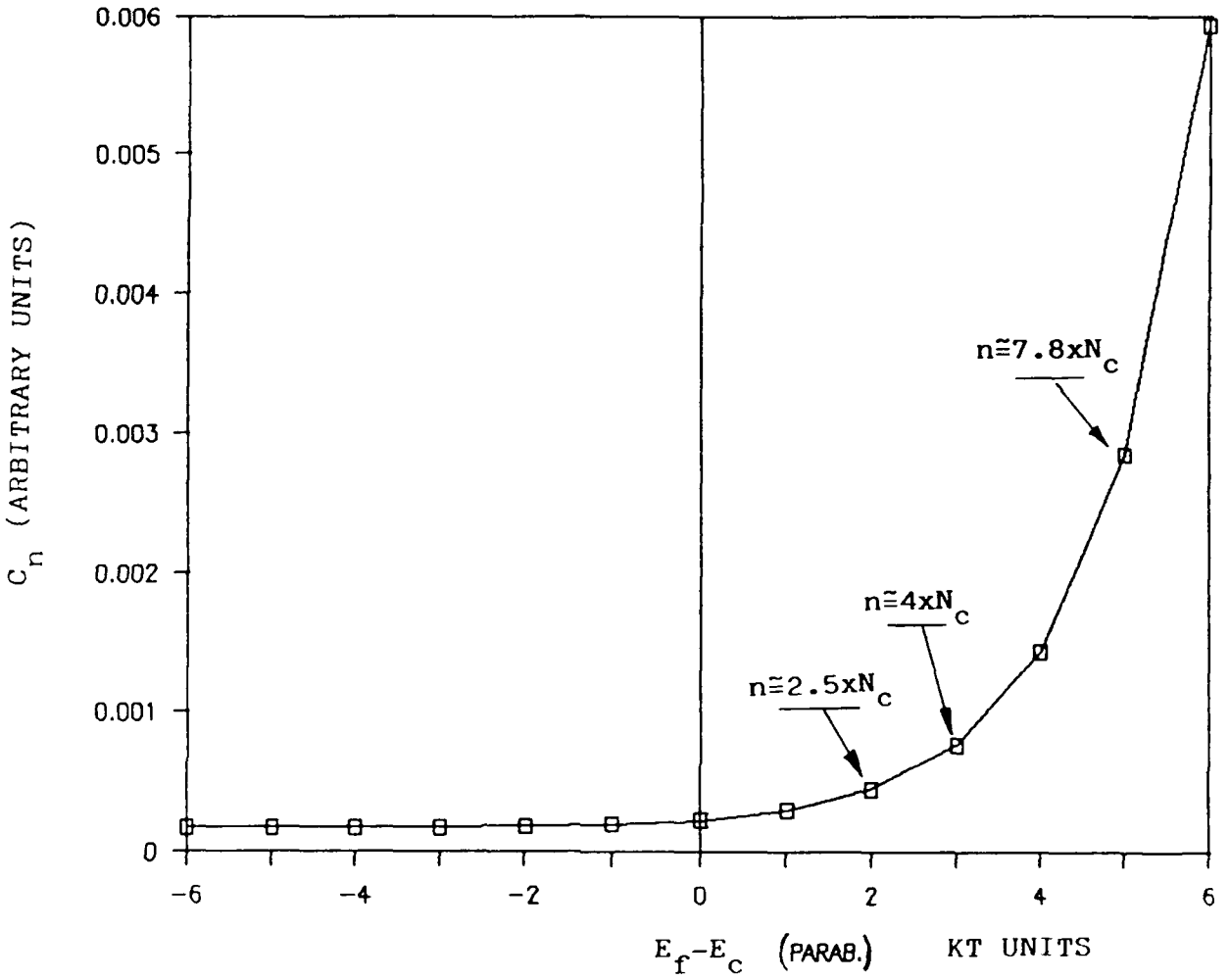

Fig. 4. Variation of the capture constant $c_n(n)$ vs. the Fermi level position relative to the C.B. bottom. The example cosider the capture over a capture barrier $E_b = 10 x kT$. Actual E_b values for AlGaAs ($\cong 30 x kT$) requires at least double precision computations, as well as a detailed knowledge of the conduction band structure. In the example we use a parabolic conduction band (only one minimum).

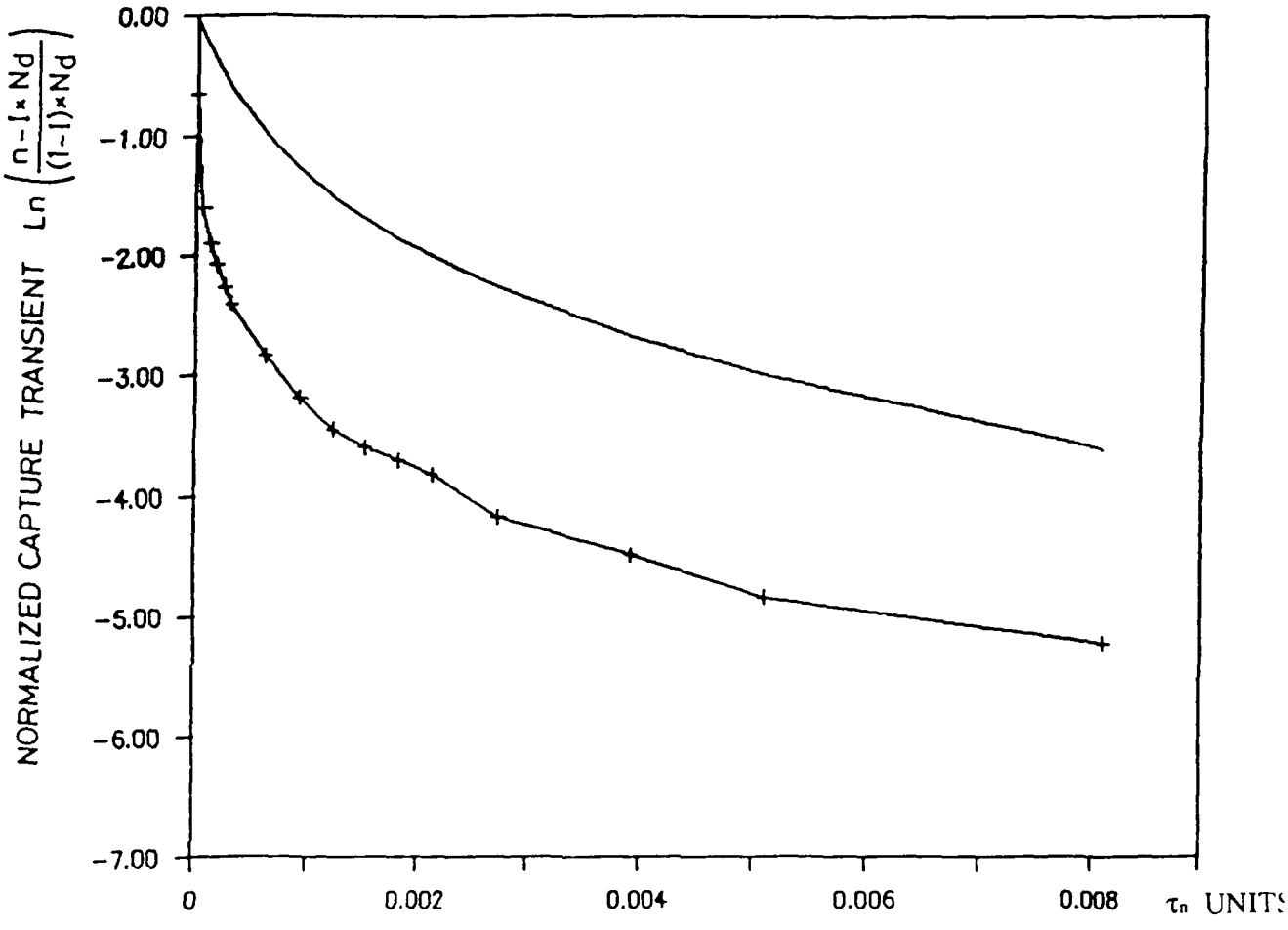

Fig. 5.a Measured (points) and theoretical (line) evolution of the normalized capture transient (see Figure 2) in $Al_{0.26}Ga_{0.74}As$. In order to use equation 6, the emission time constant at this temperature has been extrapolated as $\tau_n = 10^6$ seconds (more than 11 days) from DLTS data measured on the same sample. The non-exponential transient waveforms adds some uncertainity to this data, but it is difficult an accurate measurement. The ionization factor used is 1.9 % and the time is measured in τ_n units.

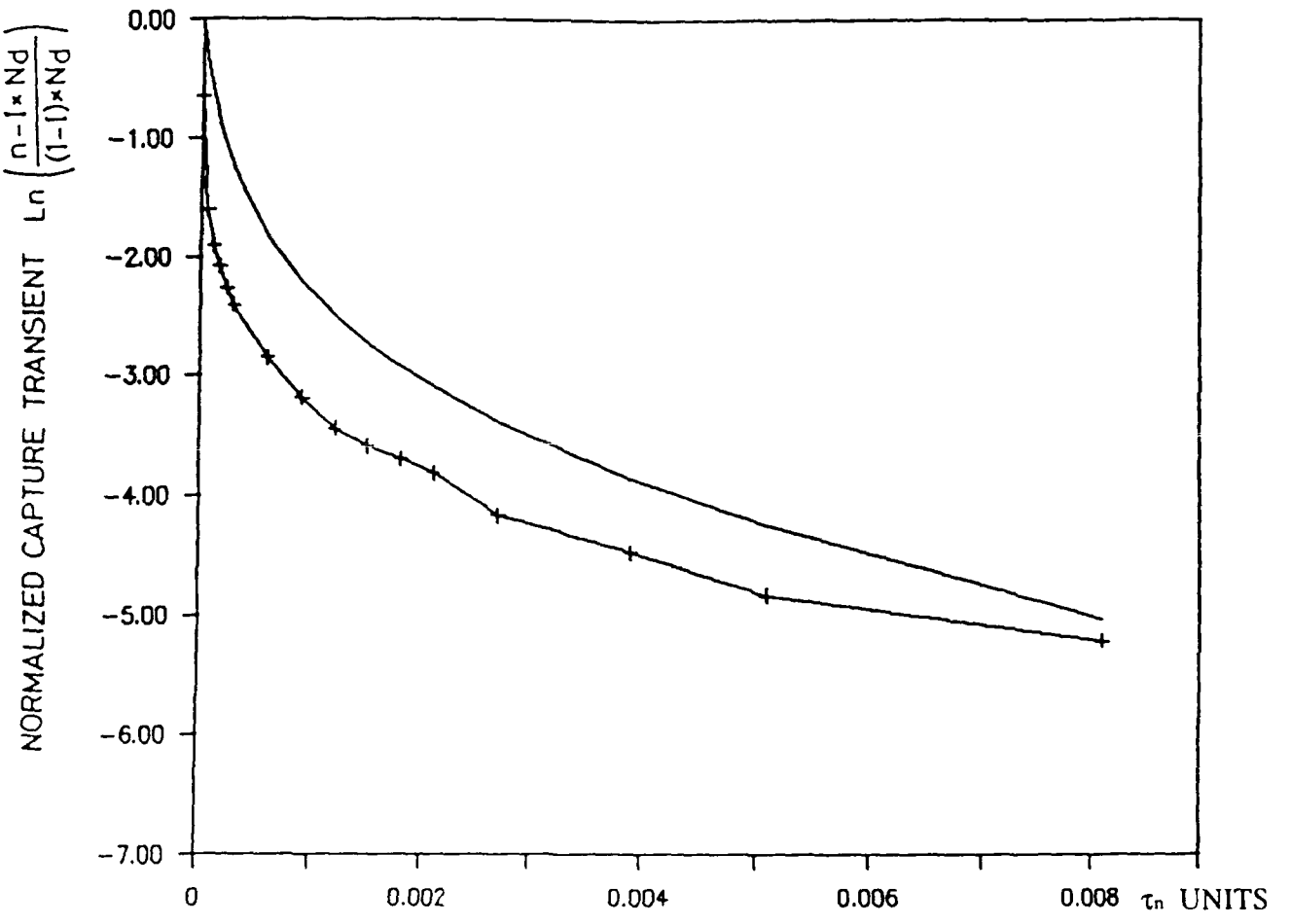

Fig. 5.b The same experimental data and a theoretical capture transient (from equation 6), obtained using the same $\tau_n = 10^6$s and a different ionization factor: I=1.1 %. The fitting seems to be better, although the final part becomes faster due to the strong influence of I in the exponential factor.

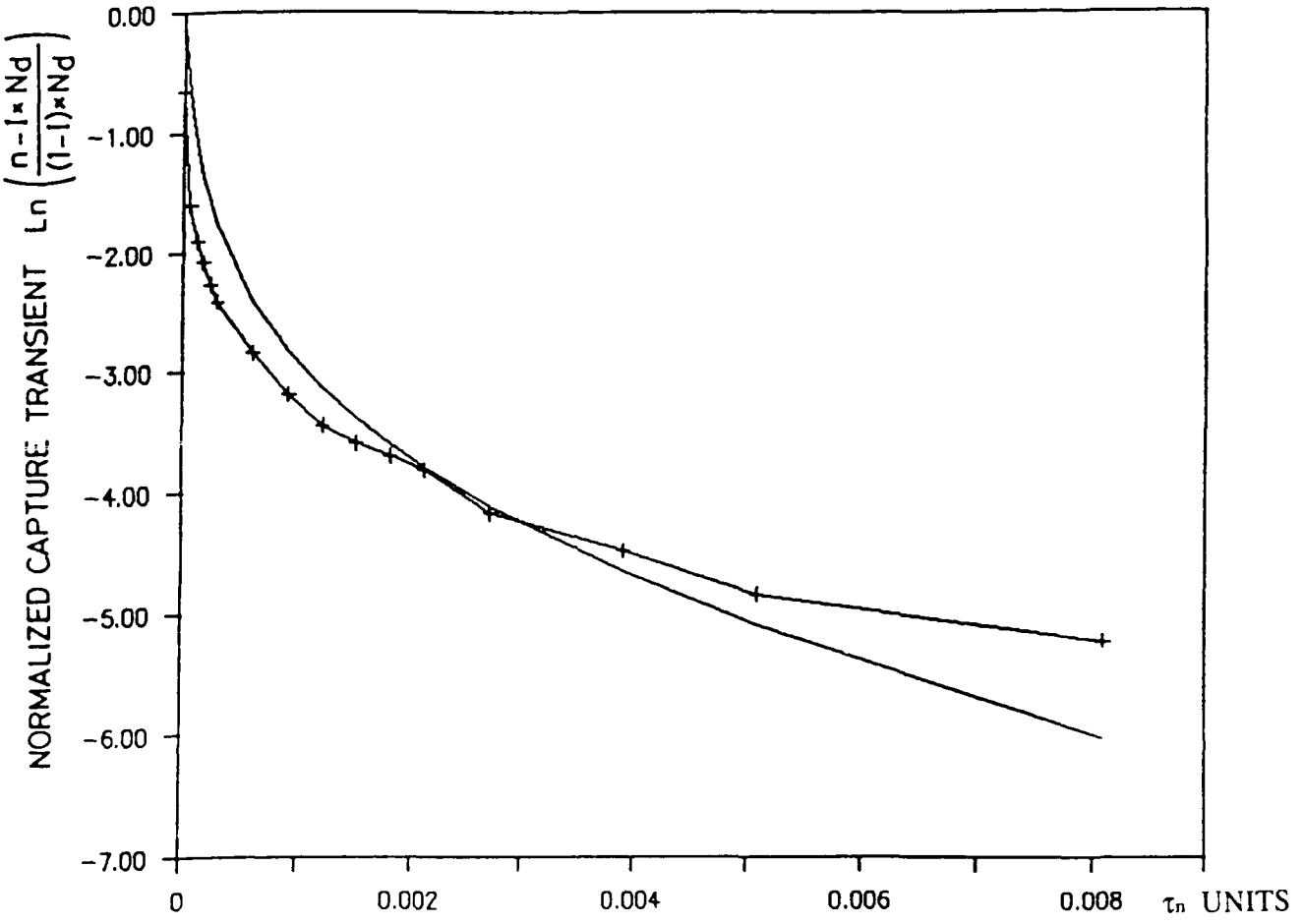

Fig. 5.c The same experimental data and a theoretical capture transient (from equation 6), obtained using the same $\tau_n = 10^6$s and a different ionization factor: I=0.8 %. Now is clear how the final part becomes faster due to the strong influence of I in the exponential factor, but even in this case we can not fit the initial, faster, part of the transient due to higher $c_n(n)$ values resulting from degeneration.

REFERENCES

1. D.V. Lang, R.A. Logan, and M. Jaros, Phys. Rev. **B19**, 1015, (1979).
2. D.V. Lang, in *Deep Centers in Semiconductors,* ed. by S.T. Pantelides (Gordon and Breach, New York, 1986), P. 489.
3. P. M. Mooney, P.M. Solomon, and T.N. Theis, Inst. Conf. Ser. **74**, p.617, (1984).
4. E. Calleja, A.I. Gomez, and E. Munoz, Solid- State Electron. **29**, 83, (1986).
5. P.M. Mooney, N.S. Caswell, and S.L. Wright, J. Appl. Phys. **62**, 4786, (1987).
6. J.C. Bourgoin, S.L. Feng, and H.J. von Bardeleben, Appl. Phys. Lett., **53**, 1841, (1988).

VI. NEAR INFRARED LUMINESCENCE IN N-TYPE $Al_xGa_{1-x}As$ ALLOYS

VI.1. INTRODUCTION

Although the main phenomenology of the DX centers (deep donor states) is already well understood, particularly in Si- doped AlGaAs alloys, there are still some aspects on debate that concern the defect microscopic structure and the physical mechanisms that drive its deep -to -shallow instability. The charge of the DX ground state (negative or positive U), the DX center link to a given conduction band minimum, if any, and the amount of the lattice distortion generated upon electron capture are topics that must be clarified. Regarding the lattice distortion, two different hypotesis are so far in conflict: the small and the large lattice relaxation models. The choice of one of them not only matters the interpretation of experimental data like the optical ionization threshold or the capture barrier energy, but it also selects between a localized or effective mass- like character of the DX center states, and between the positive and negative U models for the charge of the DX ground state.

A small lattice relaxation model (SLR) has been supported by Henning et al. [1,2], among other authors, since 1986. The detection of a small optical ionization threshold value (0.3 eV) in Si- doped AlGaAs, and the observation of a photoluminescence (PL) transition at 0.2 eV below the band gap energy, were attributed to the presence of deep donors (DX centers). Since both the thermal depth and the optical ionization threshold were comparable, a SLR model was then suggested.

A large lattice relaxation (LLR) model was proposed in 1977 by Lang et al. [3,4] to explain the observation of a much larger optical threshold in Te- doped AlGaAs. Since then, many authors have reported similar results in Si- doped AlGaAs, and very nice experiments by Legros et al. [5] and by Mooney et al. [6] confirmed a large optical ionization threshold for DX centers in Si- doped AlGaAs.

A recent model where both SLR and LLR DX configurations coexist as bistable states with different optical threshold values was proposed by

Henning et al. In their work, PL signals observed in the near infrared region (1.5 μm) are assigned to radiative transitions involving the deep donor states (DX centers) [7,8]. A different interpretation of similar infrared data is provided by Alaya et al., that assign the PL peak at 1.5 μm to an internal transition from an excited state to the ground state of the DX centers [9].

Some recent theoretical models focus on the origin of the deep donor states (DX centers) and their metastability, but none of them fully explain the vaste phenomenology of these centers. A SLR model suggests that the deep DX centers originate from effective -mass states and intervalley scattering effects [10]. On the other hand, Chadi and Chang [11] and Khachaturyan et al. [12] proposed that a LLR configuration could be stable if two electrons where localized by the donor (negative U). Besides, the model by Chadi and Chang is, so far, the only one that provides a qualitative explanation to the DX center chemical shift.

There is a lack of systematic analysis of the near infrared PL in AlGaAs alloys, since most published data refer to Si- doped material, considering a small range of alloy compositions and doping concentrations. Besides, measurements are always restricted to a narrow temperature range. In this work we present an extensive analysis of the near infrared PL spectra in Si- doped AlGaAs as a function of the alloy composition, the doping concentration and the temperature (20 to 300K). The aim of this work is to determine whether or not there is a connection between the deep donor states (DX centers) and the 1.5 μm PL peak measured by several authors.

VI.2. EXPERIMENTAL

The samples used in this work were Si-doped AlGaAs grown by molecular beam epitaxy (MBE) and metal-organic vapor phase epitaxy (MOVPE). The doping levels were in the range of 10^{16} to 10^{18} cm^{-3}, and the alloy compositions varied from 27% to 74%.

Photoluminescence measurements were performed in a closed- cycle He- cryostat over a temperature range from 20 to 300K. An Ar^{+} laser provided

the excitation with both 5145 Å and 4765 Å lines. Photoluminescence spectra were analyzed with a short focal lenght monochromator (Jobin-Yvon H25), an RCA S1 photomultiplier and a liquid nitrogen- cooled Ge- detector (North Coast). Much care was taken to avoid ghosts and replica in the infrared PL signals using band pass filters.

VI.3. RESULTS

Figure 1 represents the near- IR luminescence spectra for an MOVPE -grown AlGaAs sample doped with Si to $6x10^{17}$ cm^{-3}, and Al mole fraction of 33%. In addition to the near band gap transitions (V1, V2) and the GaAs substrate peak, two clear PL peaks appear at 1.1 and 1.5 μm, labelled as IR1 and IR2 respectively. Although not seen in this figure, we have checked that other MOVPE samples doped with Se and Sn, as well as undoped, show exactly the same PL spectra. From this data we conclude that both infrared transitions (IR1, IR2) appear at the same energy position, no matter which dopant and alloy compositions are considered.

MBE- grown Si:AlGaAs samples also show a PL peak at 1.1 μm (IR1) and a second peak (IR3) that is located between IR1 and IR2 (figure 2). As it can be seen, when the Al mole fraction increases, peak IR1 remains fixed, as it does in MOVPE material. However, peak IR3 shifts slightly towards higher energy positions.

The dependence with the temperature of the significant peaks shown in figure 1 is represented in figure 3.a. Concerning the visible region, peak V1 behavior at low temperature corresponds to donor - VB and donor -acceptor transitions. At higher temperatures, the band to band transition dominates, allowing a precise determination of the alloy composition. On the other hand, peak V2 follows a temperature dependence not predicted by a simple model, and its origin is unknown. However, this peak is not present in other samples and it might be due to some residual contaminant. We have ruled out any relation of this peak with the dopant.

The infrared peaks (IR1, IR2) that appear in figure 1 at 1.1 and 1.5 μm respectively, reproduce previous results [2,7]. Peak IR1 always

appears at the same energy position, independent of the alloy composition, the donor species and the growth method (figure 2 and table II), and it follows quite precisely the band gap temperature dependence (figures 3.a and 3.b). Peak IR2 is always present in MOVPE samples at the same energy position, which is also independent of the temperature (figure 3.a).

Finally, peak IR3, that appears in MBE samples, shows a step- like energy increase with temperature of about 60 meV (figure 3.b). Since all these samples have high Al mole fractions (indirect band gap), that might be interpreted as a transition involving the X- like effective mass donor state. This level has been recently identified in Si- doped AlGaAs by photo Hall measurements lying at 75 meV below the conduction band [13], and in Te- doped AlGaAs by FIR absorption at 60 meV below the conduction band [14].

A comparison between the sample donor concentration and the PL intensities of the infrared peaks can be established from data in table II, where Si- doped AlGaAs samples both MOVPE and MBE -grown are considered. PL amplitudes were measured at the same temperature and excitation power, and further corrected by the amplification factor, thus allowing a comparison. A bare check of these values reveals a complete lack of correlation between the Si concentration and the intensity of peaks IR1, IR2 and IR3. Moreover, there is no evidence of any relation between these intensities and the Al mole fraction.

Deep Level Transient Spectroscopy (DLTS) measurements have been performed in several Si- doped AlGaAs, both MBE and MOVPE -grown. In all cases there is a dominant peak at low temperature, corresponding to the electron thermal emission process from DX centers (figure 4). Above room temperature there is a deep trap, located at about 0.85 eV below the conduction band, that is present in all samples grown by MBE (figure 4.a, b, and c). However, in samples grown by MOVPE there are no traces of deep traps (other than the DX) (figure 4.d, e, and f).

We have also performed photoluminescence measurements as a function of the excitation power. In all samples measured, peaks IR1, IR2, and IR3 saturate at quite low excitation power. This behavior is reflected in figures 5.a, and 5.b, where the intensities are normalized to their saturation values.

VI.4. DISCUSSION

We will focus the discussion on the infrared PL data. Peaks labelled in this work as IR1 and IR2 were reported by Montie and Henning [2,7]. In their work, peak IR1 was attributed to a deep transition from the GaAs substrate, being disregarded from the discussion. On the other hand, they ascribed peak IR2 to a transition from the DX ground state, in a LLR configuration, to the valence band. If we assume that the DX centers follow the L- valley [10,15], or a weighted combination of the CB minima [11], a temperature dependence of peak IR2, following the band gap, should be expected, in contradiction with our results. Even if we consider that the DX centers are linked to the CB, no matter how, (both thermal and optical emission energies are independent of the Al mole fraction as well as of the hydrostatic pressure [4,5,14,15,16]) the above argument is valid. Moreover, following the model proposed by these authors, a shift to higher energies should be observed in peak IR2 when the Al mole fraction is increased. There is a clear evidence in this work that peak IR2 does not change its position with the Al mole fraction. Finally, the picture presented in a configuration coordinate (CC) diagram in refs. (7,8), to support the suggested bistable character of the DX center, leads to inconsistent bandgap energy values, depending on the transition path selected (LLR or SLR), as it is shown in figure 7.a.

In a recent work by Alaya et al. [9], peak IR2 was interpreted as a transition from a resonant excited state to the ground state of the DX center, assuming a SLR model and an effective- mass like origin for this center. This picture was also claimed to explain the constant value of the DX center optical threshold energy. This cannot explain why IR2 does not appear in MBE- grown samples. Besides, the energy shift of peak IR3 with the alloy composition (figure 2) rules out any relation with the above proposed PL transition, since it is the same one that drives the photoionization process, which is characterized by an energy not dependent on the alloy composition. Moreover, following the last argument, there is no explanation within this model for the constant energy value of peak IR2 in MOVPE samples, when the donor species are changed (notice that the potoionization

threshold does change with different donors). It is also difficult to reconcile such a radiative character of an effective-mass donor state with the existence of persistent photoconductivity effects and with the fact that, so far, there is no experimental evidence that the DX centers can be filled by optical excitation (photocapture) [17,18].

The step- like energy increase of peak IR3 observed in figure 3.b, that is only found in MBE- grown samples with indirect bandgap, is very close to the reported value of the donor ground state derived from the X- valley minima [13]. We can interpret this behavior considering that IR3 transition starts either from the CB or from this donor state, depending on the temperature. Then, IR3 cannot be linked to a transition between an excited state and the ground state of the DX center. A similar behavior should be expected in samples with direct bandgap, but the small value of the donor ground state derived from the Γ- valley makes its detection quite hard from our infrared PL measurements.

The summary of sample characteristics presented in table I clearly indicates that there is no relation between the infrared PL signals and the donor concentration. The same independence is applicable respect to the alloy composition. Since the apparent concentration (electron occupancy) of the DX centers depends on the Al mole fraction, and its maximum value equals the substitutional donor concentration (as it has been proved in many experiments using hydrostatic pressure), we conclude that the analyzed IR luminescence does not involve the DX centers. Moreover, the analysis of the temperature dependence of peaks IR2 and IR3, and the fact that the energy positions of peaks IR1 and IR2 do not change with the alloy composition, strengthen the above conclusion.

In order to clarify the origin of the observed infrared luminescence we should emphasize that peak IR1 is always present at the same energy in all samples. A similar behavior is observed for peak IR2, although only in MOVPE -grown samples. Finally, peak IR3, characteristic of MBE-grown samples, shifts to higher energies with increasing Al mole fraction. This dependence on the growth method, and the fact that only samples grown by MBE show a midgap level detected by DLTS (0.85 eV), led us to assign a different origin for IR2 and IR3.

Let us consider now the MBE- grown samples where both peaks IR1 and IR3 always appear together, although with different amplitudes (table II). Notice that adding the energies of peaks IR1 and IR3 gives a value that roughly follows the alloy bandgap (figure 6). When the temperature dependence of these two peaks is considered, it strongly suggests that both infrared transitions involve a midgap trap. This picture is drawn in the CC diagram of figure 7.b, where the positions of the DX center, the effective mass- like donor state, $E_d(X)$, and the midgap trap E_T are shown. This scheme explains the temperature dependence of IR1 and IR3, since one of these transitions must be independent of the temperature, and the other one must follow the bandgap temperature shift. Peak IR3 in figure 7.b represents the transition from the CB or from the "shallow" donor state, E_d, to the midgap trap, according to our interpretation of the energy shift of this peak that is shown in figure 2. Then, peak IR1 corresponds to a transition from the midgap trap to the VB. This midgap level might well be the one measured by DLTS at 0.85 eV below the CB, whose small concentration (10^{15} cm^{-3}) agrees well with the fact that both transition (IR1, IR3) intensities saturate at relatively low excitation power (figure 5). However, it must be said that the energies derived from PL and DLTS experiments might not be comparable "a priori" for an unknown trap.

There is in the literature a widespread information about a midgap level which has been characterizad in GaAs and GaAsP by DLTS, giving an emission energy between 0.8 and 0.9 eV, quite close to the one observed in our samples. This midgap level is the "well known" EL2. Moreover, two photoluminescence transitions are characteristic of EL2 in GaAs, that take place in the same way as we propose here for IR1 and IR3 (figure 7.b). The concentration of EL2 as a native defect is in the range of 10^{15} cm^{-3}, that again is what we measure by DLTS in our MBE samples.

The origin of the transition corresponding to IR2 is not so clear, since it appears only in MOVPE samples at a fixed energy. A recent study by Fockele et al. [19] reported a PL band at 1.5 μm in undoped MOVPE material that was attributed to an As- antisite defect characterizad by a constant energy level respect to the valence band. This work demonstrates that this PL signal is not originated from the GaAs substrate.

A PL peak at 1.5 μm has been also detected in SI GaAs [20], whose

amplitude follows an "W" -shape across the wafer diagonal, in a similar way as the concentration of the EL2 trap does [21]. It is hard to say if what we see in the MOVPE samples is the As- antisite or EL2, since the first is part of the second.

VI.5. CONCLUSIONS

In summary, we think that there is no evidence of infrared PL bands related to the DX centers. The observed infrared peaks, IR1, IR2, and IR3 are most likely originated from transitions involving a native defect not related to the dopant, but probably associated with As- antisite and/or EL2 defects. We also want to emphasize that IR2, and IR3, although most likely related, are not originated by the same defect, since IR2 appears only in MOVPE material whereas IR3 shows up in MBE material. Finally, we would like to point out that PL technique is not the most appropriate to determine the amount of lattice distortion that characterize the DX centers.

Table II

Summary of Sample characteristics and parameters. Si:GaAlAs.

Sample	Al %	[Si] cm^{-3}	Peak IR1 (eV)	IR1 Amplitude	IR2 Amplitude	IR3 Amplitude	DLTS (eV)	Gap (25 K) (eV)*	Remarks
A	26	5 E17	1.158	0.027		0.011		1.823	MBE Lab. 1
B	27	1 E17	1.080	0.054		0.023		1.836	MBE Lab. 1
C	28	1 E16	1.156	0.010		0.107		1.848	MBE Lab. 1
D	33	7 E17	1.129	0.065	0.163		NO	1.912	MOCVD Lab. 2
E	33	2E18		2.234	0.001		NO	1.912	MOCVD Lab. 3
F	48	6 E16	1.131	0.097		0.094	0.87	2.046	MBE Lab. 4
G	59	7 E16	1.128	0.019		0.019	0.84	2.075	MBE Lab. 4
H	74	7 E16	1.130	0.007		0.004	0.81	2.119	MBE Lab.4

T=25 K, Pow.=6mW, Excitation 476.5 nm, LN cooled Ge Detector.

* H. C. Casey & M. B. Panish: Heterostructure Lasers Part B, AP P. 9, (1978).
S. Adachi: J. Appl. Phys. 58, R1, (1985).

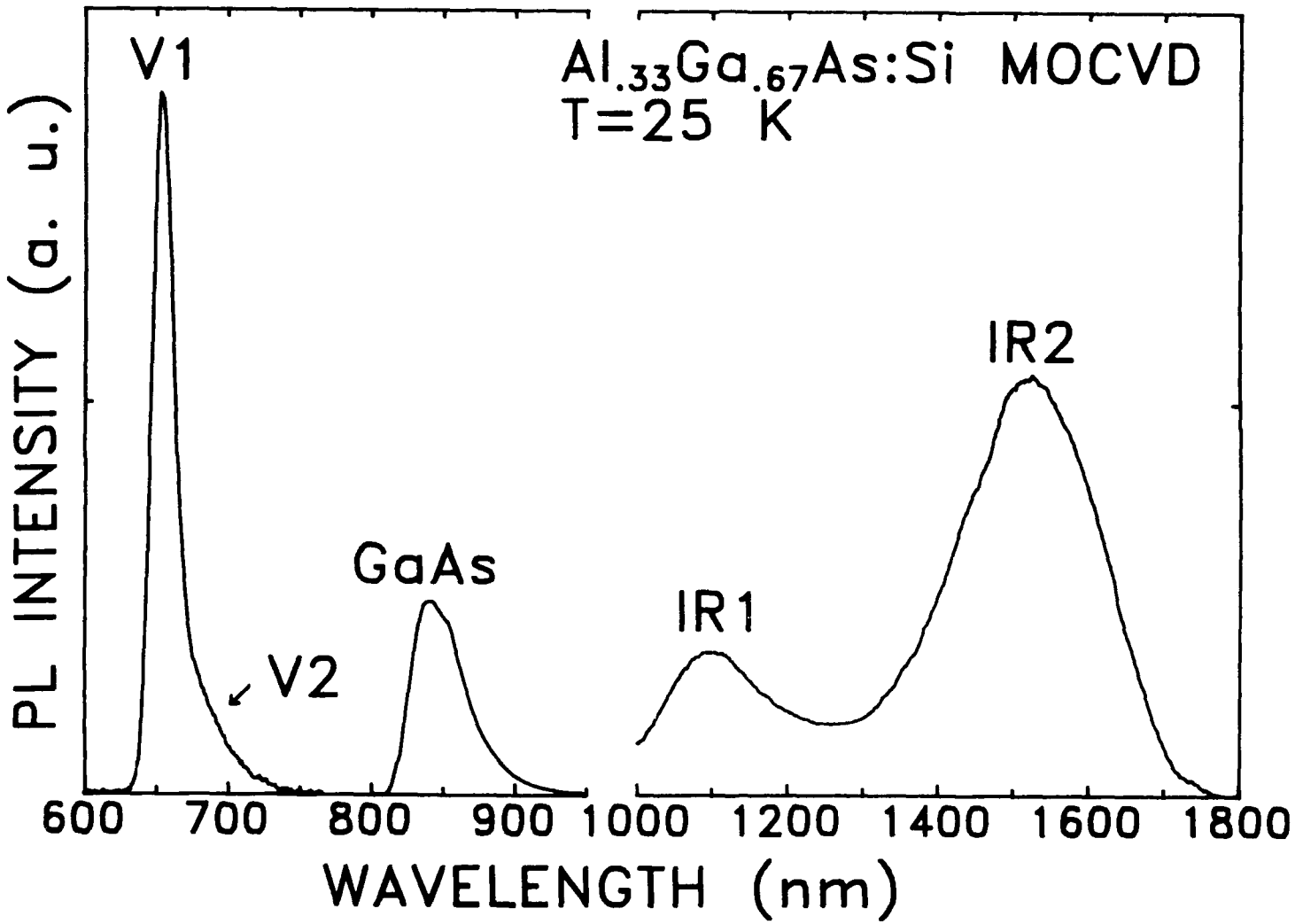

Figure 1.- Photoluminescence spectrum of a Si:AlGaAs (33%) MOCVD sample.

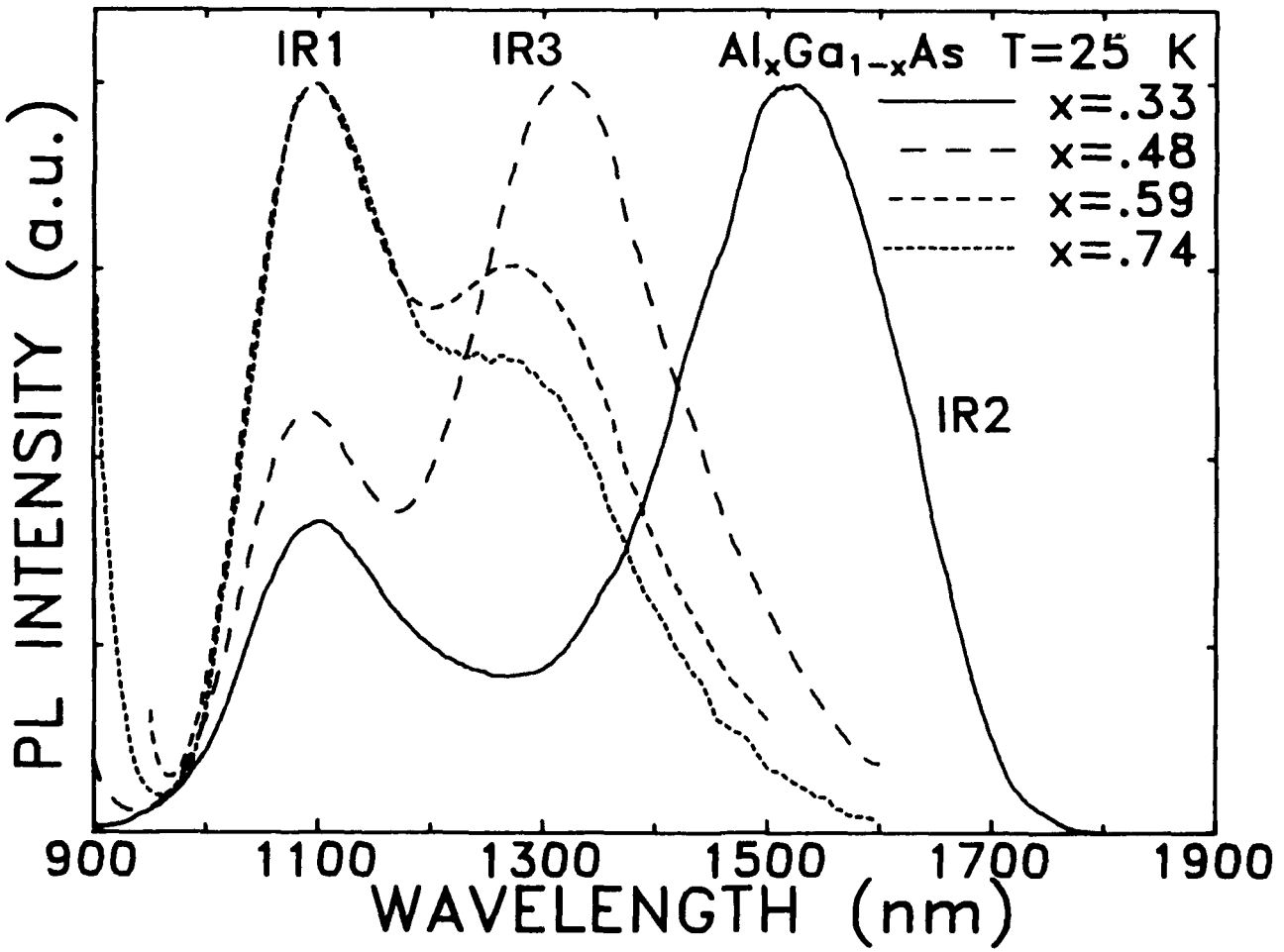

Figure 2.- Infrared PL spectra in Si:AlGaAs MBE samples (48%, 59%, 74%) and a Si:AlGaAs MOCVD sample (33%).

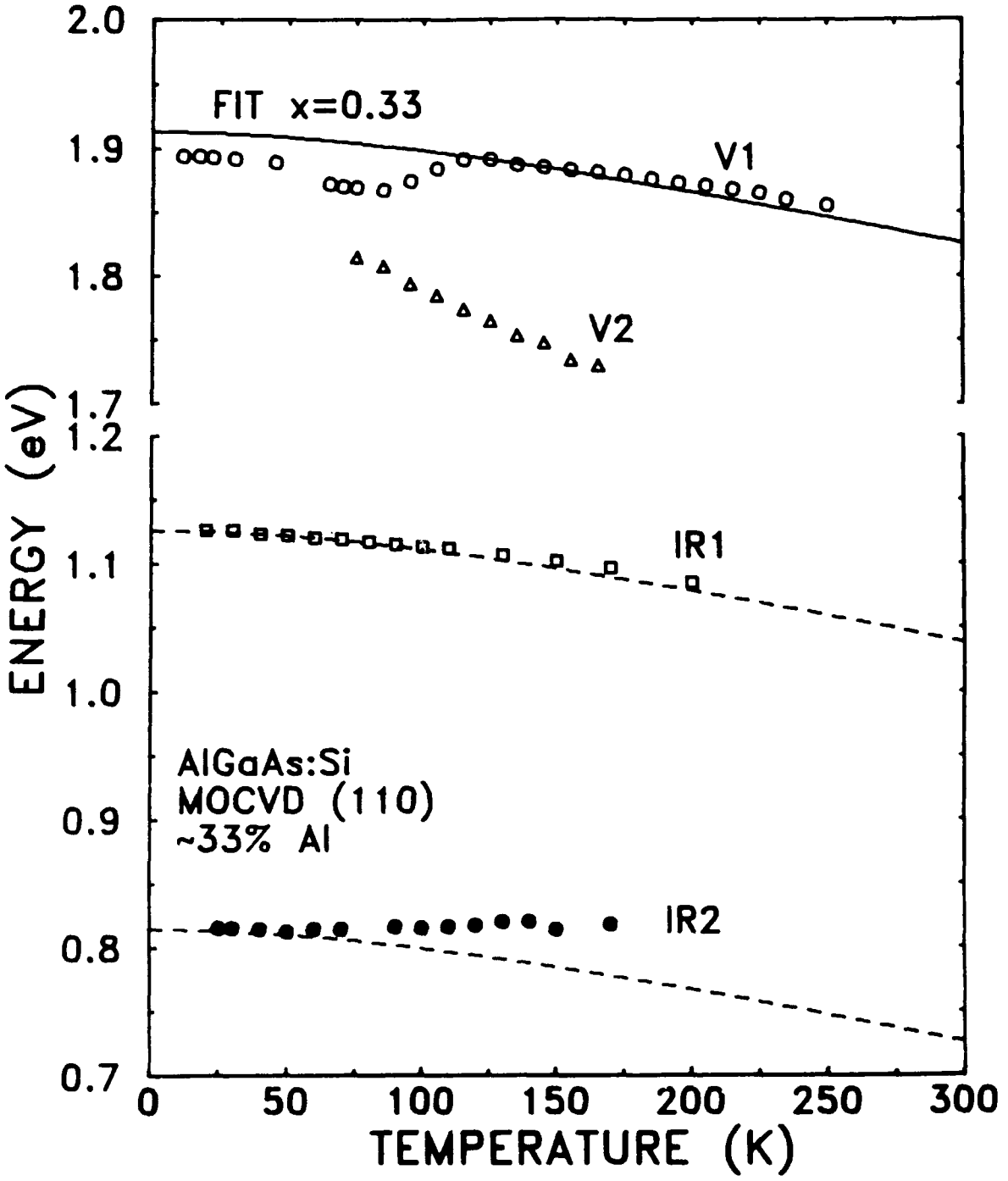

Figure 3.a.- Temperature dependence of PL peaks from figure 1.

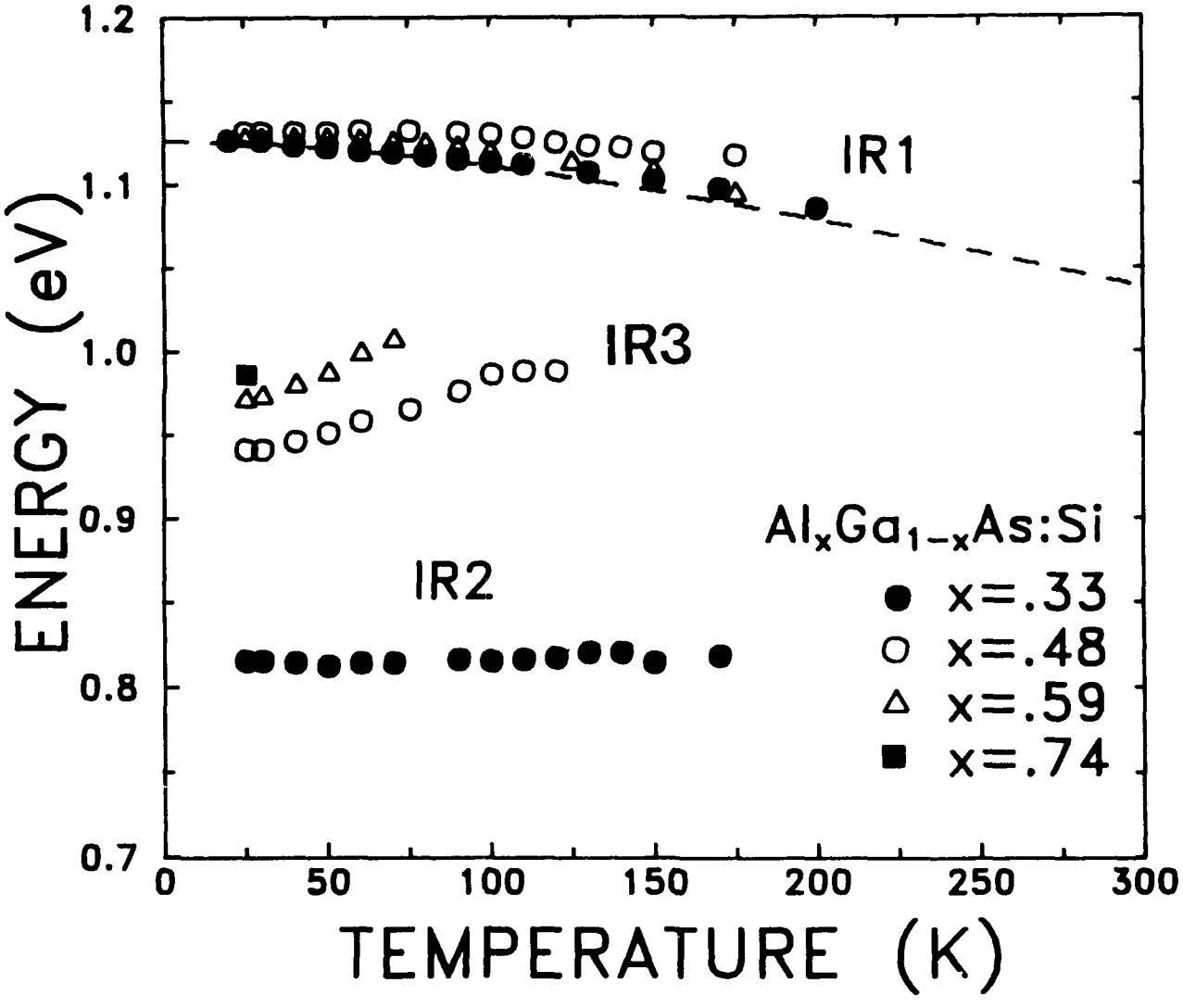

Figure 3.b.- Temperature dependence of infrared PL peaks from figure 2.

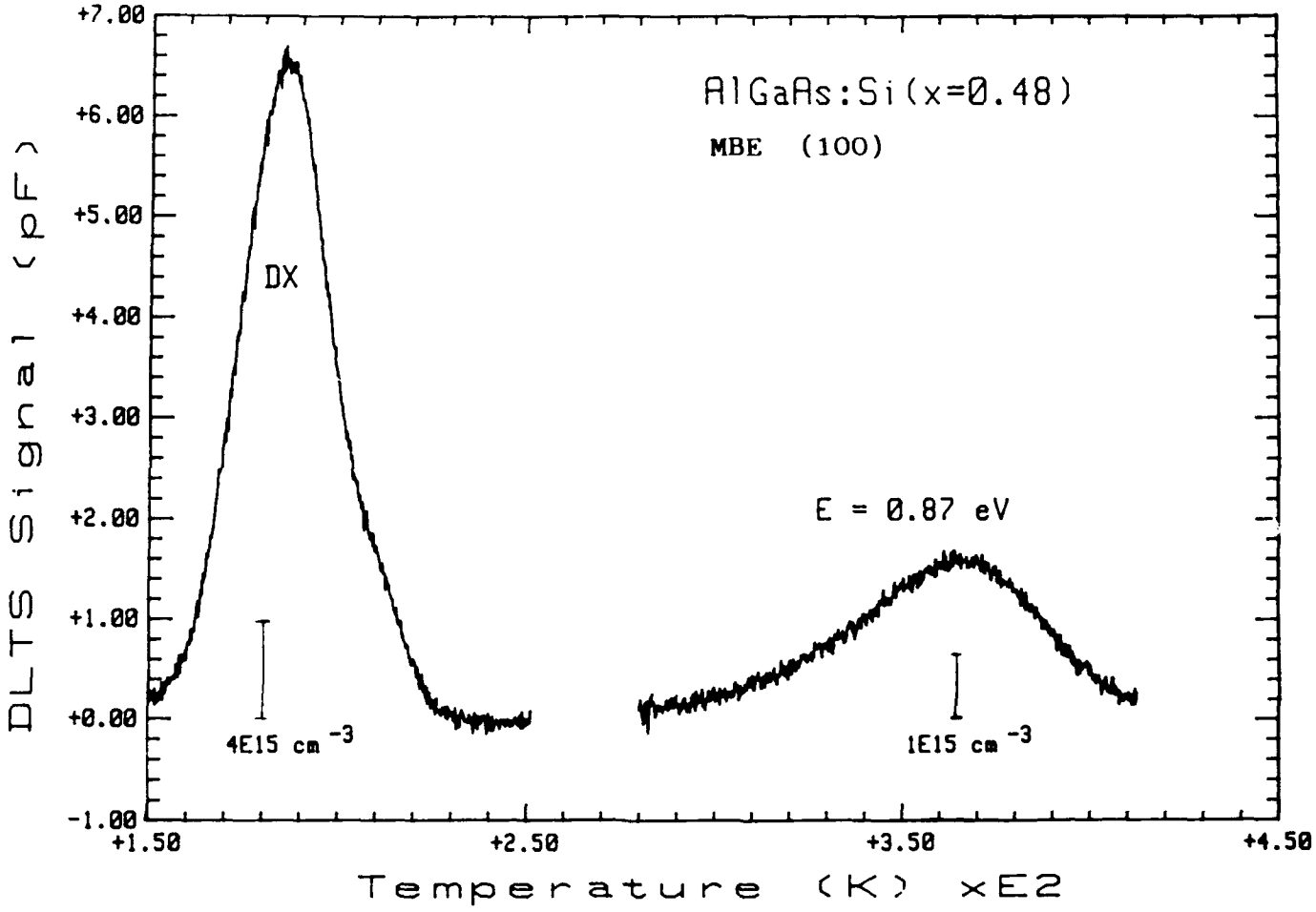

Fig. 4.a.

Figure 4.- DLTS spectra from Si:AlGaAs samples
a,b, and c, MBE grown.
d,e, and f, MOCVD grown.

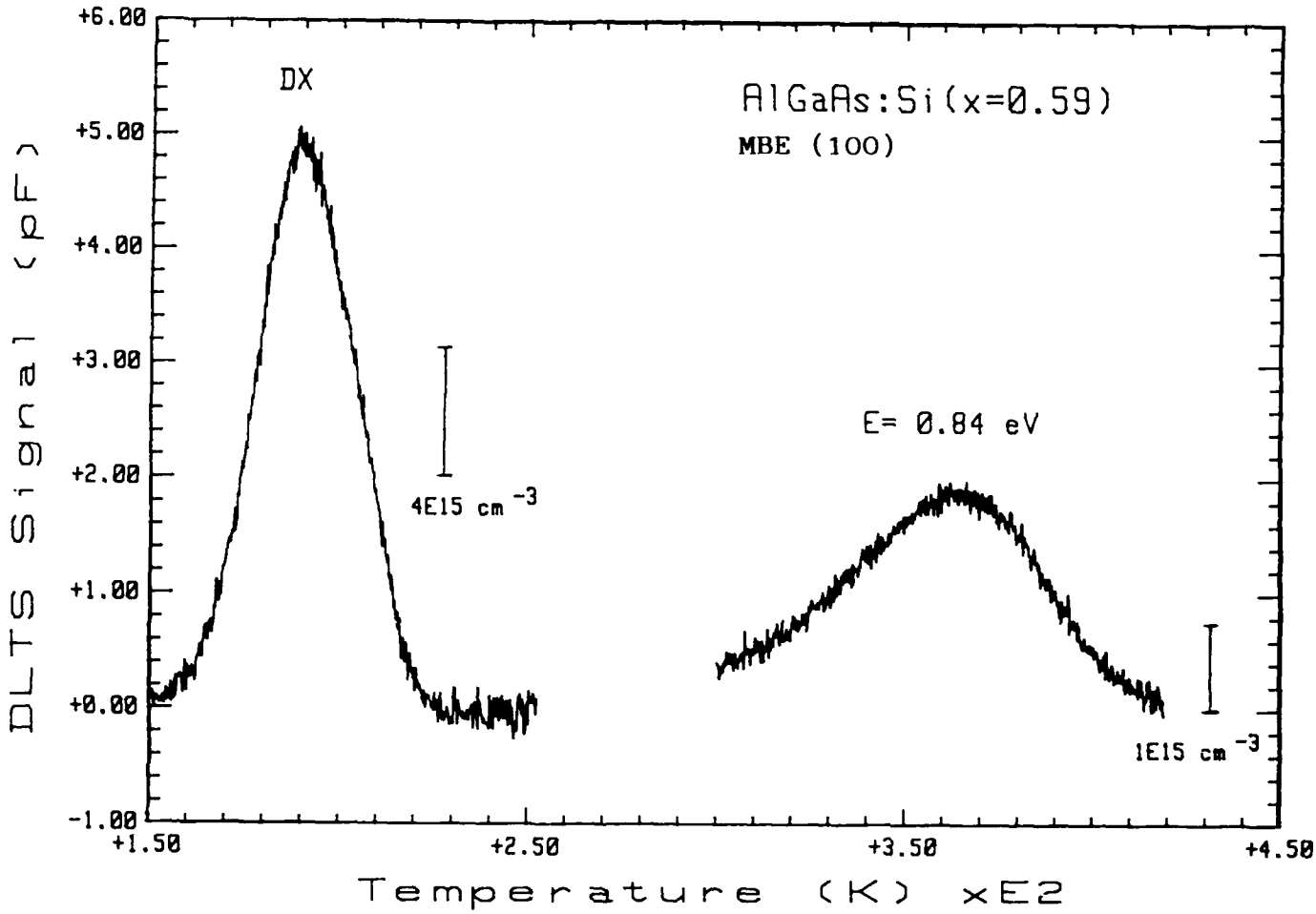
DX
AlGaAs:Si(x=0.59)
MBE (100)
E= 0.84 eV
4E15 cm -3
1E15 cm -3
DLTS Signal (pF)
+6.00
+5.00
+4.00
+3.00
+2.00
+1.00
+0.00
-1.00
+1.50
+2.50
+3.50
+4.50
Temperature (K) xE2

Fig. 4.b.

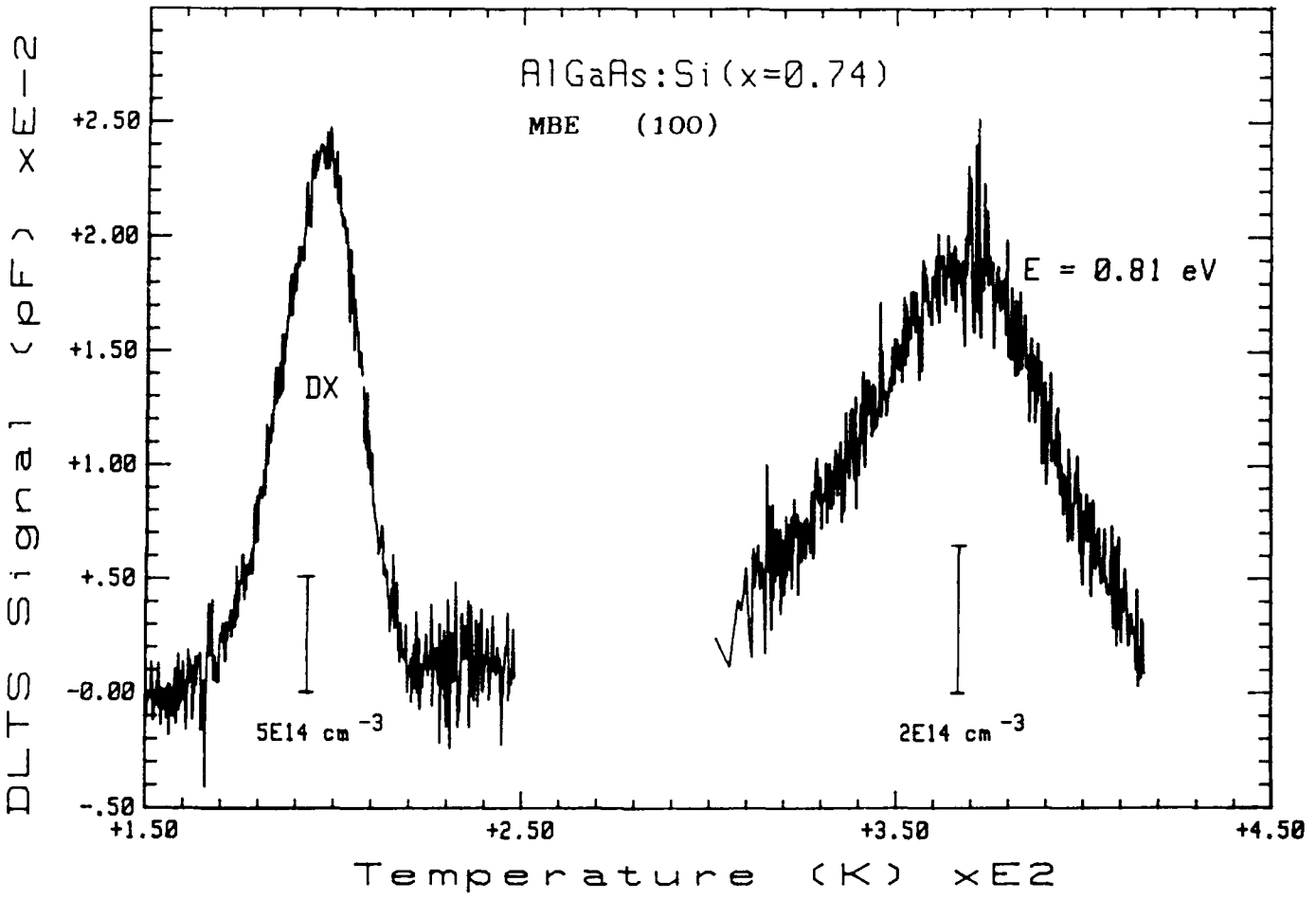
AlGaAs:Si(x=0.74)
MBE (100)
DLTS Signal (pF) xE-2
+2.50
+2.00
+1.50
+1.00
+.50
-0.00
-.50
DX
E = 0.81 eV
5E14 cm -3
2E14 cm -3
+1.50
+2.50
+3.50
+4.50
Temperature (K) xE2

Fig. 4.c.

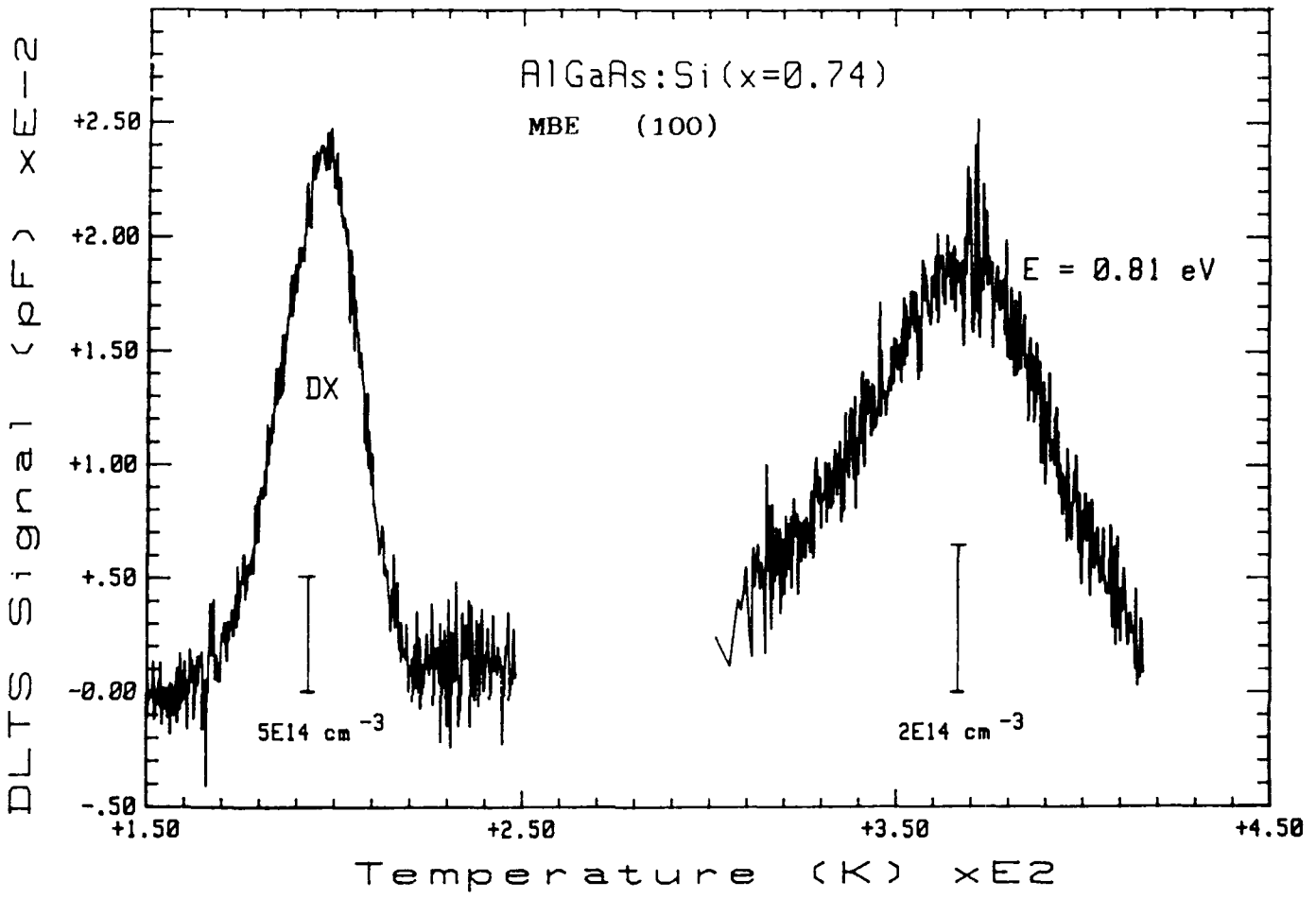
AlGaAs:Si(x=0.74)
MBE (100)
DX
E = 0.81 eV
5E14 cm -3
2E14 cm -3
DLTS Signal (pF) xE-2
+2.50
+2.00
+1.50
+1.00
+.50
-0.00
-.50
+1.50
+2.50
+3.50
+4.50
Temperature (K) xE2

Fig. 4.c.

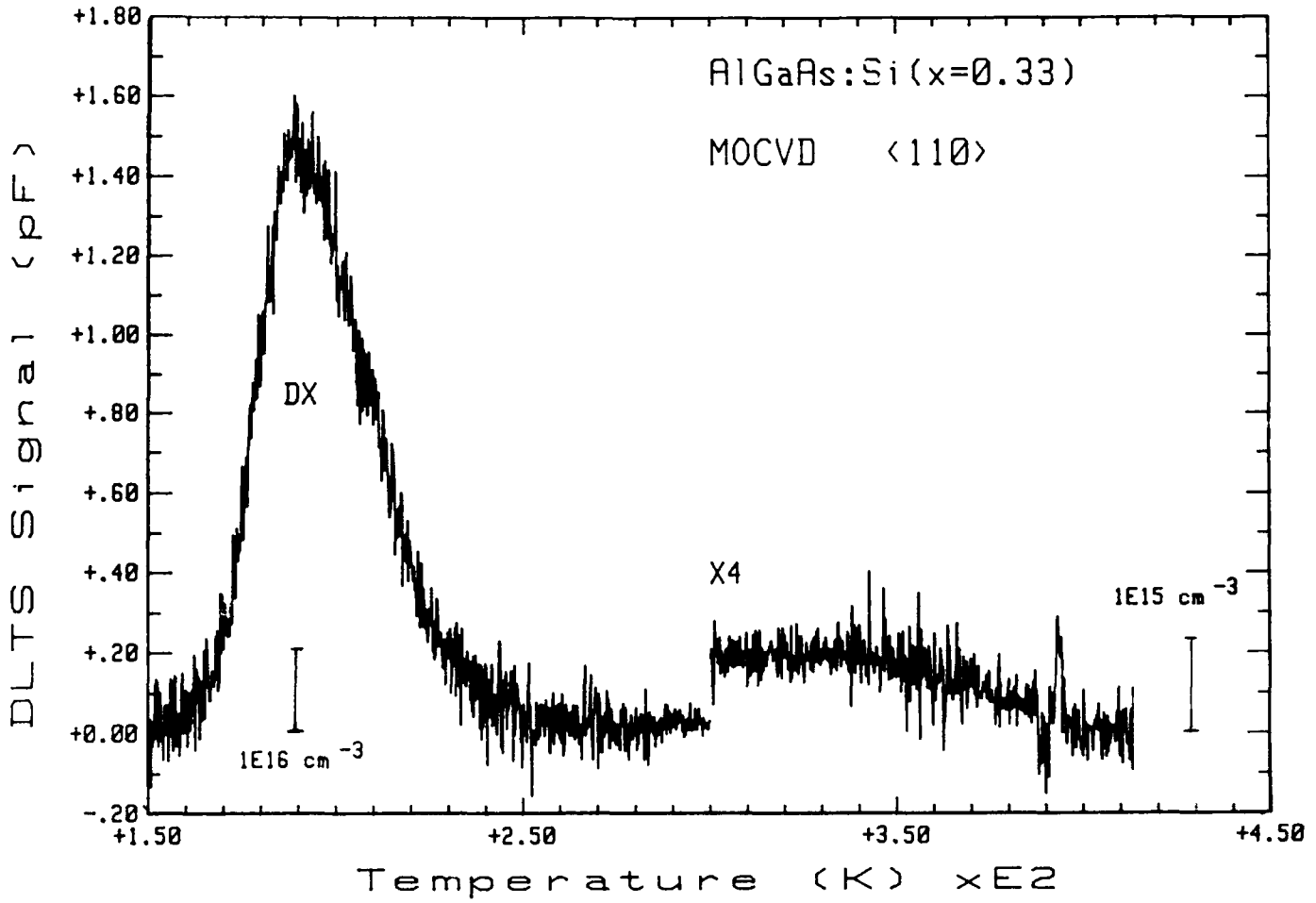
AlGaAs:Si(x=0.33)
MOCVD ⟨110⟩
DX
X4
1E16 cm -3
1E15 cm -3
DLTS Signal (pF)
+1.80
+1.60
+1.40
+1.20
+1.00
+.80
+.60
+.40
+.20
+0.00
-.20
+1.50
+2.50
+3.50
+4.50
Temperature (K) xE2

Fig. 4.d.

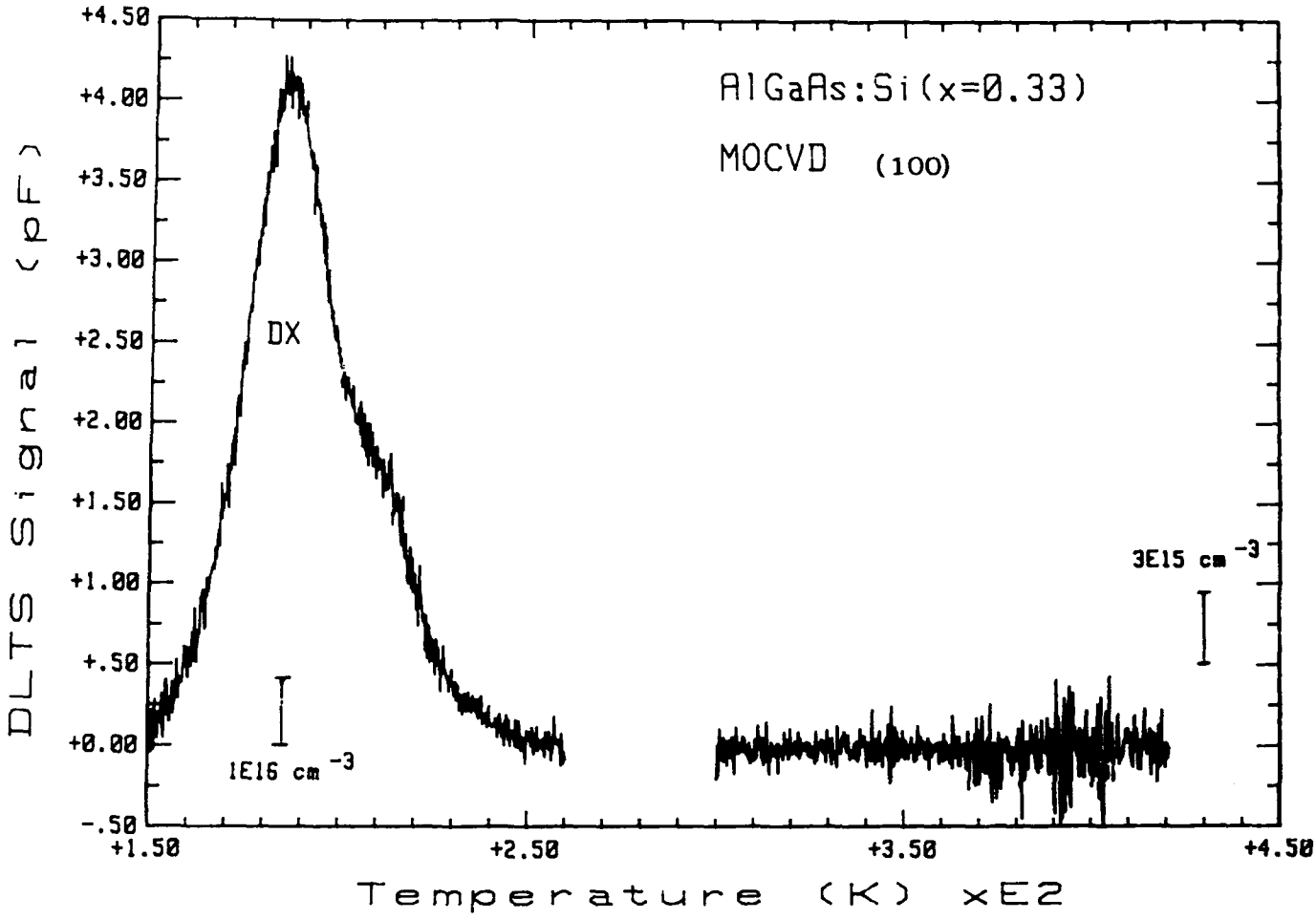
AlGaAs:Si(x=0.33)
MOCVD (100)
DX
1E16 cm -3
3E15 cm -3
DLTS Signal (pF)
Temperature (K) xE2
+4.50
+4.00
+3.50
+3.00
+2.50
+2.00
+1.50
+1.00
+.50
+0.00
-.50
+1.50
+2.50
+3.50
+4.50

Fig. 4.e.

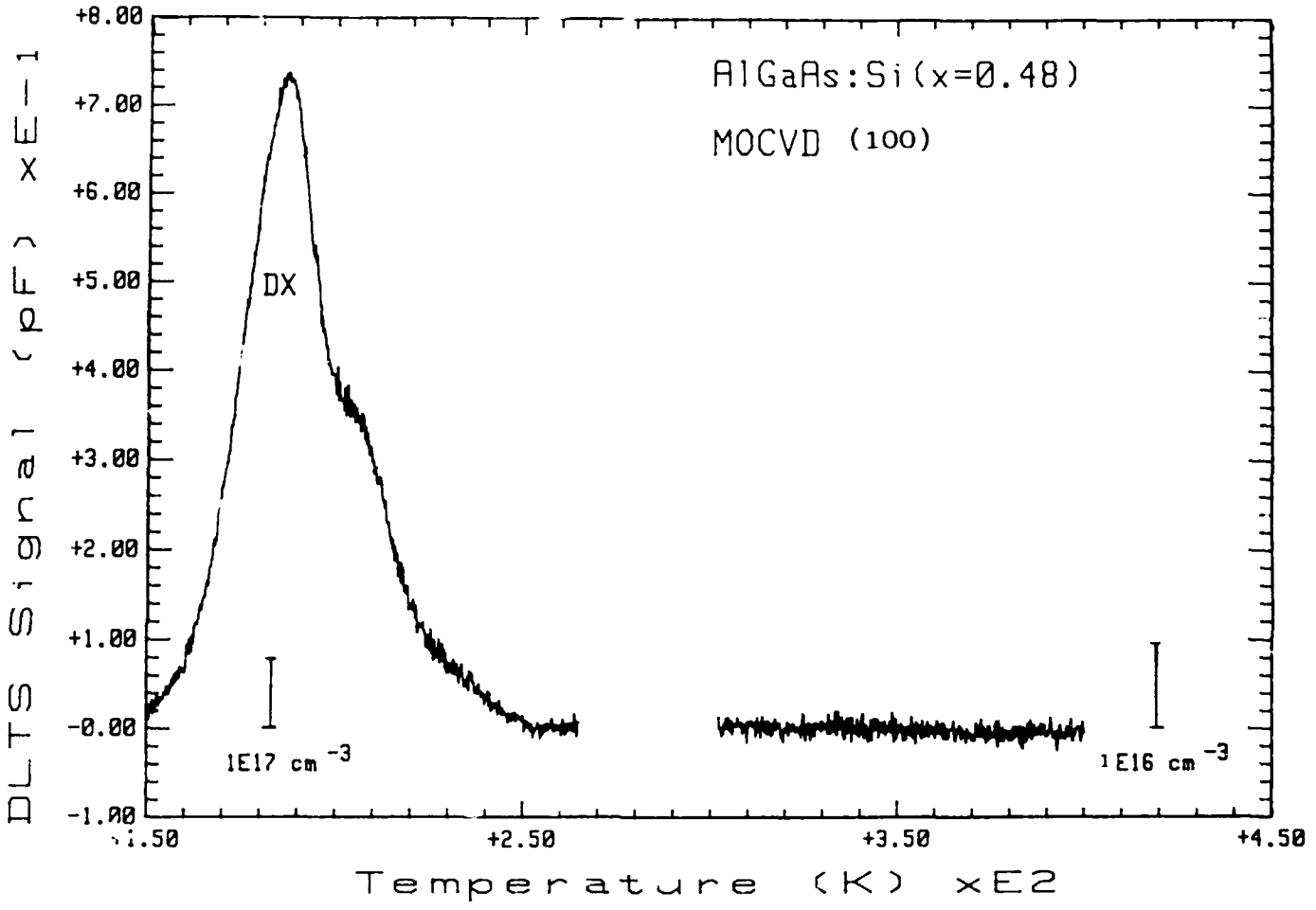
AlGaAs:Si(x=0.48)
MOCVD (100)
DX
1E17 cm -3
1E16 cm -3
DLTS Signal (pF) xE-1
+8.00
+7.00
+6.00
+5.00
+4.00
+3.00
+2.00
+1.00
-0.00
-1.00
+2.50
+3.50
+4.50
Temperature (K) xE2

Fig.4.f.

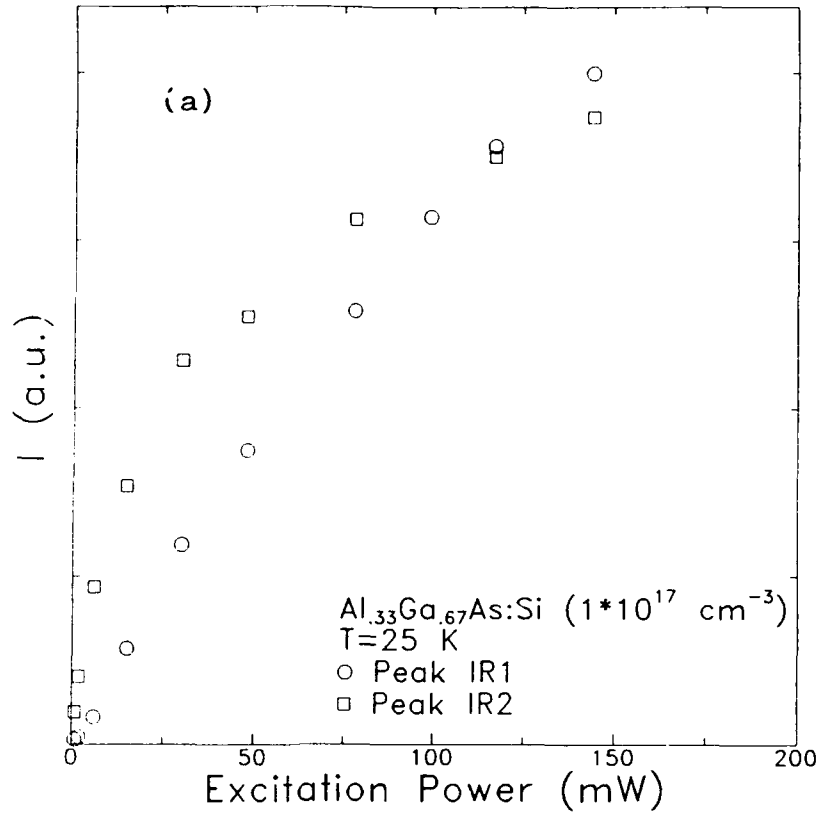

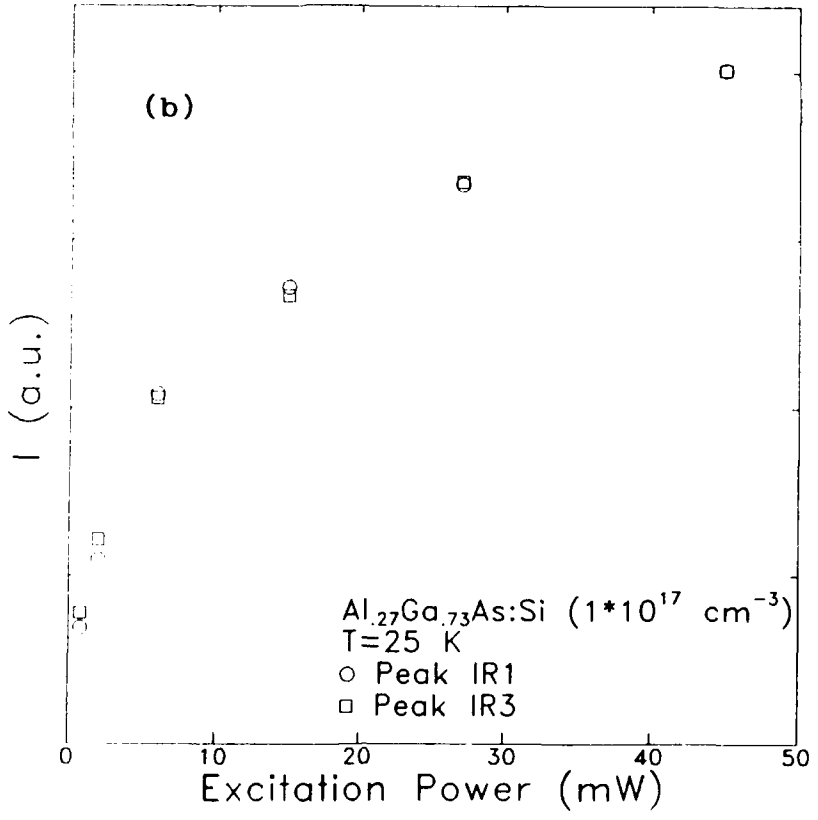

Figure 5.- PL amplitude versus excitation power
a.- Si:AlGaAs (33%) MOCVD

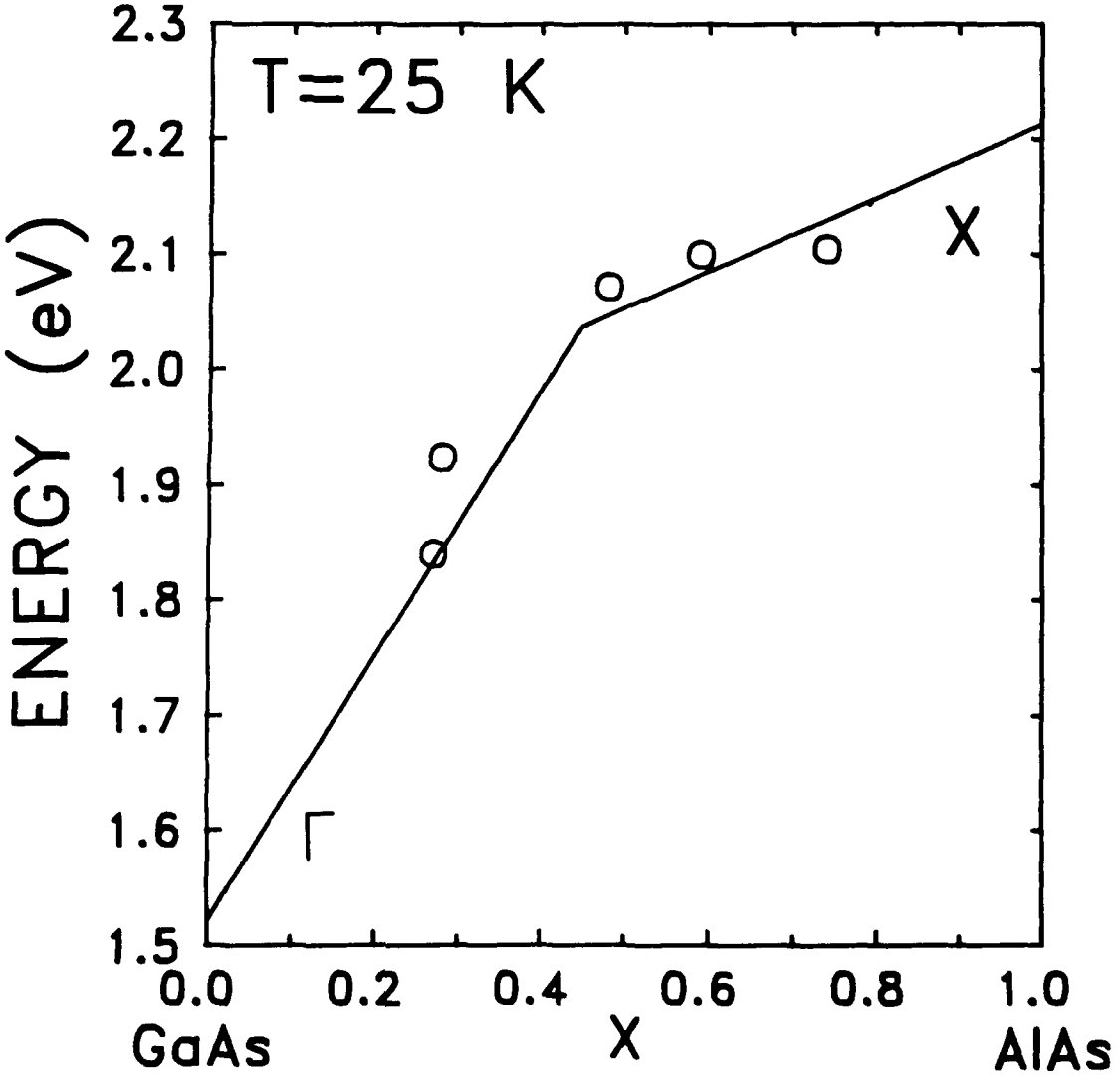

Figure 6.- Variation of (IR1 + IR3) energy versus Al composition in MBE grown Si:AlGaAs.

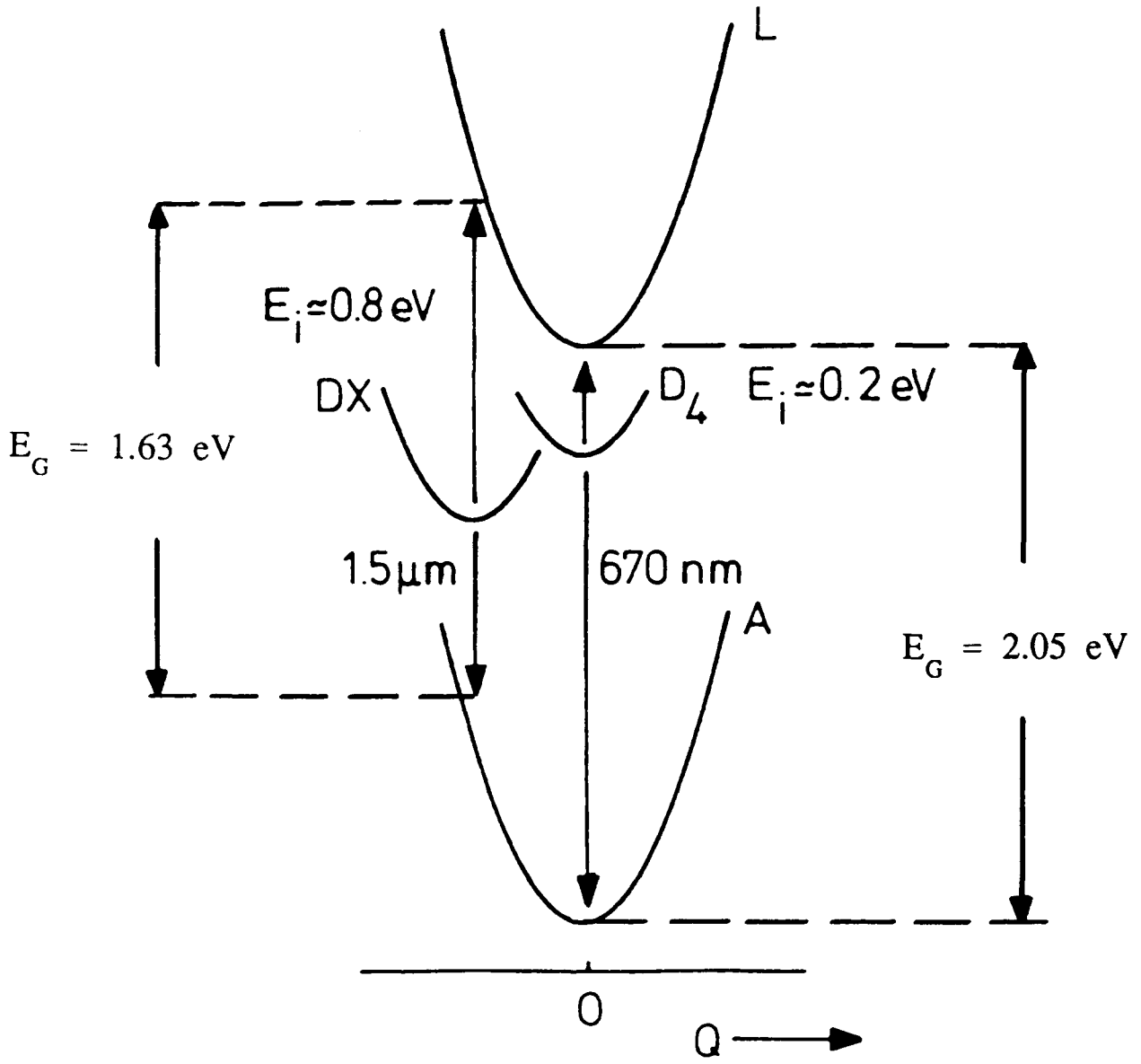

Figure 7.a

Figure 7.- Configuration coordinate diagrams showing PL transistors.
a.- from Henning in reference (1,2)
b.- from our work

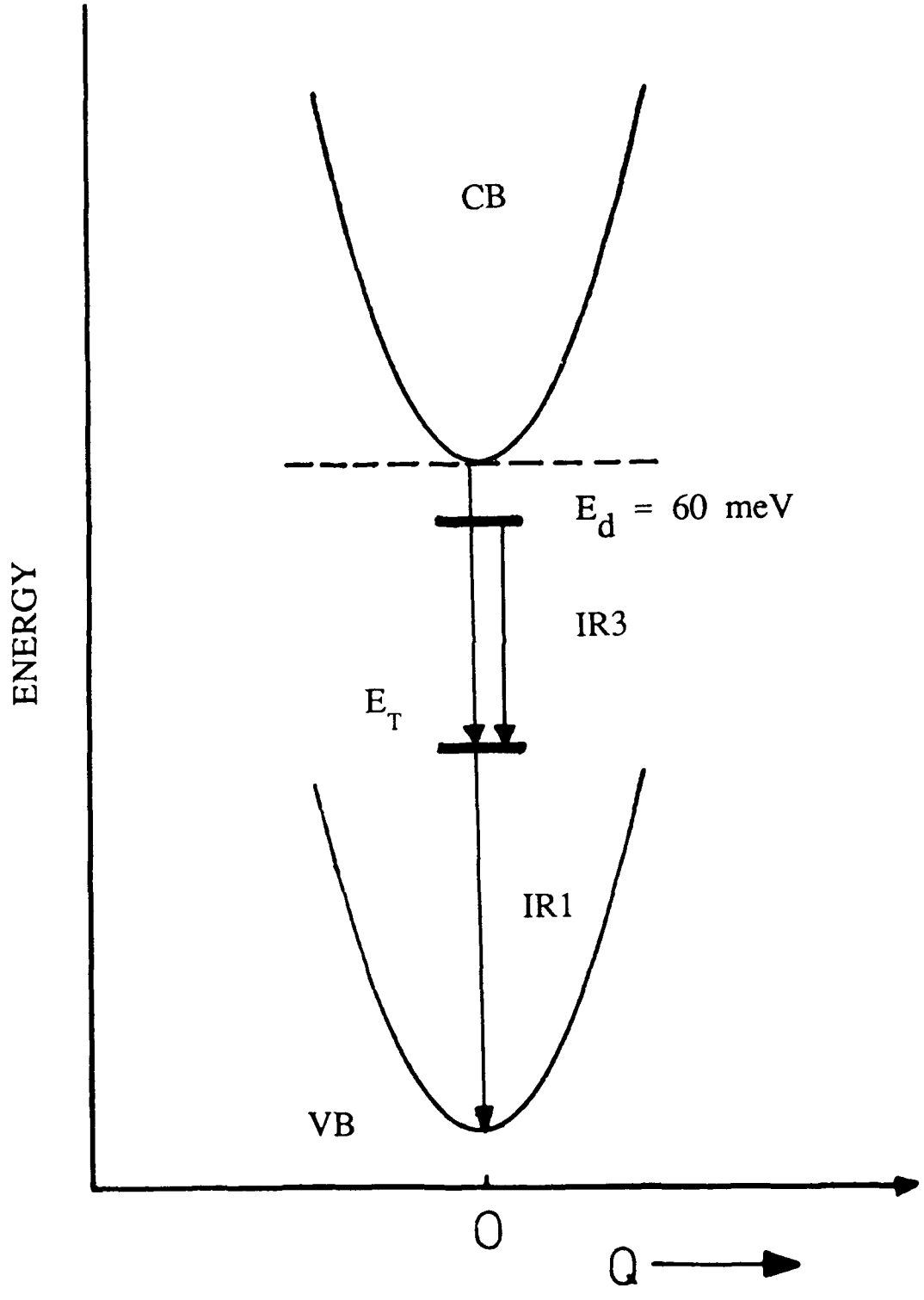

Figure 7.b.

REFERENCES

1) J.C.M. Henning and J.P.M. Ansems, Semicond. Sci. Technol., **2**, 1, (1987). Also: Appl. Phys. **A44**, 245, (1987) and Phys. Rev. **B38**, 5772, (1988).
2) J.M.C. Henning, J.P.M. Ansems, and P.J. Rosknoer, Semicond. Sci. Technol., **3**, 361, (1988).
3) D.V. Lang and R.A. Logan, Phys. Rev. Lett., **39**, 637, (1977).
4) D.V. Lang, R.A. Logan, and M. Jaros, Phys. Rev. **B19**, 1015, (1979).
5) R. Legros, P.M. Mooney, and S.L. Wright, Phys. Rev. **B35**, 7505, (1987).
6) P.M. Mooney, G.A. Northrop, T.N. Morgan, and H.G. Grimmeiss, Phys. Rev. **B37**, 8298, (1988).
7) E.A. Montie and J.C.M. Henning, J. Phys. C: Solid State Phys. **21**, L311, (1988).
8) J.C.M. Henning, E.A. Montie, and J.P.M. Ansems, in *"Defects in Semiconductors"*, Mat. Sci. Forum Vol. **38-41**, 1085, (1989), Trans. Tech. Publications, Switzerland.
9) S. Alaya, H. Maaref, and J.C. Bourgoin, Appl. Phys. Lett., **55**, 1406, (1989).
10) J.C. Bourgoin and A. Mauger, Appl. Phys. Lett., **53**, 749, (1988).
11) D.J. Chadi and K.J. Chang, Phys. Rev. Lett., **61**, 873, (1988); also: Phys. Rev. **B39**, 10063, (1989).
12) K.A. Khachaturyan, E.R. Weber, and M. Kaminska, same publication as in ref. 8, 1067.
13) T.N. Theis, Proc. 3rd Int. Conf. on Shallow Impurities in Semicond., Sweden (1988), Inst. Phys. Conf. Ser. **95**, (1989).
14) J.E. Dmochowsky, J. Langer, J. Raczynska, and W. Jantsch, Phys. Rev. **B38**, 3276, (1988).
15) E. Calleja, A. Gomez, and E. Muñoz, Appl. Phys. Lett., **32**, 383, (1988).
16) J.E. Dmochowsky, L. Dobaczewski, J.M. Langer, and W. Jantsch, Phys. Rev. **B40**, 9671, (1989).
17) H.P. Hjalmarson, S.R. Kurtz, and T.M. Brennan, unpublished.
18) G. Brunthaler, K. Ploog, and W. Jantsch, Phys. Rev. Lett., **63**, 2276, (1989).
19) M. Fockele, B.K. Meyer, J.M. Spaeth, M. Heuken, and K. Heime, Phys. Rev. **B40**, 2001, (1989).
20) W.W. Rhühle, K. Leo, and N.M. Haegel, Inst. Phys. Conf. Ser., **91**, 105, (1987).

21) M. Tajima, Appl. Phys. Rev., **46**, 484, (1985); see also: Appl. Phys. Lett., **53**, 959, (1988).

VII. INTERNAL PHOTOIONIZATION IN AlGaAs/GaAs HBT's : BENEFITS FOR THEIR LOW TEMPERATURE OPERATION

VII.1. INTRODUCTION

The low temperature behavior of GaAs/ AlGaAs devices is markedly influenced by the properties of the deep donors present in the n-type layers (for Al compositions greater than 0.2). If we consider first field effect transistors, in devices like AlGaAs/GaAs HEMT's, the carriers available in the channel proceed by thermal emission from the deep donors in the AlGaAs layer ($x \cong 0.3$). Then, any electron channel concentration change is primarily related to thermal emission and capture processes from the AlGaAs deep donors (figure 1).

As temperature is lowered, electrons tend to be captured by the deep donors and, at sufficiently low temperatures, a collapse of the HEMT I-V characteristics is produced. Such behavior has been extensively studied in Si doped HEMT's, because they do not work at 77K. In this case, Si has the largest capture barrier energy (E_b) of all deep donors studied, and T=77K is low enough to prevent any practical thermal emission from the deep donors. This result moved to fabricate HEMT's using Se, Te or Sn dopants, all of them having lower capture barrier than Si. For a given x, the relation $E_b^{Si} > E_b^{Se} > E_b^{Sn}$ is held, and at 77K Se and Sn deep donors have finite electron emission rates [1-5].

Two solutions have been engineered to avoid the Si doped HEMT collapse. One is the use of an external light source that will photoionize the deep donors, and because the large E_b^{Si}, those electrons do not come back to the deep donors at 77K. The other attempted solution is to use GaAs/AlGasAs superlattices and planar doping techniques, that prevent, partially, that the channel electrons go back to the deep donors while cooling the HEMT [6,7].

Let us now consider the behavior at low temperatures of heterojunction bipolar transistors (HBT's and DHBT's). First, the emitter base junction has an structure as described in **Section IV** of this report. As

we cool it down, electrons are captured by the deep donors, the E-B capacitance decreases, and the SCR and CDR layers, indicated in figure 1 of **Section V**, are produced. Again, depending of the Al mole fraction and the dopant being used, the capacitance collapse is produced at even lower temperatures, and if the emitter thickness is comparable to L_D at such temperatures, a markedly non neutral emitter region may be produced. Related to this fact, emitter series resistance will increase.

What is new now is that, in the HBT devices, once they are biased in their active mode, *photons are produced by radiative recombination in the GaAs, and these photons produce internal photoionization of the deep donors.* Since we use lower Al mole fractions than in MODFET's (x = 0.26 instead of x = 0.33), we have more guaranteed the PPC effect at 77 K, due to the higher capture barrier E_b, than in MODFET devices. Therefore, the internal photoionization acts in a cumulative way, and the AlGaAs region becomes an special one without trapped electrons at the deep donor levels.

In this Section, studies on the low temperature behavior of AlGaAs/ GaAs HBT's are presented. Si and Sn dopants have been basically considered, because they represent the highest and the lowest capture barrier energies for the deep donors in AlGaAs. Studies have been made mainly at 77K, as a reference.

The aim has been: to develop characterization techniques that allow to know the effective emitter donor doping level, and the free electron concentration at low temperatures, using C-V techniques; to study the internal photoionization processes in the HBT's; to obtain information about the DC and low frequency HBT performance at low temperatures, as compared to room temperature; to find criteria about which dopants to use for low temperature applications of HBT devices.

VII.2. SAMPLES

A variety of Si doped HBT's grown by MOCVD were studied in this work. A set of offset layers between emitter and base were considered, and both simple grading and SL graded E-B transitions were analyzed. The general structure is depicted in figure 2. Large area devices were used, not suitable for HF operation, but quite adequate for static and LF characterization. From the geometry indicated in figure 2, a significant base access resistance is foreseen, although it is low enough to allow good C-V measurements. Finally a set of Sn doped devices, fabricated by LPE, with simple abrupt E-B design, were prepared with the same masks set.

VII.3. THE EMITTER-BASE CAPACITANCE

The n-AlGaAs/p^+-GaAs emitter-base capacitance will behave with temperature as described in **Section IV**. Let us first consider that Si is used as the donor, and that the emitter thickness is reasonable larger than the Debye extrinsic length (L_D). As we cool down to 77K, three regions are formed in the emitter, as indicated in figure 1 of **Section V** of this report. The relative thicknesses of these layers depend on the voltage being applied to the junction while cooling to 77K. First, a region of width W_1, of fully ionized donors is formed (SCR, I≈100%) near the p^+ region. W_1 will be smaller if we have cooled under a forward junction voltage. In this region, capture of electrons in the deep donor levels *does not occur*, since there is **no** free electrons to be captured.

The second region is the charge depleted region (CDR), of width $W_2 - W_1 \cong L_D$, and that is sandwiched between the SCR and the so called quasi-neutral region, that actually becomes cuasi-neutral only $\cong 3L_D$ far away from the SCR region (figure 1 **Section V**). If we could cool down to 77 K at a *very slow rate,* the free electron concentration in the cuasi-neutral region would be given by the very low ionization factor I(77 K) corresponding to thermal equilibrium at 77 K ($I<10^{-2}$, typically). This is an unreal situation for $Al_{0.26}Ga_{0.74}As$, since from the t_a(122.5K) obtained in **Section V** for samples having this Al mole fraction, we obtain t_a(77K)≅ years. In other

words: we have Persistent Photo Conductivity. Therefore, the free electron concentration in the cuasi-neutral region after cooling down by immersion in liquid nitrogen for example, will be a low one: $I \times N_d$, but higher than the corresponding to thermal equilibrium at 77K (I>I(77K)).

If the emitter is thin, and/or it has been frozen under a large reverse voltage, it may happen that the full, short, emitter is occupied by the SCR and the CDR regions. Let us assume that this is not the case, and we perform at 77K a C-V profile in a Si doped emitter that has been cooled while O V was applied to the B-E junction. According to **Section IV**, capacitance will be due to the charges reacting at edge W_2, at the end of the CDR, and the W_1 edge *will remain fixed for practical purposes* ($t_a(77K) \cong$ years, $\tau_n = t_a/I^2(77K)$ much higher: capture and emission processes are frozen at 77K). At reverse voltages, the $1/C^2$-V plot will give information about I, or the ionized deep donors in that region. As we increase the junction voltage towards forward bias, we will reach a point where W_2 reaches the W_1 edge, and the $1/C^2$-V plot will indicate *the total* $N_d^+ = N_d$ *ionized doping level of region* W_1. Then, a marked break is produced in the $1/C^2$-V plot, like the one obtained for a p^+-n-ν structure, being $n = N_d$ and $\nu = I \times N_d$.

This is a useful technique to determine the doping level (N_d) and the *remaining* free electron concentration after cool down the sample. The break voltage, from one region to another, will be determined by the applied junction voltage while cooling down the sample. Figure 3 shows some of these results, and also indicates that under high enough reverse voltages the emitter ohmic contact is reached, allowing a direct measurement of the AlGaAs layer thickness. Figure 3 also shows that, in order to reach the ohmic contact at room temperature (W_1 *moves* as the reverse voltage increases), a reverse voltage higher than 25 volts is needed. This voltage would probably destroy the sample, being impossible to measure the layer thickness at room temperature by means of C-V measurements.

These results, at 77K, for Si-doped HBT's, are consistent with the fact that E_b^{Si} is large, and at that temperature no thermal emission or capture processes are allowed (persistent capacitance effect). For the case of Sn doped samples, and as explained in **Section IV** of the report, capacitance will be given by a combination of reacting charges at W_1 and W_2,

and the 1/ C^2-V two slope regions will be produced by cooling below 77K or having a faster C-V scanner.

VII.4. DEEP DONOR INTERNAL PHOTOIONIZATION

If we still consider the case of Si doped HBT's, as above, one of the consequences of the above technique is that the ionization coefficient in the quasi- neutral region can be tracked versus transistor operation, just by tracking the slope corresponding to the ν region (the one corresponding to the W_2 edge in the quasi- neutral region) at the 1/ C^2-V plot.

A series of experiments were made to see the evolution of the deplexable charge *(that may be approximated to the free electron concentration)* at W_2. First, while keeping the B-E short circuited, to avoid any B-E self biasing and hole injection into the emitter, the B-C heterojunction of the DHBT is forward biased. Figure 4 shows how the slope at W_2 changes with time, and in a few minutes of a collector current density of only 50 A/cm^2, all the deep donors at the emitter are fully ionized, and once the B-C junction is set at 0V, *the ionized deep donors remain ionized, as if we have a very shallow donor that is with I=100% at this temperature.* These results are explained through the deep donor internal photoionization due to the photons generated at the base- collector "light emitting diode". This photoionization process will be much faster for emitter current densities as the ones required ($\cong 10^4$ A/cm^2) to achieve good HF performances. Again the B-E heterojunction is a similar L.E.D. and there is a self-photoionization process as the emitter injects minority carriers in the base. For a DHBT device, photoionization takes place in both the emitter and collector regions.

A series of experiments were addressed to determine the role of hole injection into the emitter, as a potential path to recombine the trapped electrons at the deep donors. The E-B junction was forward biased under controlled time and current intensity conditions. Again, the evolution of the 1/C^2-V slope at W_2 allows to determine the ionized deep donors versus time. The question is to determine if the deep center ionization is

solely due to the generated photons, or there is a number of electrons at the deep donors being captured by the holes injected into the emitter. Simplified one-dimension calculations indicated to us that experimental results can be explained by an internal photoionization process, requiring for the DX centers to have a optical cross section of 10^{-16} cm^{-2} for hν=1.51 eV (GaAs bandgap at 77K). The data of ref.(8) indicate that, for such photon energy, $\sigma_{op} \cong 10^{-17} cm^{-2}$ in $Al_{0.3}Ga_{0.7}As$, not far from our estimation, taking into account the very simple 1D model used.

The role of hole injection was estimated determining a lower limit for $J_n/J_p \geq 10^{-2}$, for our structure, and then requiring a hole capture cross section larger than $3 \times 10^{-9} cm^{-2}$ to explain our experimental results. Evenmore, no capture barrier for holes was considered. The required such large hole capture cross section is not consistent with experimental facts in compensated layers. In layers where Zn has moved into the n-type layer, there is no indication of recombination currents (ideality factor ≅ 2) due to such high hole capture cross section.

Then, as a conclusion, we think that the emitter deep donor ionization process, once the transistor starts to work in their active mode, is due to internal photoionization caused by the photons generated in the GaAs region.

For the case of Si at 77 K, THE IMPORTANT POINT IS THAT THE Si ATOMS WILL REMAIN IONIZED. However, for Sn atoms at 77 K, thermal capture and emission processes are produced, and a dynamic equilibrium will be produced with the internal photoionization processes. But the net consequence is that Sn atoms in the HBT emitter are not fully ionized, thus increasing both bulk and contact emitter series resistance.

A detailed analysis of the $1/C^2$-V plots after photoionization revealed a curvature, as shown in figure 5. This result is understood as reflecting the fact that, near the base, the photon density is greater than inside the emitter, due to reflections and lateral illumination effects. Then, a waveguiding effect takes place (photons in the base region are randomly emitted, not only perpendicular to the B-E and B-C junctions), and the photoionization rate is lower inside the emitter than near the base: photons traveling in both directions: perpendicular and parallel to the

interfaces. Speaking from an optical point of view, the DHBT structure is similar to the semiconductor laser one, without optical feedback.

VII.5. HETEROJUNCTION BIPOLAR TRANSISTORS AT LOW TEMPERATURES

The operation of HBT's at low temperatures has several aspects related to base transport factor, injection efficiency, DC current gain, etc. We focused our work on the emitter layer behavior at low temperatures, and as a function of the dopant used. We try to link the results presented in **Section VII.3** with the HBT operation. The small signal low frequency behavior of the HBT has been also studied.

At 77K, a reduction by a factor of 2 is found in the DC current gain, for both Si and Sn dopants. As indicated above, for Si, once the transistor is in operation, the emitter free electron concentration is increased. The effects in the AC transistor performance have been studying by using the HBT as an emitter follower, and comparing, for the same conditions, Si and Sn doped devices.

For the Si doped emitters it was found that the emitter resistance is practically the same at 77K *than* at room temperature. It is envisaged that the low frequency noise will be markedly reduced at 77K. We conclude that the operation of Si doped HBT's at 77K needs to be explored, because a reduction of parasitics and GR noise may be obtained. On the other hand, Sn doped transistors present a degraded behavior at 77K, with an increase in the emitter series resistance by more than two orders of magnitude. Figure 6 summarizes the circuit and parameters determined in a series of samples.

This result may open a door for a positive property of the Si deep donor in HBT's working at 77K. We may remember than in HEMT's its effect is always deleterious.

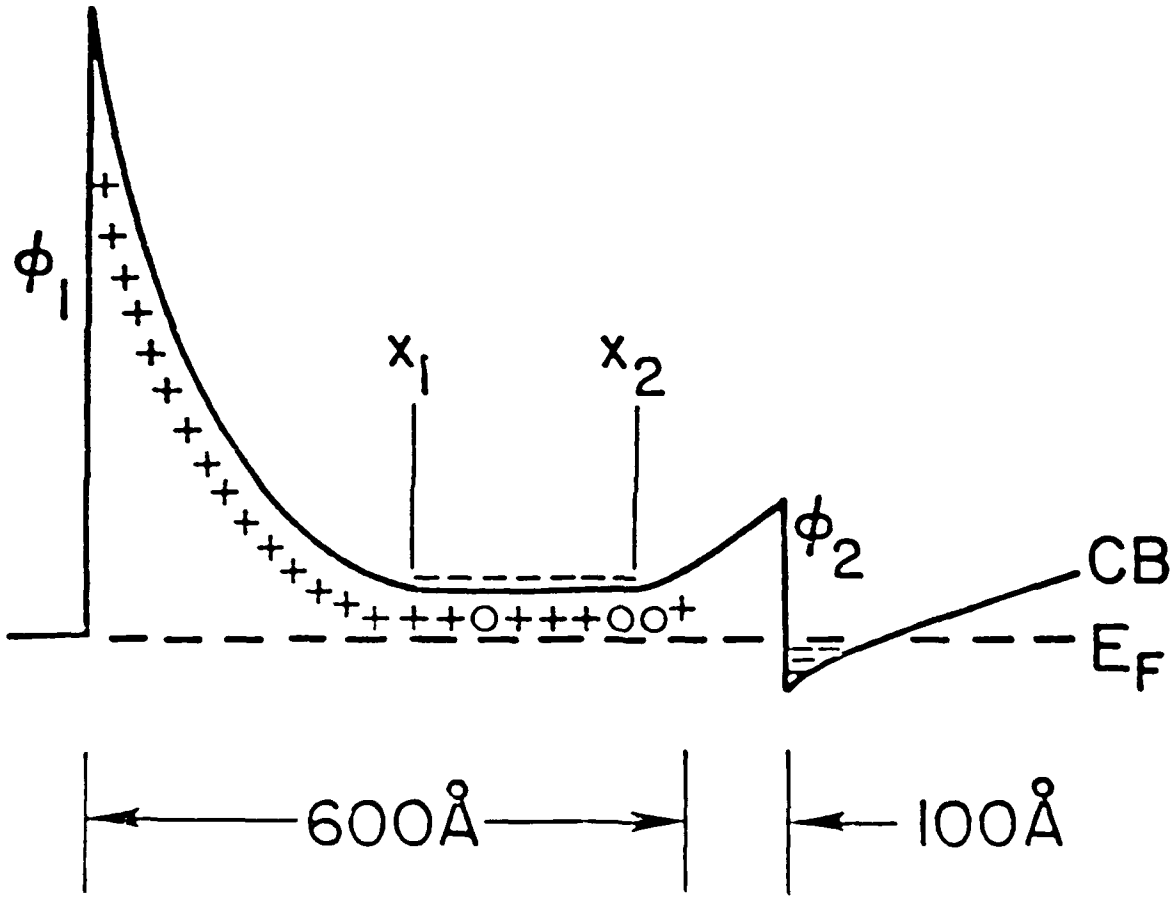

Figure 1. Conduction band diagram of a HEMT

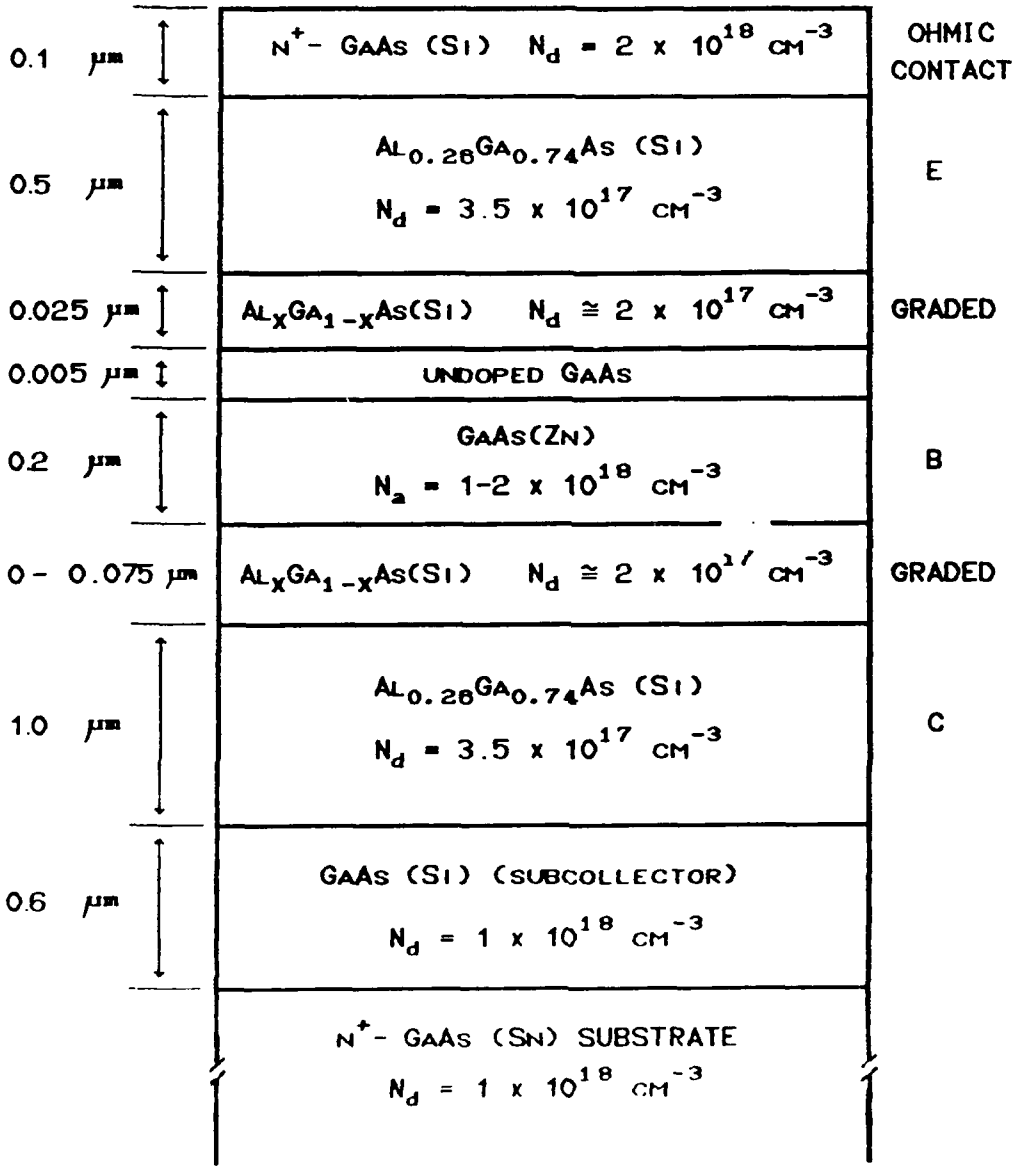

Figure 2. DHBT structure grown by MOCVD.

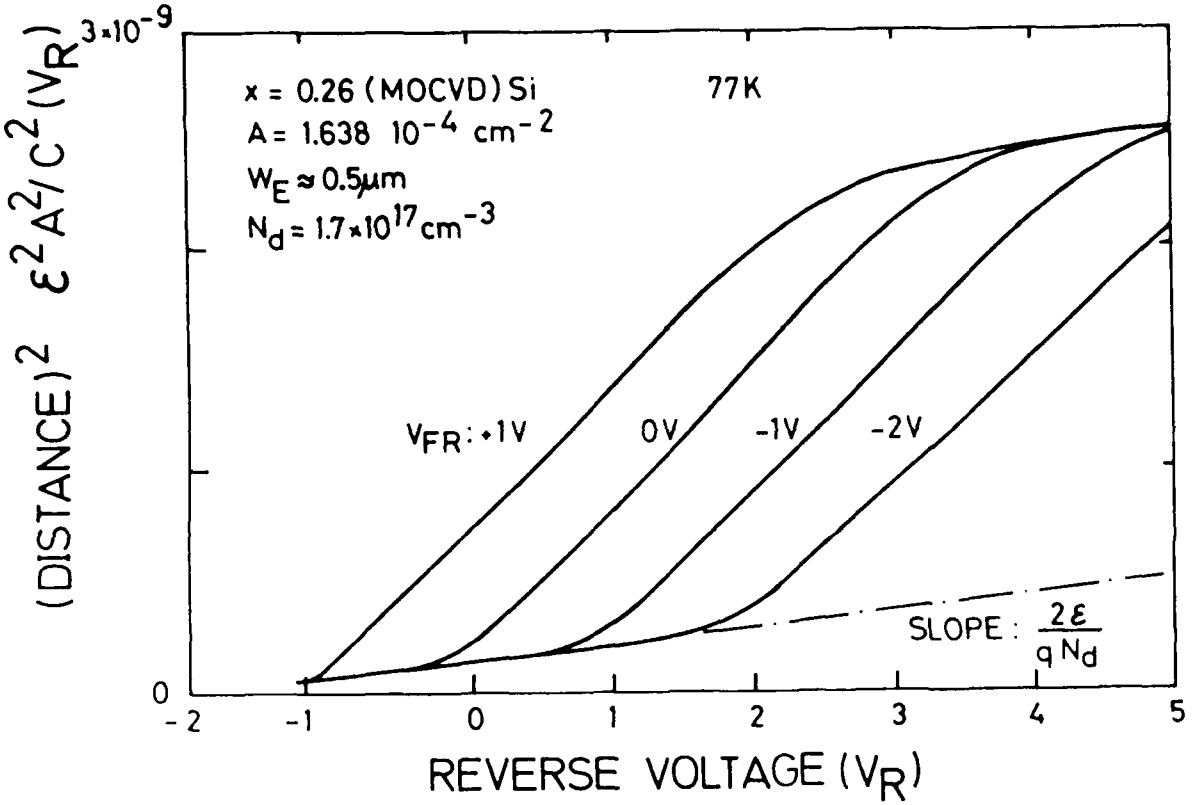

Fig. 3. Capacitance-voltage plots in an E-B junction (Si doped) at 77K. The two slopes indicate the total ionized dopant (N_d)at the SCR region, and the ionized dopant at the quasi-neutral region (IxN_d). Depending on the voltage applied while coaling the break point is obtained at different voltages.

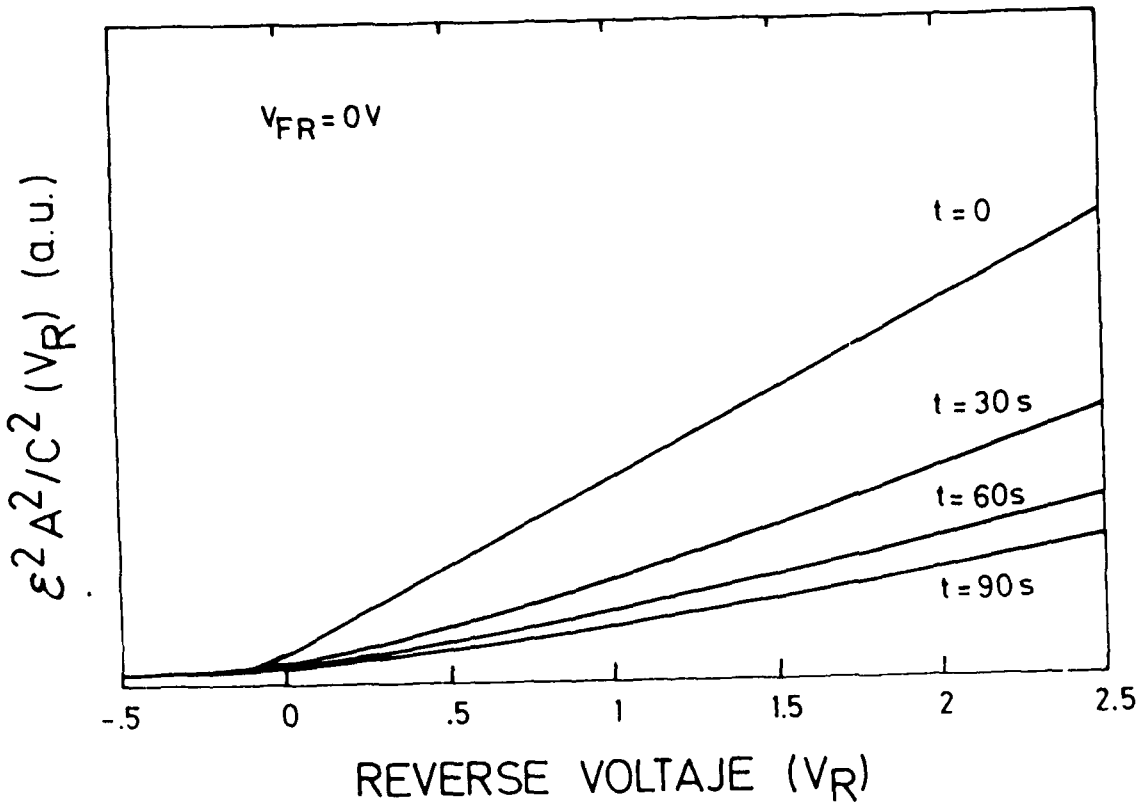

Fig. 4. Photoionization of the deep Si centers due to the photons generated at the GaAs.

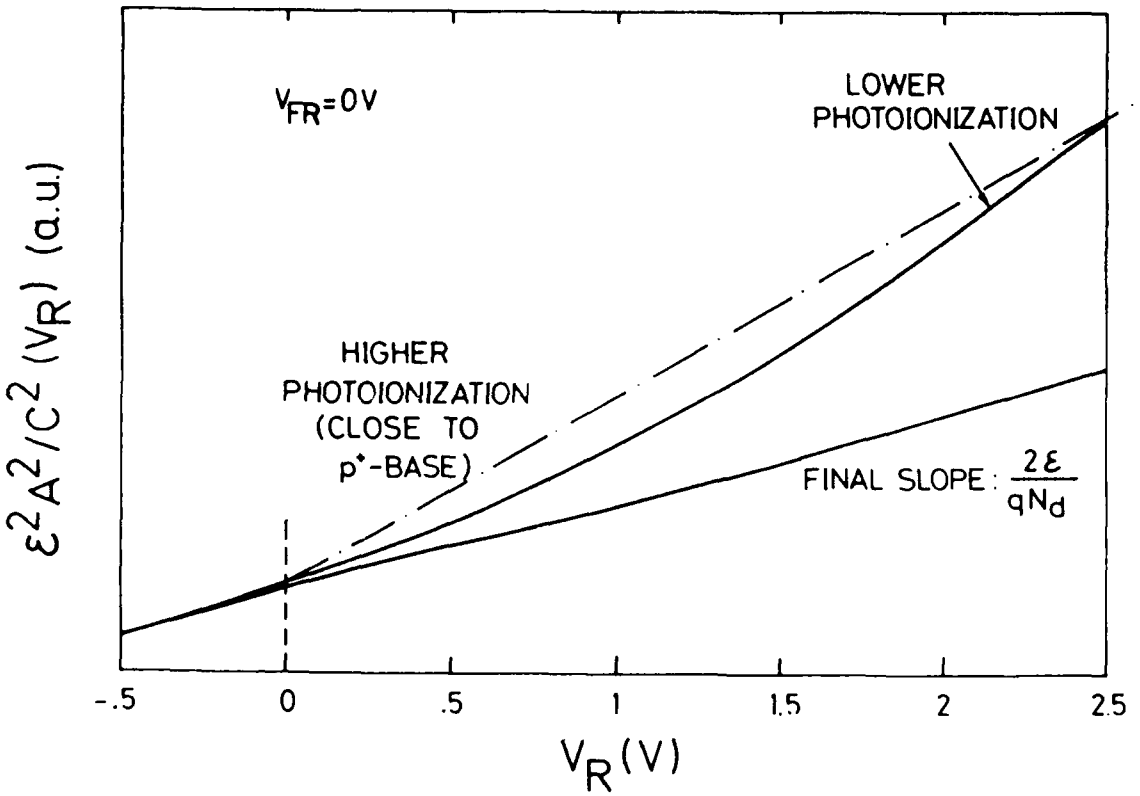

Fig. 5. Detail of the $1/c^2$-V slope at low and higher reverse voltages, indicating that the ionizing photon flux is higher near the GaAs base (larger I), than at the emitter interior (lower I).

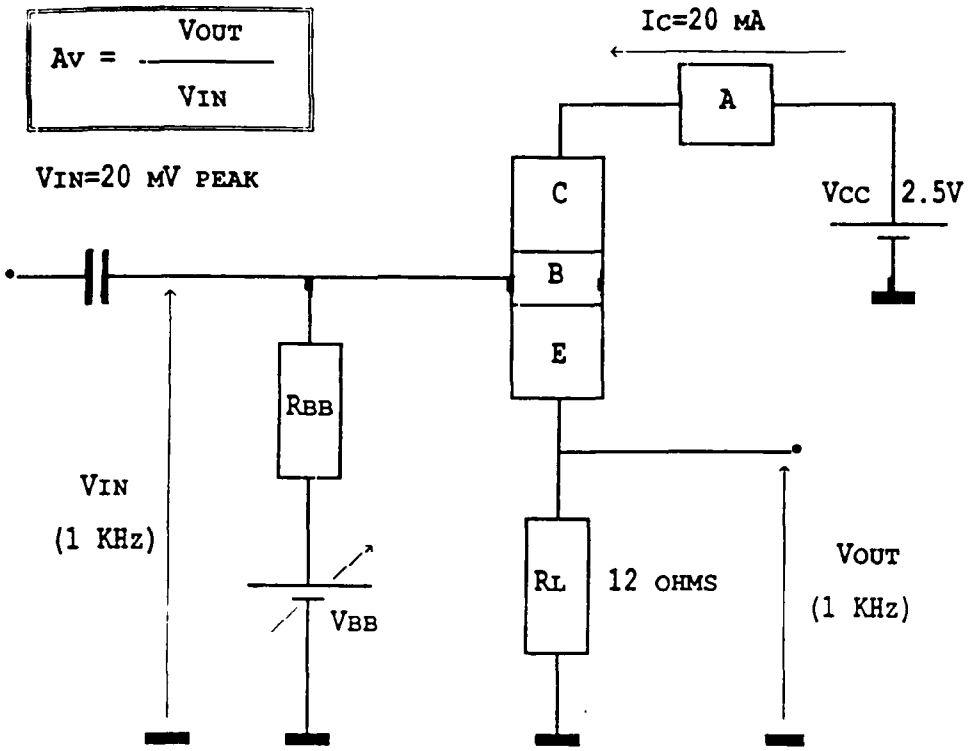

SAMPLE	DONOR	β(300 K) AT Ic=20 mA	β(77 K) AT Ic=20 mA	Av(300 K)	Av(77 K)
HBT DT153-9	Sn	110	30	0.825	0.287
HBT DT153-10	Sn	110	30	0.812	0.250
HBT DT153-13	Sn	110	35	0.812	0.250
DHBT MV268-1	Si	105	62	0.840	0.830
DHBT MV268-9	Si	105	62	0.850	0.815
DHBT CPM468-7	Si	95	60	0.825	0.775

Figure 6. Emitter follower voltage gain at 300 and 77 K for several HBT Sn-doped devices and DHBT Si-doped ones.

REFERENCES

1. D.V. Lang, in *Deep Centers in Semiconductors,* ed. by S.T. Pantelides, (Gordon and Breach, New York, 1986).
2. J.F. Rochette, P. Delescluse, M. Lavin, D. Delagebeaudeuf, J. Chevrier, and N.T. Linh, Inst. Conf. Ser. **65**, 385, (1982).
3. A. Kastalsky and R.A. Kiehl, IEEE Trans. Electron Devices **ED-33**, 414, (1986).
4. M.I. Nathan, Solid-State Electron. **29**, 167, (1986).
5. M.I. Nathan, S. Tiwari, P.M. Mooney, and S.L. Wright, J. Appl. Phys. **62**, 3234, (1987).
6. T. Baba, T. Mizutani, M. Ogawa, and K. Ohata, Japan. J. Appl. Phys. **23**, L654, (1983).
7. Y.K. Chen, D.C. Radulescu, P.J. Tasker, G.W. Wang, and L.F. Eastman, Inst. Phys. Conf. ser. No. 83, 581, (1987).
8. P.M. Mooney, G.A. Northrop, T.N. Morgan, and H.G. Grimmeiss, Phys. Rev. **B37**, 8298, (1988).

VIII. IMPACT IONIZATION OF Se AND Si RELATED DX CENTERS IN AlGaAs

VIII.1. INTRODUCTION

The behavior of n- type dopants in III-V compounds has been shown to be a very complex one. The presence of deep states related to the donors was already detected in $GaAs_{1-x}P_x$ alloys, but was in $Al_xGa_{1-x}As$ where the research has been more systematic. Current views indicate that, as an intrinsic behavior of the donor atoms, each chemical donor species generates two types of electronic states [1,2,3]. One is a shallow and delocalized effective mass state associated with the Γ or X minima, and related to the substitutional site configuration of the donor atom. The second one is a more localized and deeper state, labelled DX, apparently correlated with the L minima, and generated by a lattice distortion around the donor atom. Since both types of state belong to the same donor atom, their steady state electron population is just determined by their relative distance respect to the conduction band. Concerning the microscopic structure of DX centers, one of the remaining most important problems refers to the charge state determination of the DX ground state (DX^0 or DX^-), that is, the positive or negative-U nature of the DX centers[4].

The electron ionization by thermal and optical processes has been analyzed in detail, mainly for Si-related DX centers[1-3]. In this section we want to report, for the first time, that the electrons trapped by the Si and Se- related DX centers can be impact ionized to the conduction band. The electron emission kinetics under high reverse bias conditions is presented.

VIII.2. EXPERIMENTAL AND RESULTS

MOVPE grown AlGaAs layers with 30% and 34% Al content were used in this work. These samples were 1 μm thick and Se- doped to 10^{18} cm^{-3}. An undoped GaAs cap layer, 100 Å thick, was needed to obtain Ti/ Au Schottky

diodes with reasonable reverse characteristics. High frequency capacitance bridges (Boonton 72BD and HP-4191), dedicated hardware, and computer systems allowed to obtain capacitance transients at constant voltage, constant capacitance, and *constant reverse current.* Low temperature measurements were performed in a closed cycle He- cryostat down to 20K range. Two- terminal capacitance and quality factor parameters were determined in all measurements to detect any device series resistance effect.

An initial sample characterization revealed a Se doping level of 1.1×10^{18} cm^{-3}. It was determined by C-V profiling at room temperature and at 77K under white light illumination. Deep level transient spectroscopy (DLTS) spectra showed that only the Se- related DX peak was present in the temperature range considered. A thermal emission activation energy, E_e, of 240 ± 20 meV was obtained in samples with 30%, 34%, 48%, and 77% Al content[5]. The thermal capture barrier, E_b, was determined in a sample with 30% Al content following the technique developed by Criado et al. [6], giving a value of 160 ± 20 meV.

It is worth to mention the difficulties to determine the DX center electron occupation in a quasi neutral region by capacitance techniques. C-V profiling tends to give the total N_d doping level, even at temperatures where the donor ionization factor (I) is small [7]. A way to overcome this problem is to perform *fast* 1/ C^2-V scans at various temperatures, from which both the free electron density profile and its evolution with time are determined[7]. *Fast* means that the C-V scanning time must be much smaller than the electron thermal emission time constant from the DX center. Then, the 1/ C^2-V plot produces a slope that is inversely proportional to the non-trapped electron concentration at the quasi- neutral region (Direct Electron Concentration Spectroscopy, DECS). Figure 1 schematizes the shape of the space charge region (SCR) in a Schottky barrier governed by DX centers. The SCR tail and the regions labelled as #1 and #2, where the 1/ C^2-V slopes are obtained by DECS (figure 1.b), are also represented. Scanning times must be smaller than the capture times involved.

This technique has been applied to Schottky barriers on Se: AlGaAs layers, at 77K. A sudden drop in the 1/ C^2-V slope is observed at a given reverse voltage. This effect is depicted in figure 2, for a 34% Al

content sample. Near $V_r \cong$ -1.3 V, the slope of the DECS characteristic changes abruptly (ABCD line) and a further increase of the reverse voltage switches the $1/C^2$ value to the one corresponding to room temperature (slope inversely proportional to N_d). Note that this slope is the same as the one obtained at 77K after DX photoionization (AED line). The shape of the ABCD line in figure 2 depends on the delay time before each voltage scan, because at 77K the thermal emission time from Se- related DX centers is about 10^4 seconds while the capture time is in the 10^2 second range. If we stay longer at point A, curve AB' is then obtained, that corresponds to a smaller electron concentration at the conduction band. Finally, once point D is reached, a backward voltage scan tracks the DEA line, which proves that all DX centers are ionized.

It is the sudden drop in the $1/C^2$-V slope (BC line in figure 2) what we relate to an enhanced electron emission mechanism from the DX centers. Capacitance measurements as a function of the temperature provide a further check that this enhanced electron emission process corresponds to a real DX ionization. Cooling down the sample at 0 volts, from 300 to 20K, a capacitance drop is observed. Once at 20 K, *the very same capacitance recovery* is obtained either illuminating with white light or biasing the sample *in the dark* at a given reverse voltage and returning back to 0 volts. In this case, the time needed to recover the capacitance depends on the value of the reverse bias used. Beyond a critical value (point B in figure 2) a higher reverse voltage implies a shorter recovery time.

VIII.3. DISCUSSION

Since for Se- related DX centers the electron thermal emission rates at 77K are too small ($\cong 10^4$ s), we have to consider other physical mechanisms to account for such a fast ionization rates observed. One possibility is a Poole- Frenkel effect (PFE). Whether PFE affects or not the thermal emission rate from DX centers is still a subject of controversy [8-9]. A rough estimation indicates that at 77K and for an electric field at the SCR edge of 10^5 V/cm, PFE would enhance the electron thermal emission by a factor of 10^4. This is comparable to the enhancement experimentally

observed (curve ABCD in figure 2). However, small changes in the reverse voltage would not significantly modify the electric field at the SCR edge of the Schottky diodes under study. Moreover, the enhanced ionization mechanism described here shows a clear voltage threshold instead of a monotonous dependence on the reverse voltage V_r.

To consider alternative ionization mechanisms, it is worth to notice that, because the doping levels involved in these devices, an electron tunneling current flows from the the metal barrier to the semiconductor. In fact, the barrier breakdown region is a soft one ($I \cong V^n$), and from its dependence on temperature, the dominance of the tunneling processes was confirmed. Then, a DX ionization mechanism might be due to an impact process due to such flowing electrons. The reverse current will now be the key parameter.

The electron emission kinetics has been first characterized by an analysis of the isothermal emission transients at very small reverse bias, under constant capacitance conditions. Clear non-exponential transients with very large time constants were found (figure 3.a), confirming that a range of emission rates is involved in the thermal process [10,11]. Let us remember that in isothermal transients at constant capacitance, the applied reverse voltage increases with time. In our case, depending on the temperature and the capacitance set point, this voltage reaches the critical value (point B in figure 2), and the strong emission enhancement is produced (figure 3.a). The voltage transients are limited (flat regions) by a protection circuit. The analysis of the enhanced emission transients under constant capacitance conditions is not easy, because while the reverse voltage increases the reverse current also increases. If there is an impact mechanism involved, the shape of the transient will be affected by this reverse current variation. A similar problem arises when emission transients at constant voltage are considered. As the DX centers ionize, the SCR shrinks and the reverse current also increases. This feedback mechanism is shown in figure 3.b, where an initial slow transient is followed by a region characterized by a decreasing time constant. On the other hand, it is clear in figure 3.b, that the emission enhancement increases with increasing reverse voltage.

Following the above considerations, we have studied capacitance transients under constant- reverse current conditions. These measurements might provide the clearest information about an enhanced emission process driven by an impact mechanism. As it is shown in figure 3.c, the transient waveforms obtained are much more exponential than the ones in figure 3.b. The involved emission time constants are now roughly inversely proportional to the reverse current. Evenmore, an emission transient at 30K, obtained under a constant reverse current of 30 μA, has a time constant about **one half** than at 77K and reflects the weak temperature dependence of an impact mechanism. For a thermal activation energy of 240 meV (Se -DX centers), and even if we consider at 30K a PFE enhancement in the 10^{10} range (electric field $\cong 10^5$ V/cm), it is clear that any thermal emission process would not be detectable at 30K and would show a temperature coefficient with **opposite** sign to the impact ionization temperature dependence. Finally, in samples with 30% Al content, all the above phenomenology is reproduced except that transient amplitudes are smaller, as it is expected from a lower DX electron occupancy.

From above experimental data, PFE cannot be considered the origin of the reported electron emission enhancement. The dependence of the enhanced emission rates on the reverse current move us to propose that the emission mechanism described in this work is due to the *impact ionization of the Se- related DX centers*. This mechanism is started by the electrons leaking from the metal barrier. Similar studies have been made in AlGaAs:Si/ GaAs double heterojunction bipolar transistors (DHBT). In these devices the transistor effect allows to establish a controllable reverse electron current collected by the junction where Si- DX centers are going to be ionized. Besides the internal photoionization of DX centers by photons emitted from the base[12], DX impact ionization is found to depend on the energy of these collected electrons (collector- base reverse voltage).

VIII.4. CONCLUSIONS

In summary, we report a new enhanced emission process from DX centers in Se and Si- doped AlGaAs, which is not of thermal origin. This

electron emission appears under reverse bias and low temperatures where the thermal emission rate is many orders of magnitude lower. Although other processes cannot be fully disregarded, we propose an electron impact ionization mechanism as the origin of this enhanced emission. These findings must be considered in breakdown voltage and noise analysis in AlGaAs/ GaAs-based heterojunction bipoiar and high electron mobility transistors.

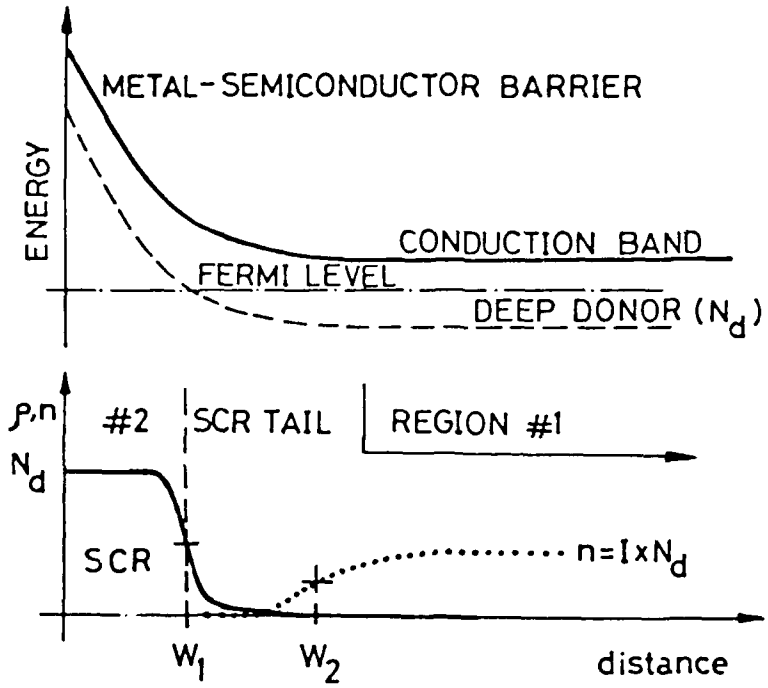

(a)

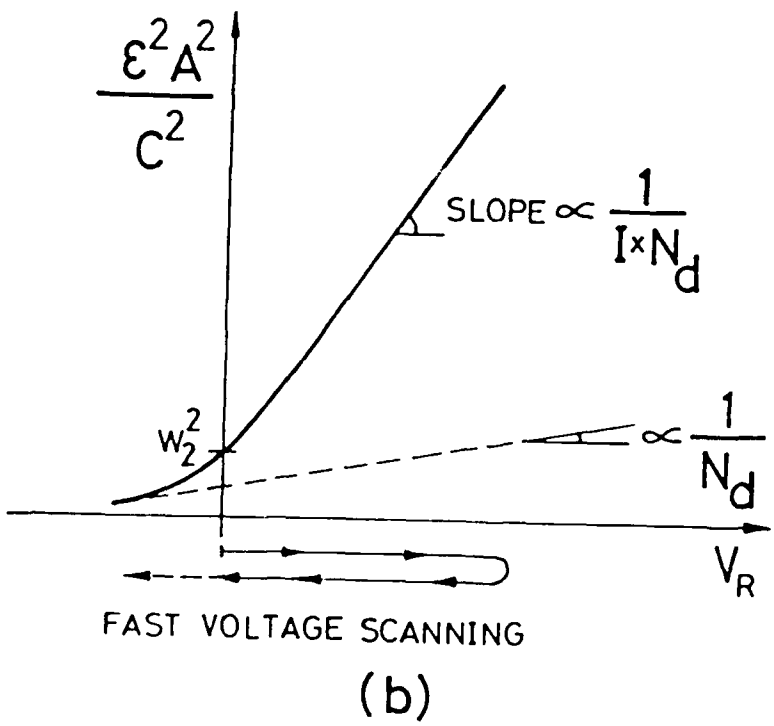

(b)

Figure 1.- a) space charge region shape in a metal/n-AlGaAs barrier, at low temperatures, when the donor has a low ionization factor, I. A long Debye tail is present.

b) $1/C^2$-V plot by performing a fast C-V scanning. The two slopes corresponding to concentrations N_d (region II) and to IxN_d (region I) are obtained.

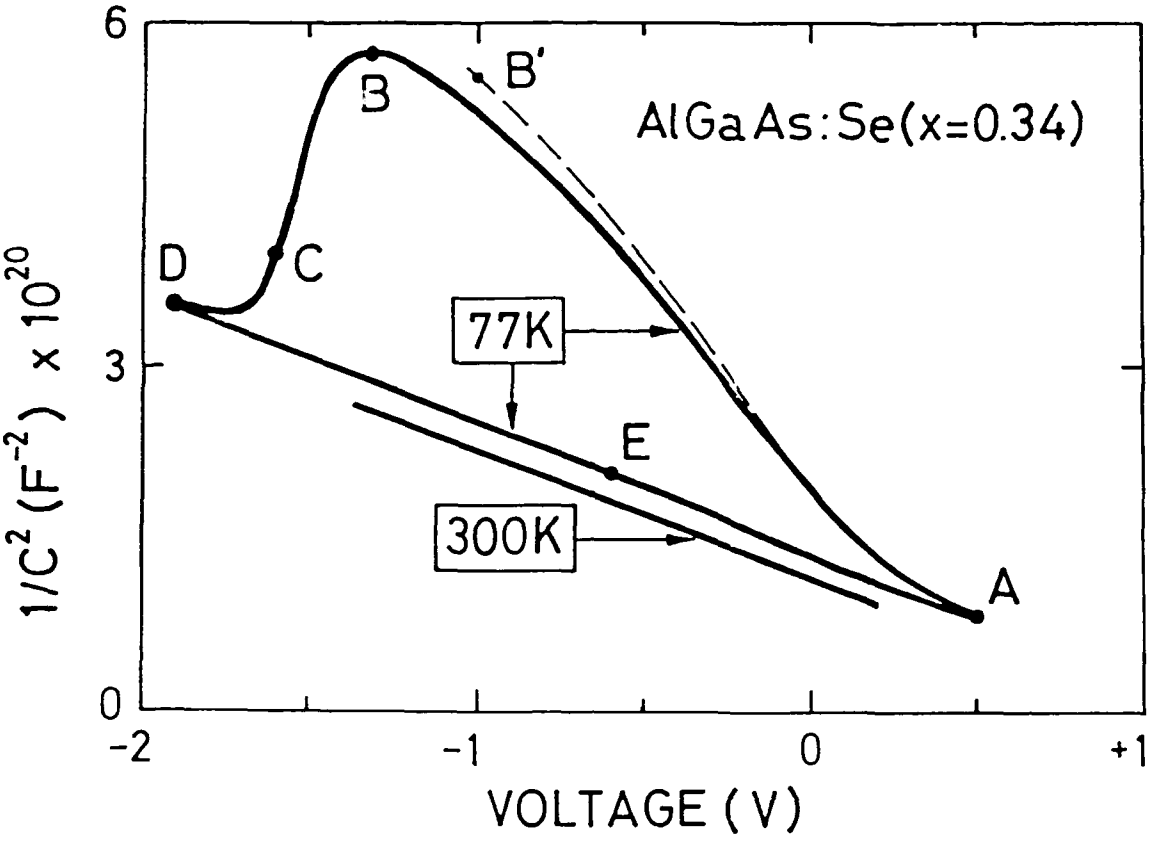

Figure 2.- Direct electron concentration spectroscopy applied at 77K to a metal-$Al_{0.34}Ga_{0.66}As$:Se barrier. From A to B' a fast C-V scanning would allow to determine the IxN_d net ionized DX centers. At $V_r \cong .3V$ (B), a sudden slope change is produced towards the N_d concentration (line AED): the flowing electrons have impact ionized the DX centers. A fast scanning towards forward voltages follows the DEA path, the same slope than at room temperature (N_d).

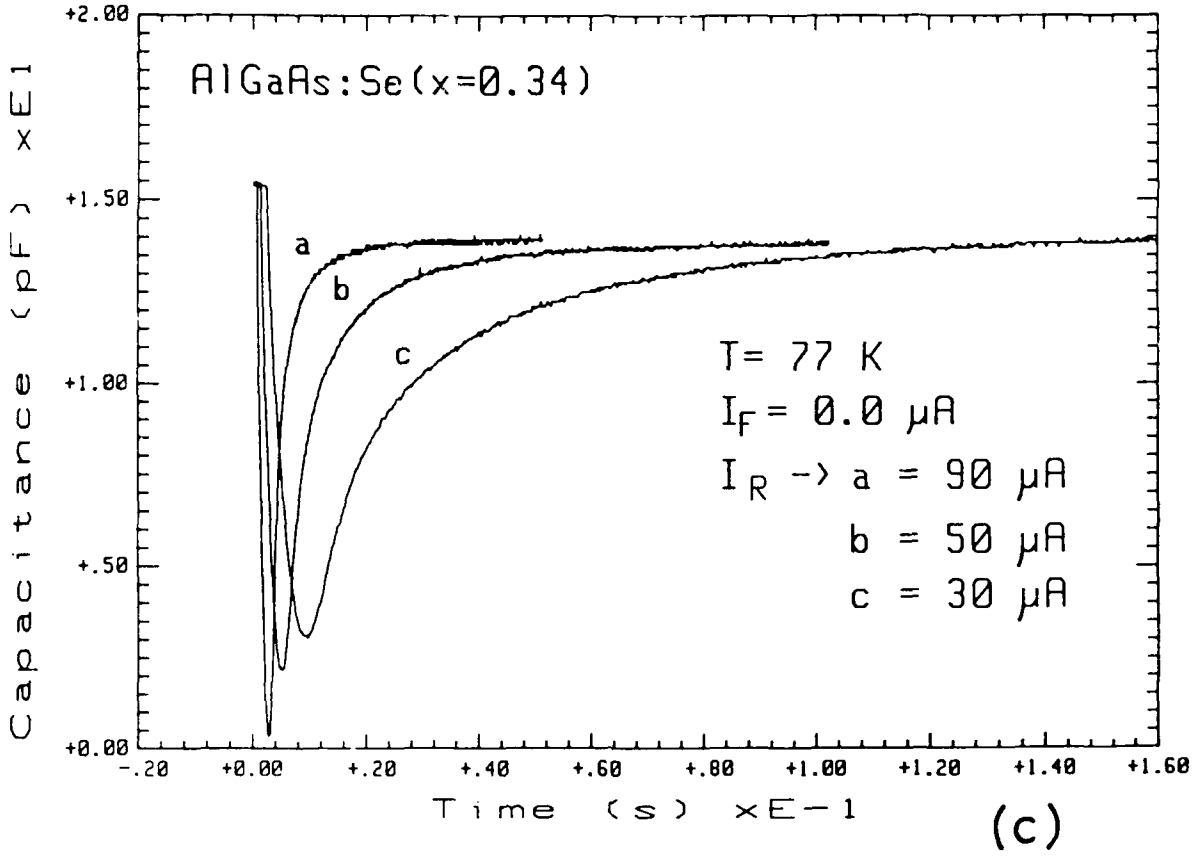

Figure 3.- Transient waveforms due to the electron ionization of Se-related DX centers, under various excitation mechanisms.

a) Voltage transients under constant capacitance conditions;

b) capacitance waveform under constant voltage transient;

c) capacitance transient under constant reverse current excitation.

In a) and b) an initial thermal excitation component, much slower, is detected, followed by a fast impact ionization once the reverse voltage and current increase. In c) much more exponential capacitance transients are registered, with time constants roughly proportional to the inverse of the reverse current. The waveform front is distorted by the charging of the bridge DC-decoupling capacitance.

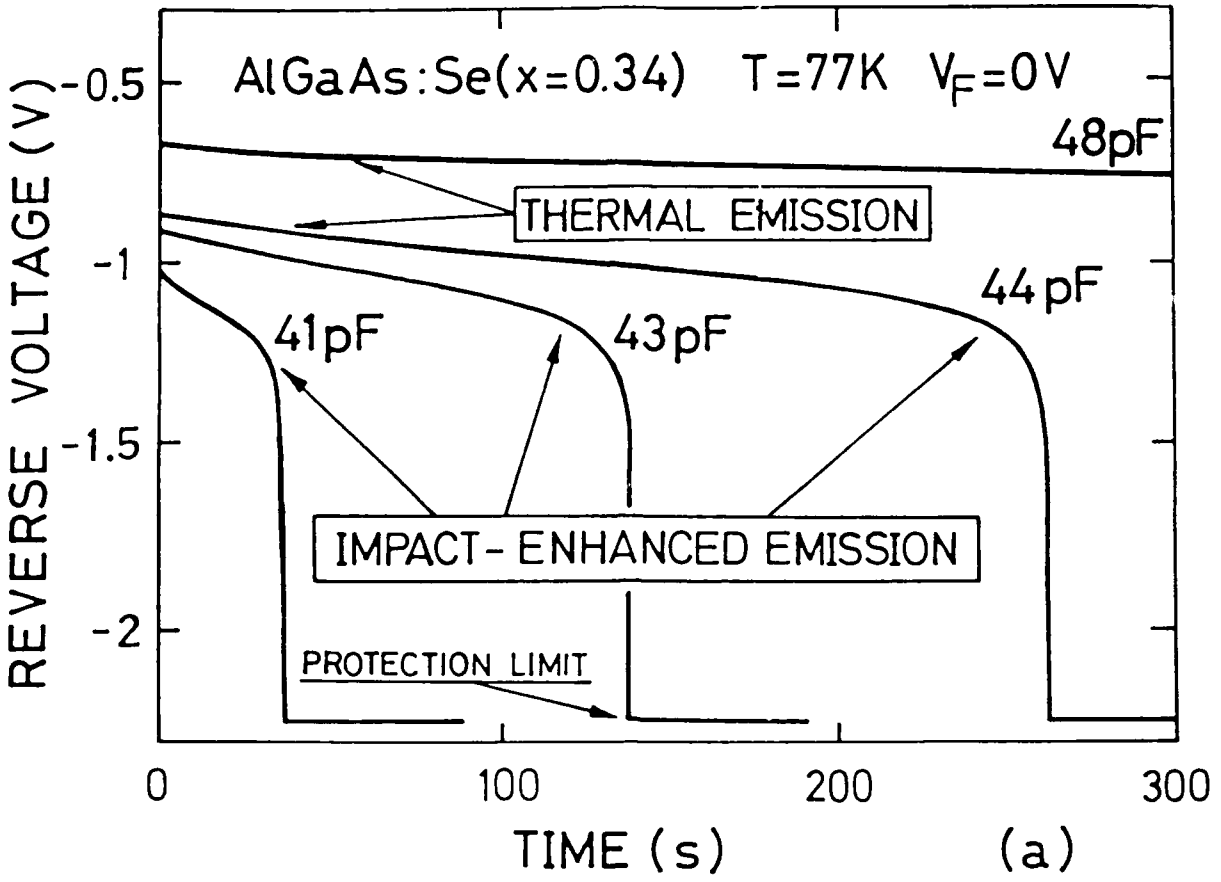

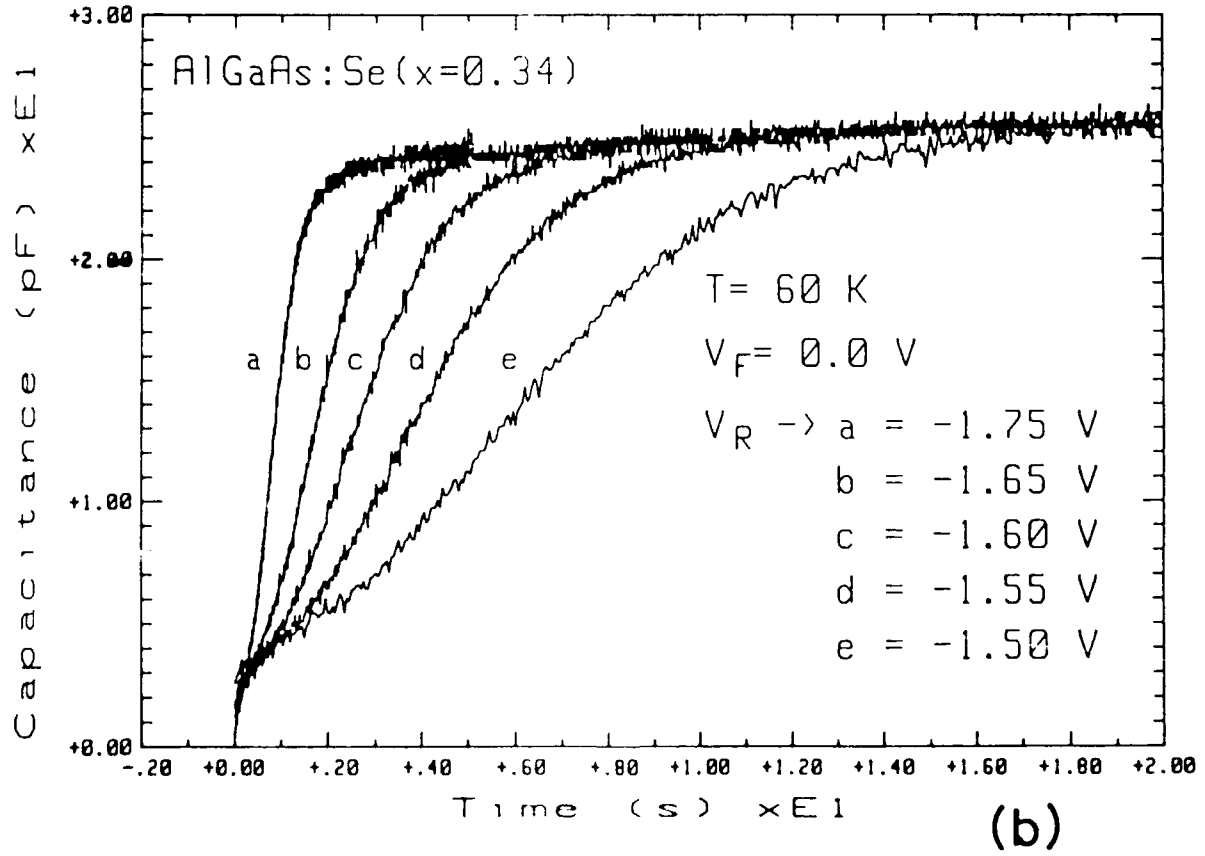

Figures 3a and 3b

REFERENCES

1. D. V. Lang, in *Deep Centers in Semiconductors,* edited by S. T. Pantelides (Gordon and Breach, New York, 1986), p. 489.
2. P. M. Mooney, J. Appl. Phys., **67**, R1, (1990).
3. J. C. Bourgoin, editor, *Physics of DX Centers in GaAs Alloys*, Sci. Tech. Publications, Liechtenstein, 1990.
4. D. J. Chadi and K. J. Chang, Phys. Rev. **B39**, 10063, (1989).
5. E. G. Oh, M. Hanna, Z. Lu, D. Szmyd, and A. Majerfeld, Electron. Mater. Conf., 1988, Boulder, USA.
6. J. Criado, A. Gómez, E. Calleja, and E. Muñoz, Appl. Phys. Lett., **52**, 660, (1988).
7. I. Izpura, E. Muñoz, G. Hill, J. Roberts, M. A. Pate, P. Mistry, and N. Y. Hall, Appl. Phys. Lett., **55**, 2414, (1989).
8. J. M. Langer, J. E. Dmochowski, L. Dobaczewski, W. Jantsch, and G. Brunthaler, p. 233 in ref.3.
9. M. Zazoui, S. L. Feng, J. C. Bourgoin,, and J. von Bardeleben, MRS Fall Meeting, Boston, 1989.
10. E. Calleja, P. Mooney, S. Wright, and M. Heiblum, Appl. Phys. Lett., **49**, 657, (1986).
11. E. Calleja, P. M. Mooney, T. N. Theis, and S. L. Wright, Appl. Phys. Lett., **56**, 1934, (1990).
12. I. Izpura, E. Muñoz, and E. Calleja, Int. Conf. on the Science and Tecnology of Defect Control in Semiconductors, Sept. 1989, Yokohama.

IX. SUGGESTIONS FOR FUTURE WORK

The behavior and model of DX centers has shown to be a very complex one. The nature and structure of DX centers is still under debate. Considered as a defect, it is a real complex point defect!. Two of the basic problems relate to determining the charge state of the DX ground state, and the nature of the intermediate state(s) to which electrons are emitted by thermal or optical excitation. It has not been definitevely anwsered if the ground state is DX° or DX^{-}, and if excited states are implicated in the emission and capture traffic. From present electrical and optical characterization such information might not be obtained.

From a device viewpoint, the idea that deep donors are intrinsic to donor behavior in III-V compounds has moved device design to conduction band engineering and doping techniques that minimize such effects: δ- doping techniques, supelattices, In- doped AlGaAs layers, use of strain InGaAs channels in HEMT devices, InGaP- based devices (its lattice matched composition on GaAs seems to be below bandgap crossover), AlInAs/ InGaAs/InP LM- HEMT's, etc.

We summarize here some suggestions for further study concerning the device limitations due to DX centers:

* study of δ- doping structures in both AlGaAs (for PM- HEMT's) and in AlInAs (in InP- based LM- HEMT's).

* as a related problem, to investigate high doping effects in n- type GaAs and AlGaAs, to determine how emission and capture activation energies evolve at very high doping levels.

* to fully investigate alternative dopants to Si in GaAs and AlGaAs technology. Some results are already available for Se, Te, and Sn. From the electrical viewpoint all of them offer advantages over Si. New dopants like Pb should be investigated.

* in relation to the charge state of the DX centers, careful double

doping experiments should be performed. Co- doping with Si and Sn, and Si- Se should be studied.

* to further pursue the experiments and modeling of local environment effects on the capture barrier.

* to study and model In doped AlGaAs (5 - 10% of In) for, at least, one group VI donor. In these quaternary alloys, hydrostatic pressure experiments for both Si, and Se (or Te) dopants, will be quite interesting.

X. PUBLICATIONS

The following publications have been made during the contract period, acknowledging the AFOSR support:

- I. Izpura, and E. Muñoz, "Electron capture by DX centers in AlGaAs and related compounds", Appl. Phys. Lett., **55**, pp. 1732-1734, Oct 1989.

- I. Izpura, E. Muñoz, G. Hill, J. Roberts, M. A. Pate, P. Mistry, N. Y. Hall, "Capacitance properties in n-type AlGaAs", Appl. Phys. Lett. **55**, pp.2414-2416, Dec 1989.

- I. Izpura, E. Muñoz, and E. Calleja", "DX centers and the low temperature behavior of AlGaAs/GaAs heterojunction bipolar transistors", The International Conference on the Science and Technology of Defect Control in Semiconductors, Yokohama, Japan, Sept. 1989, proceedings to be published.

- E. Muñoz, "DX centers and III-V device performance", invited paper, Materials Research Society Spring Meeting, San Francisco, April 1990. To be published in Volume 84 MRS Symposium Proceedings series.

- *The project senior investigators have published the following book chapters, summarizing previous and present research efforts on DX centers:*

- E. Calleja and E. Muñoz, "Thermal Emission Processes from DX Centers", in Solid State Phenomena Vol. 10, (Sci-Tech Publications Ltd, Liechtenstein, 1990), pp. 73-98.

- E. Muñoz and E. Calleja, "Carrier Capture Processes at DX Centers", in Solid State Phenomena Vol. 10, (Sci-Tech Publications Ltd., Liechtenstein, 1990), pp. 99-120.

The following paper has been submitted for publication:

- I. Izpura, E. Muñoz, F. García, E. Calleja, A. L. Powell, P. I. Rockett, C. C. Button, J. S. Roberts, "Impact Ionization of Se-related DX Centers in AlGaAs", submitted to Appl. Phys. Lett.